Analog Impairments Compensation in OFDM Direct-Conversion Receiver

Analog Impairments Compensation in OFDM Direct-Conversion Receiver

Umut Yunus

February 2010

Doctoral Thesis at Osaka Prefecture University

Analog Impairments Compensation in OFDM Direct-Conversion Receiver

A dissertation submitted to the
Graduate School of Engineering
in partial fulfillment of
the requirements for the
degree of Doctor of Engineering

Umut Yunus

Sakai, February, 2010

INTELLIGENT INFORMATION COMMUNICATION LABORATORY
Department of Electrical & Electronic Systems
Graduate School of Engineering
Osaka Prefecture University

Submitted version, January, 2010.
Revised version, February, 2010.

Typeset by the author with the LaTeX 2ε Documentation System, with AMS-LaTeX Extensions, in 12/18pt Sabon and Pazo Math fonts.

INTELLIGENT INFORMATION COMMUNICATION LABORATORY
Department of Electrical & Electronic Systems
Graduate School of Engineering
Osaka Prefecture University
1-1 Gakuen-cho, Sakai, Osaka, 599-8531, JAPAN

Acknowledgments

WITH utmost sincerity, I would like to express my gratitude to my supervisor, Professor Katsumi Yamashita for his constant encouragement and valuable advices that guided me throughout this research, and for his enthusiasm and devotion that always inspired me during my hard times. My deepest thanks go to Prof. Yamashita.

I would like to thank Professors Yutaka Katsuyama, Masaharu Ohashi, for serving as members of my dissertation committee and their vital suggestions. They assured the quality of this research.

I am specially grateful to Dr. Hai Lin for his encouragement and full support during my hard time. I would like to thank all my colleagues in the Intelligent Information Communication lab, for their great support.

I would also like to gratefully acknowledge the financial support received from the Japanese Government-Monbu Kagakusho Scholarship.

I would like to thank Professors Masanobu Kominami and Yiwei He in Osaka Electro-Communication University for their valuable advices and encouragement.

I would like to thank Xinjiang University for their great support. I am specially grateful to Professors Zhenhong Jia and Dilmurat Tursun for their encouragement and full support.

Finally, I am extremely grateful to my family for all their unconditional support, patience, trust and love during these hard times while I was working at a distance. I dedicate this work to them.

Contents

List of Figures

List of Tables

List of Acronyms

ADSL	Asymmetric Digital Subscriber Line
AGC	Automatic Gain Control
AWGN	Additive White Gaussian Noise
BER	Bit Error Rate
BPSK	Binary Phase Shift Keying
CATV	Cable Television
CFO	Carrier Frequency Offset
CP	Cyclic Prefix
DAB	Digital Audio Broadcasting
DCR	Direct-Conversion Receiver
DCO	DC Offset
DFT	Discrete Fourier Transform
DMC	Differential Method Coarse estimation
DMF	Differential Method Fine estimation
DSP	Digital Signal Processor
DVB	Digital Video Broadcasting
FDE	Frequency Domain Equalization
FDM	Frequency Division Multiplexing

FFT	Fast Fourier Transform
FIR	Finite Impulse Response
FTTH	Fiber To The Home
GI	Guard Interval
HPF	High Pass Filter
HSDPA	High Speed Downlink Packet Access
ICI	Inter-Carrier Interference
IDFT	Inverse Discrete Fourier Transform
IF	Intermediate Frequency
IFFT	Inverse Fast Fourier Transform
IICM	Iteration based ISI Cancellation Method
I/Q	In phase / Quadrature phase
IRR	Image Rejection Ratio
ISI	Inter-Symbol Interference
ISM	Industrial, Scientific and Medical
LMC	Least square Method Coarse estimation
LMF	Least square Method Fine estimation
LNA	Low Noise Amplifier
LO	Local Oscillator
LPF	Low Pass Filter
LTS	Long Training Sequence
MC-CDMA	Multi-Carrier Code Division Multiple Access
MSE	Mean Square Error

MUI	Multi-User Interference
OFCDM	Orthogonal Frequency and Code Division Multiplexing
OFDM	Orthogonal Frequency Division Multiplexing
PICM	Proposed ISI Cancellation Method
PP	Periodic Pilot
P/S	Parallel to Serial
QAM	Quadrature Amplitude Modulation
QPSK	Quadrature Phase Shift Keying
RF	Radio Frequency
SER	Symbol Error Rate
S/P	Serial to Parallel
STS	Short Training Sequence
SNR	Signal to Noise Ratio
TV-DCO	Time-Varying DCO
VSF	Variable Spreading Factor
WLAN	Wireless Local Area Network

CHAPTER 1

Introduction

THE history of wireless communications began in 1886, when Hertz generated electromagnetic waves. Around 1897, Marconi successfully demonstrated wireless telegraphy, for that he was awarded the Nobel Price in 1909. Based on this, the radio communication by Morse code across the Atlantic Ocean had been established in 1901. More than one century has passed, since then. Today, telecommunication has become so indispensable that we almost cannot imagine our lives without it. From satellite transmission, radio and television broadcasting to the now ubiquitous mobile telephone, wireless communications have revolutionized human society. In contrast to the poor information-carrying ability of the early telecommunication system, instantaneous transferring of a large number of information, such as multimedia information, becomes possible.

Under the increasing demand to high-speed, high-spectral efficiency of radio communication, the digital-communication employing orthogonal frequency division multiplexing (OFDM) had emerged. The origin of OFDM started in 1966, when Chang proposed the structure of OFDM in [32], where the concept of using orthogonal overlapping multi-tone signals was given. At that time, although the theory of OFDM was well developed, the implementation of OFDM systems still had some difficulties [33, 34] due to the hardware. In 1971, Weinstein [34] introduced the idea of using a discrete Fourier transform (DFT) to perform baseband modulation and demodulation of the signals.This presented an opportunity of an easy implementation of OFDM, especially with the use of fast Fourier transform (FFT). Another important contribution was due to Peled and Ruiz in 1980 [3], who introduced the cyclic prefix (CP) to combat mutipath fading. Then, communication of OFDM had become possible according to the development of digital

signal processor (DSP) circuit. As a result, in 1987, OFDM was used in the European digital audio broadcasting (DAB) standard. Nowadays, OFDM is well-known modulation scheme, which has been adopted in many wireless communication systems such as DAB, digital video broadcasting (DVB), and IEEE 802.11 wireless local area network (WLAN) [1].

1.1 TENDENCY OF WIRELESS COMMUNICATION SYSTEMS

The total number of mobile subscribers is about 100 million in Japan, which increased 10 times in 10 years. At the end of 2005, there were 80 million internet subscribers in Japan, that occupied 62% of the population [20]. There were 20 million broadband users, accessing from asymmetric digital subscriber line (ADSL), fiber to the home (FTTH), and cable television (CATV) [20]. In 2005, the number of 3G subscribers is 41 million [20].

As a 3.5G system, high speed downlink packet access (HSDPA) was used to start the service in 2006, and can achieve a transmission speed of up to 14 Mbit/s, even when using the same 5MHz frequency bandwidth as 3G [20]. As a 3.9G system, transmission speed of 100 Mbit/s can be achieved at the downlink [17]. This means that the transmission speed of cellular phone increased 10 thousand times during these 20 years. As a result, the cellular phone, which was just used for audio communication, is able to access multimedia freely. For next generation systems, a very high-speed wireless access of approximately 1 Gbit/s is required. One possible technology that satisfies the requirements is variable spreading factor orthogonal frequency and code division multiplexing (VSF-OFCDM) .

On the other hand, IEEE 802.11g, which uses OFDM technology in the 2.4 GHz band with a bit rate of 54 Mbit/s, was established in 2003 [20]. Currently, a new standard, IEEE 802.11n can achieve maximum 600 Mbit/s. Furthermore, new standards IEEE 802.11ac and IEEE 802.11ad, which are expected beyond 1Gbit/s in the future, have being discussed [17].

1.2 THE RECEIVER ARCHITECTURE

According to the receiver architecture, the receivers can be classified to the superheterodyne receiver and direct-conversion receiver (DCR). In the following subsection, we will

give brief explanations to these receivers.

1.2.1 Superheterodyne Receiver

The superheterodyne principle was introduced in 1918 by the U.S. Army major Edwin Armstrong in France during World War I, which is generally thought to be the receiver of choice owing to its high selectivity and sensitivity. About 98% of radio receivers use this architecture. In a superheterodyne receiver, the input signal is first converted by an offset-frequency local oscillator to a lower intermediate frequency (IF), and substantially amplified in a tuned IF containing highly-selective passive bandpass filters. Therefore, the superheterodyne receiver needs two stages of detection and filtering.

1.2.2 Direct-Conversion Receiver

Direct-conversion receiver (DCR) is very attractive by its smaller size, lower cost, and lower power consumption over the traditional superheterodyne receivers. DCR, also known as homodyne, synchrodyne, or zero-IF receiver was developed in 1932 by a team of British scientists searching for a method to surpass the superheterodyne. DCR is a radio receiver that demodulates the incoming signal by a local oscillator signal synchronized in frequency to the carrier of the wanted signal. Therefore, the wanted modulation signal is obtained immediately by low-pass filtering, without further detection. Thus a direct-conversion receiver requires only a single stage of detection and filtering.

1.3 A Brief Review of OFDM-DCR

In recent years, OFDM-DCR system, which is a combination of OFDM technique with DCR, has attracted a lot of attention. The main reason is that, in OFDM-DCR, not only high-speed and high spectral efficiency, but also small size, low cost, and low power consumption can be achieved. Although OFDM-DCR has many considerable merits, it leads to additional analog impairments, which causes severe performance degradation of the system. In OFDM-DCR, carrier frequency offset (CFO), DC offset (DCO), and I/Q (in-phase and quadrature-phase) imbalance [4] are considered to be the most serious impairments. In order to obtain good performance, it is necessary to estimate and compensate the analog impairments. In this thesis, we focus on the compensation of these analog impairments. To better understand the background of this study, we will give brief reviews of above mentioned analog impairments.

1.3.1 CFO

The main drawback of OFDM systems is it's sensitivity to carrier frequency offset (CFO). Orthogonality among subcarriers is the fundamental of OFDM systems. CFO, mainly caused by frequency mismatch between the transmitter and receiver local oscillators (LOs). While CFO occurs, the spectrum of the received signal will be shifted. This will destroy the required orthogonality and result in severe performance degradation. Therefore, the estimation/compensation of CFO is very crucial in OFDM systems. Conventionally, the CFO can be estimated easily from the autocorrelation of periodic pilot (PP) [14, 26, 30, 40].

1.3.2 DCO and I/Q Imbalance

DCO is induced by the self-mixing associated with the imperfect isolation and is known as the most serious problem [2] of DCR. The I/Q imbalance is caused by the mismatched components between the in-phase (I) and quadrature-phase (Q) branches, i.e., is basically any mismatch between the I and Q branches from the ideal case. Therefore, the estimation/compensation of CFO in the presence of I/Q imbalance and the DCO is a critical problem in an OFDM-DCR.

In the absence of DCO, the CFO can be estimated easily from the autocorrelation of periodic pilot (PP) [14, 26, 30, 40]. The CFO estimators in the presence of DCO and of I/Q imbalance in OFDM DCRs have been proposed in [7,12,15,37] and [9,11,19,35,36], respectively. Also, the joint estimation of CFO, I/Q imbalance and DCO can be found in [12]. However, all of these works treated the DCO as time-invariant.

1.3.3 Time-Varying DCO Caused by AGC

In practice, automatic gain control (AGC) is usually used to keep the received signal amplitude proper fixed level. Also, a high pass filter (HPF) is often employed in the DCR to reduce DCO [47]. Therefore, the gain shift in the low noise amplifier (LNA) will cause a time-varying DCO (TV-DCO) [38], whose high frequency components may pass through the HPF. As a result, the ordinary CFO estimation in [7, 12, 15, 37] will be corrupted by the residual TV-DCO. Until now, there is only one CFO estimator taking the residual TV-DCO into account [25]. In this scheme, a differential filter is used to eliminate the residual TV-DCO, and then the CFO is estimated by the conventional autocorrelation-based method. Since the differential filter increases the noise variance and the residual TV-DCO cannot be eliminated completely, this method will cause per-

formance loss. To the best of our knowledge, until now, only [24] considered the scenario of the coexistence of CFO, I/Q imbalance, and TV-DCO. The idea in [24] is to employ a differential filter to ease the effect of the TV-DCO, and then estimate the CFO by the conventional autocorrelation-based method. However, the differential filter not only fails to completely eliminate the TV-DCO, but also enhances the noise. Also, the CFO estimation is severely biased by the remaining uncompensated I/Q imbalance. Moreover, in [24], only a CFO estimator was proposed and how to estimate/compensate the I/Q imbalance in this situation was not mentioned.

1.4 Inter-Symbol Interference Cancellation in OFDM Systems without Guard Interval

The one reason of that OFDM has been selected for high-speed communication systems, is its good performance in multipath channels. In order to fight multipath, the cyclic prefix (CP), which is also referred to as guard interval (GI), is inserted between symbols. While the length of GI is longer than channel delay spread, it can protect received signal from inter-symbol interference (ISI). However, the price is the transmission speed.

On the other hand, in order to increase the transmission speed, several attempts [8, 13, 18, 21–23, 31, 39, 48] have been made to the cancellation of ISI and ICI (inter-carrier interference) in the OFDM systems with insufficient GI [8, 13, 18, 21–23, 31] or without GI [39, 48]. In [21, 31], time domain equalizer is used to shorten the channel impulse response to combat ISI and ICI. FIR (Finite impulse response) tail cancellation and FIR cyclic reconstruction techniques are used in [18] to cope with ISI and ICI. Precoding techniques and oversampling techniques are used to mitigate ISI and ICI in [22] and [23], respectively. In [8, 13], a decision feed back loop is proposed, which not only result in feedback delay increment and error propagation, but also increase the computational complexity. All these methods only consider the OFDM systems with insufficient GI. Since GI insertion reduces transmission efficiency, beside the common GI insertion, some studies [39, 48] discussed the OFDM systems without GI. In the absence of GI, eliminating ISI between adjacent symbols is a crucial problem. A method [39] was proposed for compensation of ISI distortion by using null subcarriers, i.e., inactive subcarriers, which is usually being placed at the edges of the frequency band and the DC to avoid aliasing and ease transmit filtering. In [48], an iteration method is proposed to eliminate the ISI and ICI. However, the iteration in [48] increases the complexity of computing and also results in error propagation, specially for high-degree constellation.

1.5 OVERVIEW OF THE THESIS

1.5.1 Contributions of the Thesis

In this thesis, in order to improve bit error ratio (BER) performance in the presence of analog impairments as mentioned in Section 1.3, we propose a novel CFO estimation method and a novel joint estimation method of CFO and I/Q imbalance respectively. Furthermore, since ISI in OFDM systems without guard interval (GI) degrades the system performance as introduced in Section 1.4, in order to improve it, we propose a novel ISI cancellation method for OFDM systems without GI. They can be described as follows.

A Robust CFO Estimator in the Presence of Time-Varying DCO

Until now, there is only one CFO estimator taking the residual TV-DCO into account [25]. In this scheme, a differential filter is used to eliminate the residual TV-DCO, and then the CFO is estimated by the conventional autocorrelation-based method. Since the differential filter increases the noise variance and the residual TV-DCO cannot be eliminated completely, this method will cause performance loss. We develop a novel CFO estimation method in the presence of TV-DCO. It was shown the residual DCO after high-pass filtering varies in a linear fashion. Based on this observation, we model the residual DCO using a linear function. Then, from the periodicity of the training sequence, we derive a CFO estimator in closed-form in Chapter 3.

A Novel Joint Estimator of CFO and I/Q Imbalance in the Presence of TV-DCO

To the best of our knowledge, until now, only [24] considered the scenario of the coexistence of CFO, I/Q imbalance, and TV-DCO. The idea in [24] is to employ a differential filter to ease the effect of the TV-DCO, and then estimate the CFO by the conventional autocorrelation-based method. However, the differential filter not only fails to completely eliminate the TV-DCO, but also enhances the noise. Also, the CFO estimation is severely biased by the remaining uncompensated I/Q imbalance. Moreover, in [24], only a CFO estimator was proposed and how to estimate/compensate the I/Q imbalance in this situation was not mentioned. We develop a novel joint estimation method for CFO and I/Q imbalance in the presence of TV-DCO, where similarly we approximate TV-DCO by linear function. From the periodicity of the pilot, we derive a low-complexity estimator in Chapter 4, which can obtain the necessary estimates in closed-form.

A Novel ISI Cancellation Method for OFDM Systems without GI

Since GI insertion reduces transmission efficiency, beside the common GI insertion, some studies [39, 48] discussed the OFDM systems without GI. In [48], an iteration method was proposed to eliminate the ISI and ICI. However, the iteration in [48] increases the complexity of computing and also results in error propagation, specially for high-degree constellation. To obtain a good performance with the low-complexity, a novel ISI cancellation method is developed in Chapter 5. While the channel is minimum phase, we derive a novel ISI cancellation method, by using the channel information and signal achieved at the tail part of OFDM symbols. For the channel which is not minimum-phase, the proposed method is also applicable after converting the channel into minimum-phase by using a proper filter.

1.5.2 Thesis Organization

This thesis primarily is a collection of our published works in [27, 29, 42–46] and is organized as follows: Chapter 2 introduces the model of OFDM DCR systems, where the reasons of CFO and I/Q imbalance are explained and the basic concepts are given. In addition to this, ISI and ICI problems are given to the OFDM systems without GI. Chapter 3 investigates the problem of CFO in the presence of TV-DCO and drives a novel estimation method. Chapter 4 focuses on the joint estimation of CFO and I/Q imbalance in the presence of TV-DCO and drives a novel estimation method. We propose a novel ISI cancellation method for OFDM systems without GI in Chapter 5. Finally, Chapter 6 concludes this thesis.

In this thesis, superscript $(\cdot)^{\mathcal{H}}$, $(\cdot)^{T}$, $(\cdot)^{*}$ and $(\cdot)^{\dagger}$ denote Hermitian, transpose, conjugate and pseudoinverse, respectively. The subscript $(\cdot)_I$ and $(\cdot)_Q$ denote the I and Q component respectively.

CHAPTER 2

OFDM Systems with Direct Conversion Receiver

MAXIMUM speed of communication including wireless communication was derived by Shannon in 1948 [5, 6]. Shannon's theorem gives an upper bound to the capacity of a link, in bits per second (bps), as a function of the available bandwidth and the signal-to-noise ratio of the link. It can be expressed as follows

$$C = B \log_2 \left(1 + \frac{S}{N}\right) \tag{2.1}$$

where C is the channel capacity in bits per second, B is the bandwidth of the channel, S is the total received signal power over the bandwidth, and N is the total noise or interference power over the bandwidth. This indicates that the high-speed communication is possible by widening signal bandwidth or raising SNR. Since OFDM technology can efficiently increase the bandwidth, it is possible to obtain high-speed communication. Therefore, in broadband communication, OFDM is a key-word. Figure 2.1 shows the trends of wireless communication systems [17].

2.1 MULTIPATH CHANNEL AND ISI

One of the main reasons to use OFDM modulation is it's robustness to multipath delay spread. In OFDM, the data is divided into several parallel data streams called as symbols, then the closely-spaced orthogonal sub-carriers are used to carry these symbols. However, after passing through the channel, inter-symbol interference (ISI) is caused by the multipath channel. To completely eliminate the ISI, a guard time is inserted in

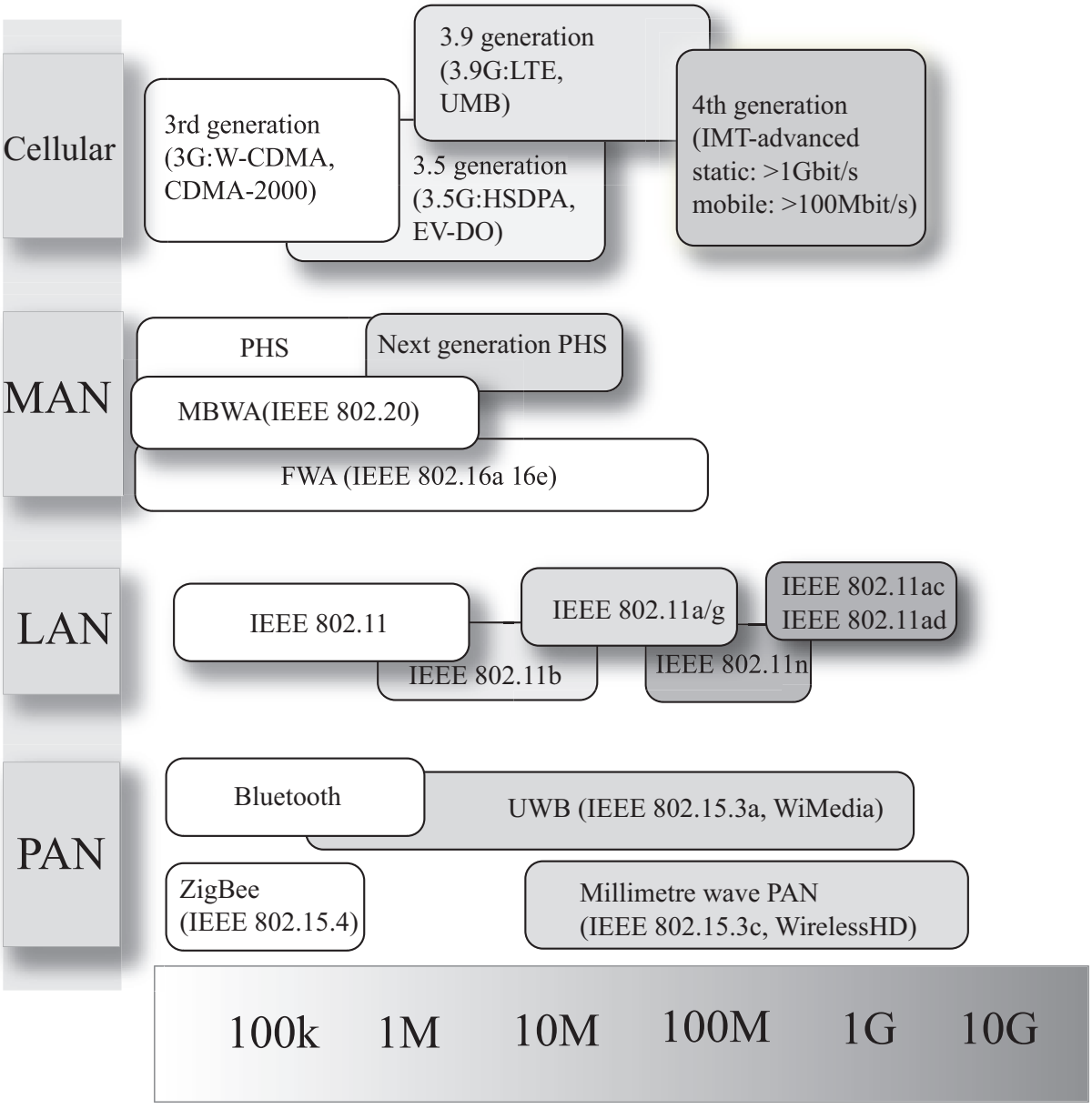

Fig. 2.1. Trends of wireless systems

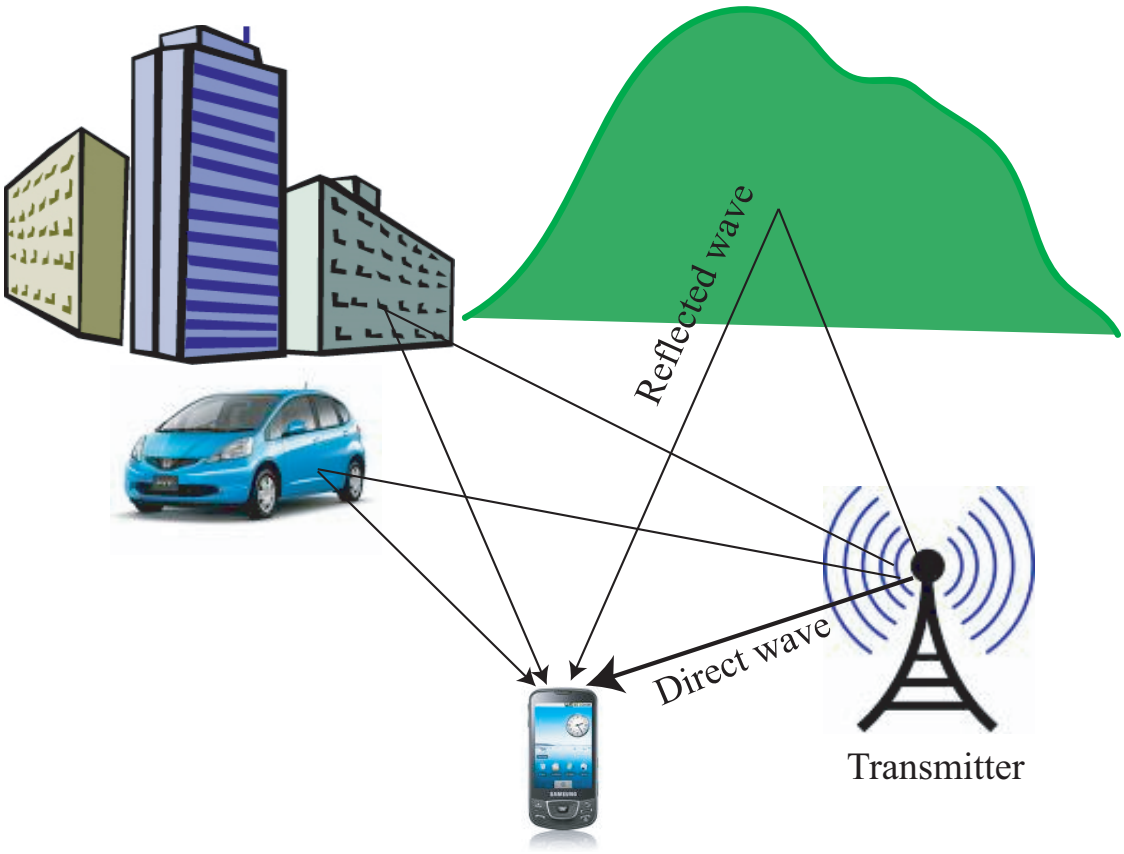

Fig. 2.2. Multipath channel

each OFDM symbol. The duration of the guard time is chosen in accordance with the multipath characteristics of the channel. To avoid the creation of ISI and inter-carrier interference (ICI), a cyclic extension should be longer than the length of channel delay spread. The price to be paid is transmission speed. For this reason, OFDM system designers always keep the guard time duration as short as possible. The multipath of the channel introduces delayed echoes of transmitted signal as shown in Fig. 2.2, where we can see that the received signal is consist of direct wave and reflected waves.

2.2 Comparison of FDM and OFDM

Frequency division multiplexing (FDM) extends the concept of single carrier modulation by using multiple subcarriers within the same single channel. The total data rate to be sent in the channel is divided between the various subcarriers. Advantages of FDM include using separate modulation/ demodulation customized to a particular type of data,

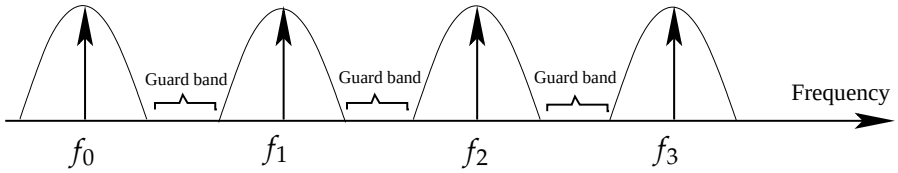

(a) FDM

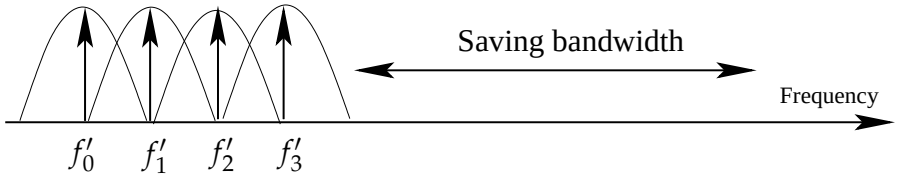

(b) OFDM

Fig. 2.3. Comparison of spectral efficiency

or dissimilar data can be best sent using multiple modulation schemes. FDM systems usually require a guard band between modulated subcarriers to prevent the spectrum of one subcarrier from interfering with another. These guard bands lower the system's effective information rate when compared to a single carrier system with similar modulation. If the above FDM system had been able to use a set of subcarriers that were orthogonal to each other, a higher level of spectral efficiency could have been achieved. The guardbands that were necessary to allow individual demodulation of subcarriers in an FDM system would no longer be necessary. The use of orthogonal subcarriers would allow the subcarriers spectra to overlap, thus increasing the spectral efficiency. As long as orthogonality is maintained, it is still possible to recover the individual subcarriers signals despite their overlapping spectrums. This is the fundamental of OFDM. The comparison of spectral efficiencies of FDM and OFDM is shown in Fig. 2.3.

2.3 OFDM Baseband System Model

In OFDM systems, modulation and demodulation are implemented by using IFFT and FFT, respectively as shown in Fig. 2.4. At the transmitter side, after mapping and serial to parallel (S/P) conversion to the information data, IFFT will be performed. Then the

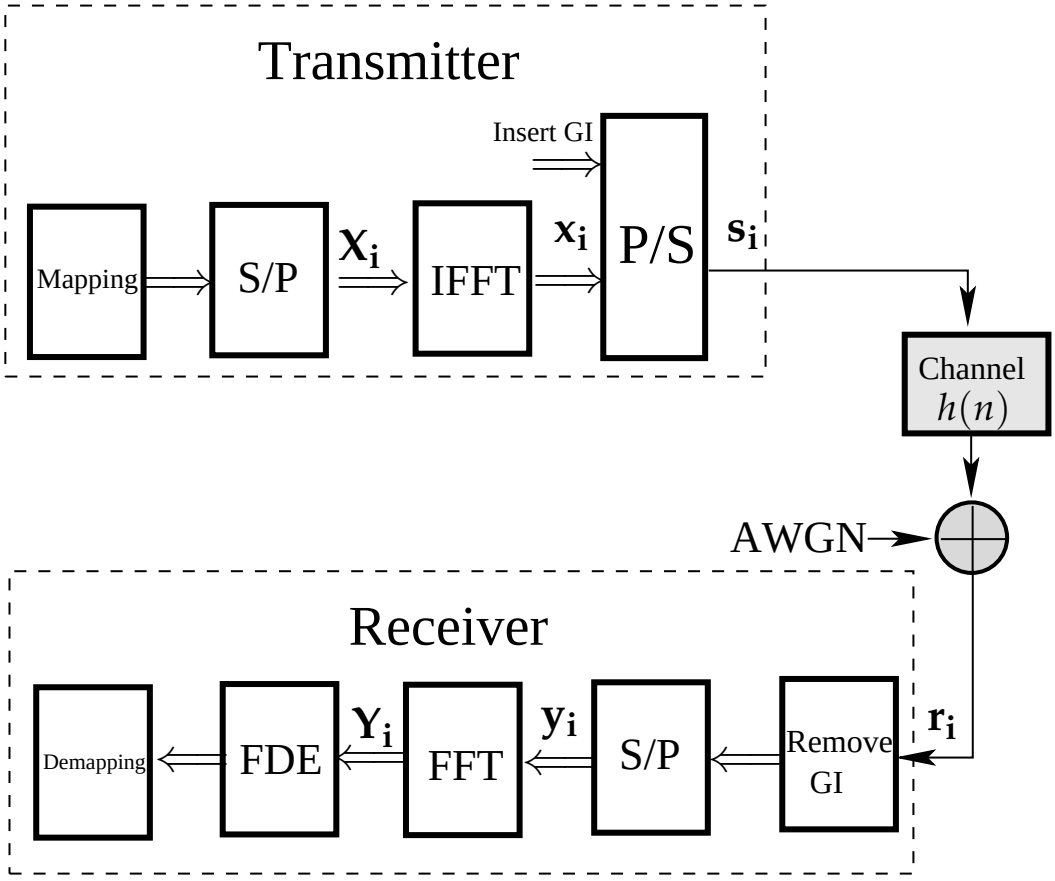

Fig. 2.4. OFDM system model.

*i*th OFDM symbol with N length becomes

$$\mathbf{x}_i = \mathbf{F}^{\mathcal{H}}\mathbf{X}_i, \tag{2.2}$$

where, $\mathbf{x}_i = [x_0,\ x_1, \ldots, x_{N-1}]^T$ and $\mathbf{X}_i = [X_0,\ X_1, \ldots, X_{N-1}]^T$ correspond to the OFDM symbols in time and frequency domains respectively, and $\mathbf{F}^{\mathcal{H}}$ is an IFFT matrix as follows

$$\mathbf{F}^{\mathcal{H}} = \frac{1}{\sqrt{N}} \begin{bmatrix} 1 & 1 & \ldots & 1 \\ 1 & e^{j\frac{2\pi}{N}} & \ldots & e^{j\frac{2\pi(N-1)}{N}} \\ \vdots & \vdots & \ddots & \vdots \\ 1 & e^{j\frac{2\pi(N-1)}{N}} & \ldots & e^{j\frac{2\pi(N-1)(N-1)}{N}} \end{bmatrix}. \tag{2.3}$$

Then, after GI insertion and parallel to serial (P/S) conversion, the OFDM signal is ready for transmitting. We assume that the signal pass through the channel, also the channel length L is less than GI length, and additive white Gaussian noise (AWGN) is added to the received signal. Based on this assumption, after GI removal and S/P conversion, we can obtain the ith received symbol $\mathbf{y}_i$ as follows

$$\mathbf{y}_i = \mathbf{h}\mathbf{s}_i + \mathbf{z}_i, \tag{2.4}$$

where, $\mathbf{z}_i$ is an AWGN vector corresponding to the ith symbol,

$$\mathbf{s}_i = \begin{bmatrix} x_{N-L} \\ \vdots \\ x_{N-1} \\ x_0 \\ \vdots \\ x_{N-1} \end{bmatrix}, \tag{2.5}$$

and the channel matrix $\mathbf{h}$ is an $N \times (N+L-1)$ Toeplitz-like matrix

$$\mathbf{h} = \begin{bmatrix} h_{L-1} & \dots & h_0 & 0 & \dots & \dots & 0 \\ 0 & \ddots & & \ddots & \ddots & & \vdots \\ \vdots & \ddots & h_{L-1} & \dots & h_0 & \ddots & \vdots \\ \vdots & & \ddots & \ddots & & \ddots & 0 \\ 0 & \dots & & 0 & h_{L-1} & \dots & h_0 \end{bmatrix}. \tag{2.6}$$

Then, Eq.(2.4) can be rewritten as

$$\mathbf{y}_i = \mathbf{h}_{cycl}\mathbf{x}_i + \mathbf{z}_i, \tag{2.7}$$

where, $\mathbf{h}_{cyc}$ is a cyclic channel matrix as follows

$$\mathbf{h}_{cycl} = \begin{bmatrix} h_0 & 0 & \dots & h_{L-1} & \dots & h_0 \\ \vdots & \ddots & & & \ddots & \vdots \\ h_{L-2} & \dots & h_0 & & & h_{L-1} \\ h_{L-1} & h_{L-2} & \dots & h_0 & & \vdots \\ 0 & h_{L-1} & h_{L-2} & \dots & h_0 & \vdots \\ 0 & \dots & h_{L-1} & h_{L-2} & \dots & h_0 \end{bmatrix}. \tag{2.8}$$

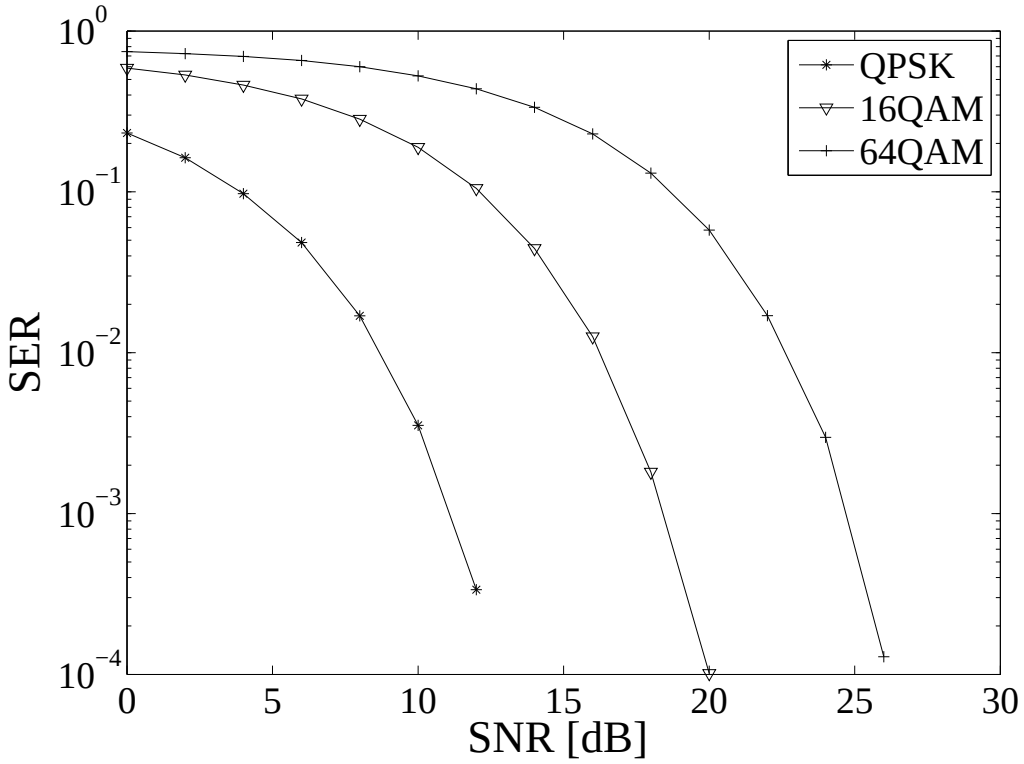

Fig. 2.5. BER versus SNR

After performing FFT to the received symbol in Eq.(2.7), we have

$$\begin{aligned} \mathbf{Y}_i &= \mathbf{F}\mathbf{h}_{cycl}\mathbf{x}_i + \mathbf{F}\mathbf{z}_i \\ &= \mathbf{F}\mathbf{h}_{cycl}\mathbf{F}^{\mathcal{H}}\mathbf{X}_i + \mathbf{Z}_i, \end{aligned} \tag{2.9}$$

where, $\mathbf{Z}_i$ denotes an AWGN vector in frequency domain, and $\mathbf{F}$ is FFT matrix as follows

$$\mathbf{F} = \frac{1}{\sqrt{N}} \begin{bmatrix} 1 & 1 & \dots & 1 \\ 1 & e^{-j\frac{2\pi}{N}} & \dots & e^{-j\frac{2\pi(N-1)}{N}} \\ \vdots & \vdots & \ddots & \vdots \\ 1 & e^{-j\frac{2\pi(N-1)}{N}} & \dots & e^{-j\frac{2\pi(N-1)(N-1)}{N}} \end{bmatrix}. \tag{2.10}$$

Since $\mathbf{F}\mathbf{h}_{cycl}\mathbf{F}^{\mathcal{H}}$ becomes diagonal matrix, from Eq.(2.9), we have

$$\mathbf{Y}_i = \mathbf{H}_{diag}\mathbf{X}_i + \mathbf{Z}_i. \tag{2.11}$$

Finally, the information can be recovered easily, by using frequency domain equalization (FDE) as follows

$$\hat{\mathbf{X}}_i = \mathbf{H}_{diag}^{-1}\mathbf{Y}_i. \tag{2.12}$$

Figure.2.5 shows the results of bit error rate (BER) versus signal to noise ratio (SNR) to QPSK, 16QAM, and 64QAM respectively. We can see that the BER performance becomes worse with the increasing order of constellation.

2.4 ISI IN OFDM SYSTEMS WITHOUT GI

In this section, let us consider the effect of ISI in OFDM systems without GI. After passing through the channel, the ith received OFDM symbol without guard interval can be expressed as follows

$$\mathbf{r}_i = \dot{\mathbf{h}} \cdot \mathbf{s}_{i-1,i} + \mathbf{z}_i, \tag{2.13}$$

where, $\mathbf{s}_{i-1,i} = \begin{bmatrix} \mathbf{s}_{i-1} \\ \mathbf{s}_i \end{bmatrix}$ is a $2N \times 1$ vector consist of two consecutive transmitted symbols and $\mathbf{s}_i = [s_i^0,\ s_i^1,\ \dots,\ s_i^{N-1}]^T$ is an $N \times 1$ vector corresponding to ith symbol, and $\dot{\mathbf{h}} = [\mathbf{h_t}\ \ \mathbf{h_x}]$, where

$$\mathbf{h_x} = \begin{bmatrix} h_0 & 0 & \dots & \dots & \dots & 0 \\ \vdots & \ddots & \ddots & & & \vdots \\ h_{L-1} & \dots & h_0 & \ddots & & \vdots \\ 0 & h_{L-1} & \dots & h_0 & \ddots & \vdots \\ \vdots & \ddots & \ddots & & \ddots & 0 \\ 0 & \dots & 0 & h_{L-1} & \dots & h_0 \end{bmatrix}, \tag{2.14}$$

$$\mathbf{h_t} = \begin{bmatrix} 0 & \dots & 0 & h_{L-1} & \dots & h_1 \\ \vdots & \ddots & & \ddots & \ddots & \vdots \\ \vdots & & \ddots & & \ddots & h_{L-1} \\ \vdots & & & \ddots & & 0 \\ \vdots & & & & \ddots & \vdots \\ 0 & \dots & \dots & \dots & \dots & 0 \end{bmatrix}. \tag{2.15}$$

Obviously, these two matrices satisfy

$$\mathbf{h_x} + \mathbf{h_t} = \mathbf{h}_{cycl}, \tag{2.16}$$

where $\mathbf{h}_{cycl}$ is the "ideal" channel matrix, i.e., the matrix that results in a cyclic convolution between the transmitted signal and the channel. Then, we have

$$\mathbf{r}_i \;=\; \mathbf{h_x} \cdot \mathbf{s}_i + \mathbf{h_t} \cdot \mathbf{s}_{i-1} + \mathbf{z}_i. \tag{2.17}$$

we can rewrite

$$\mathbf{r}_i = \mathbf{h}_{cycl} \cdot \mathbf{s}_i - \mathbf{h_t} \cdot \mathbf{s}_i + \mathbf{h_t} \cdot \mathbf{s}_{i-1} + \mathbf{z}_i, \tag{2.18}$$

where, $\mathbf{h}_{cycl} \cdot \mathbf{s}_i$, $\mathbf{h_t} \cdot \mathbf{s}_i$ and $\mathbf{h_t} \cdot \mathbf{s}_{i-1}$ represent the desired, ICI and ISI components respectively. From Eq.(2.18), we can see that the desired signal is effected by ISI and ICI. This will result in severe performance degredation.

2.5 DCR ARCHITECTURE

As indicated in introduction, the receivers can be classified to the superheterodyne receiver and direct-conversion receiver (DCR). To better understand DCR architecture and

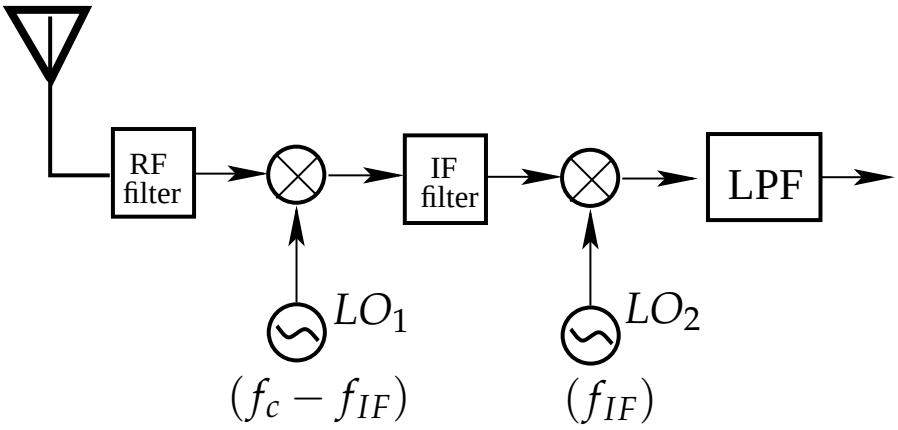

Fig. 2.6. Superheterodyne receiver.

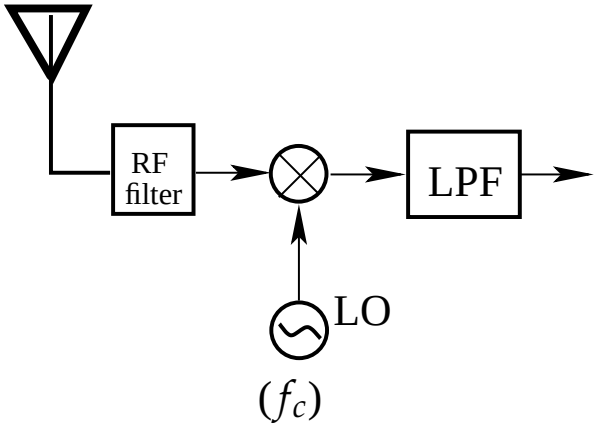

Fig. 2.7. Direct-conversion receiver.

make clear the difference between DCR and superheterodyne receiver, we give simple diagrams of superheterodyne receiver and DCR respectively in Figs.2.6 and 2.7. As shown in Fig.2.6, superheterodyne receiver filters the received radio frequency (RF) signal with carrier frequency f_c and converts it to a lower intermediate frequency (IF) f_{IF} by mixing with an offset local-oscillator LO_1 with frequency $f_c - f_{IF}$. Then, the resulting IF signal is converted again by LO_2 at an intermediate frequency f_{IF}, and finally base-band signal is obtained by using low pass filter (LPF). However, the signal amplification requires IF filters to be biased with large currents, causing substantial power dissipation. Furthermore, these filters need many off-chip passive components, adding to receiver size and cost.

The process of frequency translation to zero IF is called direct-conversion and is illustrated in Fig.2.7. Since IF is zero, the desired signal is translated directly to the baseband. Therefore, the direct-conversion receiver (DCR) architecture relaxes the selectivity requirements of RF filters and removes all IF analog components, thus a small-size, low-cost and low-power can be achieved. Due to these merits, DCR is an attractive receiver for wireless communication.

2.6 Impairments Caused by DCR

Although DCR has many considerable merits, it leads to additional analog impairments such as CFO, DCO, and I/Q imbalance, which causes severe performance degradation of the system. In this section we will discuss these impairments in detail.

2.6.1 CFO Caused by DCR

CFO is mainly caused by the frequency mismatch between transmitter and receiver local oscillators (LO's) as shown in Fig.2.9, where f_c is carrier frequency, and $\triangle f_c$ is the frequency error. After downconversion, let us see the effect of CFO to the system. For the simpilicity, we just consider one block of OFDM symbols. The total system bandwidth B is divided into N subcarriers, at a spacing of $\Delta f = B/N$. Then, the downconverted received signal with CFO can be expressed as follows (see Appendix A)

$$d(k) = y(k)e^{j\frac{2\pi\varepsilon k}{N}}, \tag{2.19}$$

where, $d(k)$ denotes the kth sample of downconverted signal, $y(k)$ is baseband equivalent signal of received signal $r(k)$, and ε is the CFO normalized to the subcarrier spacing, which equals the actual CFO Δf_c divided by the OFDM subcarrier spacing Δf. As shown in Eq.(2.19), since the received samples are actually affected by the normalized CFO ε, the normalized CFO is often called as CFO in CFO estimation, for the simplicity. Eq.(2.19) can be expressed by matrix form as

$$\mathbf{d} = \mathbf{\Gamma}(\varepsilon)\mathbf{y}, \tag{2.20}$$

where, the matrix $\mathbf{\Gamma}(\varepsilon)$ is corresponding to the CFO as

$$\mathbf{\Gamma}(\varepsilon) = \mathrm{diag}(1, e^{j\frac{2\pi\varepsilon}{N}}, e^{j\frac{4\pi\varepsilon}{N}}, e^{j\frac{6\pi\varepsilon}{N}}, ..., e^{j\frac{2\pi\varepsilon(N-1)}{N}}). \tag{2.21}$$

This can be rewritten as

$$\mathbf{d} = \mathbf{\Gamma}(\varepsilon)\mathbf{F}^{\mathcal{H}}\mathbf{Y}, \tag{2.22}$$

where $\mathbf{Y} = \mathbf{Fy}$. While CFO occurs, since OFDM spectrum will be shifted, the orthogonality between subcarriers should be distroyed. The effect of the CFO is shown in Fig.2.8, where the solid wave and the dashed wave indicate original OFDM spectrum and OFDM spectrum with the effect of CFO, respectively. In this figure, from the observation point at a and b on the solid wave, we can see that subcarriers maintain its orthogonality in original OFDM spectrum. However, from the observation point at a' and b' on the dashed wave, we can see that the orthogonality is distroyed with CFO $\triangle f_c$, since the spectrum is shifted. Therefore, in OFDM systems, CFO compensation is very important.

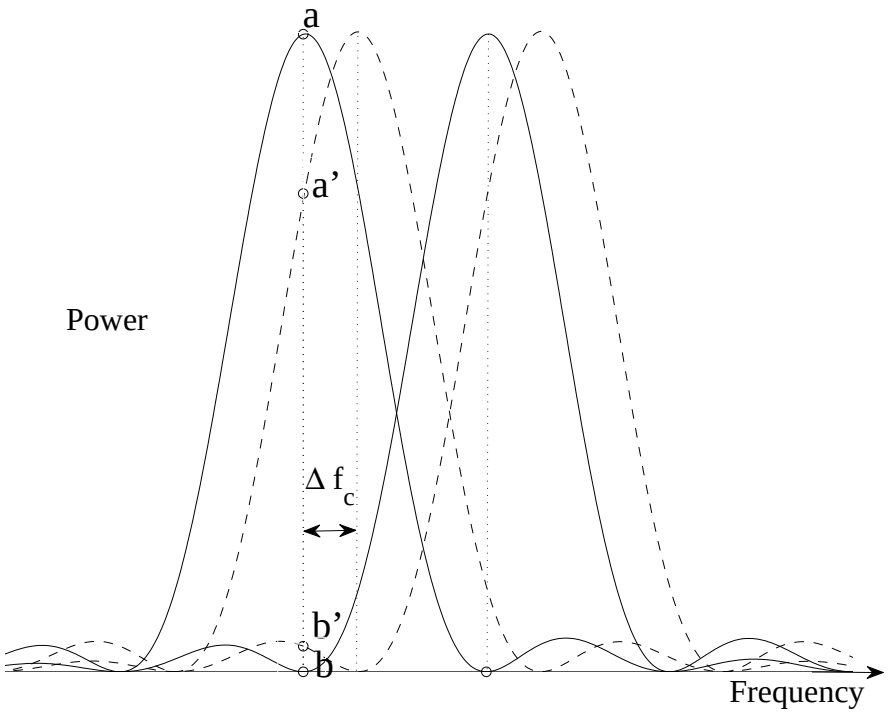

Fig. 2.8. Spectrum shift of OFDM due to CFO

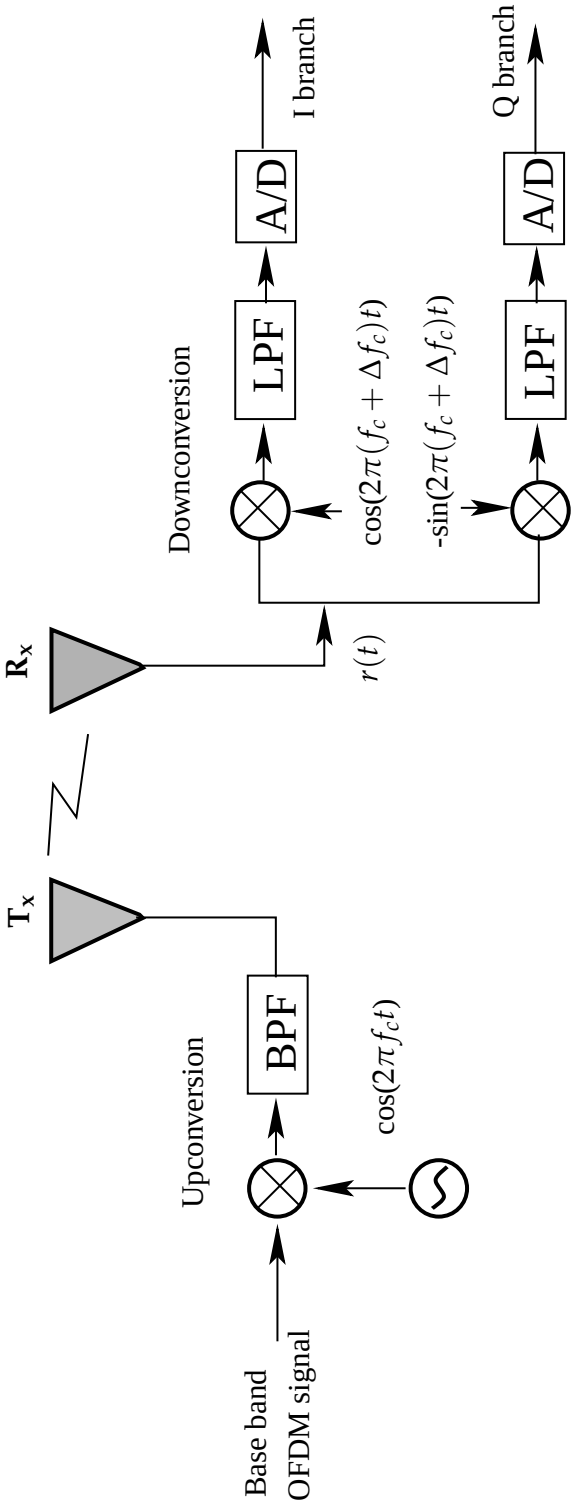

Fig. 2.9. Model of CFO.

2.6.2 I/Q Imbalance Caused by DCR

The I/Q imbalance is caused by the mismatched components between the in-phase (I) and quadrature-phase (Q) branches. Let us assume that the amplitude mismatch is g and phase error is ϕ. Based on this assumption, the mathematical model of I/Q imbalance is shown in Fig.2.10. In the figure, the received signal $r(t)$, which is centered at f_c with bandwidth B, can be written as

$$r(t) = 2\mathrm{Re}[s(t)e^{j2\pi f_c t}] = s(t)e^{j2\pi f_c t} + s^*(t)e^{-j2\pi f_c t}, \tag{2.23}$$

where $s(t) = s_I(t) + s_Q(t)$ is baseband equivalent signal of $r(t)$. The local oscilator signal $x_{LO}(t)$ with I/Q imbalance experessed by

$$x_{LO}(t) = \cos(2\pi f_c t) - jg \cdot \sin(2\pi f_c t + \phi). \tag{2.24}$$

This can be rewritten as follows

$$\begin{aligned} x_{LO}(t) &= \frac{e^{j2\pi f_c t} + e^{-j2\pi f_c t}}{2} - jg \cdot \frac{e^{j(2\pi f_c t+\phi)} - e^{-j(2\pi f_c t+\phi)}}{2} \\ &= C_1 \cdot e^{-j2\pi f_c t} + C_2 \cdot e^{j2\pi f_c t}, \end{aligned} \tag{2.25}$$

where $C_1 = \frac{1+ge^{-j\phi}}{2}$ and $C_2 = \frac{1-ge^{j\phi}}{2}$.

As shown in Fig.2.10, the received signal $r(t)$ is downconverted to baseband by mixing it with LO signal $x_{LO}(t)$. Therefore, the downconverted signal can be written as

$$\begin{aligned} r(t) \cdot x_{LO}(t) &= \{s(t)e^{j2\pi f_c t} + s^*(t)e^{-j2\pi f_c t}\}(C_1 \cdot e^{-j2\pi f_c t} + C_2 \cdot e^{j2\pi f_c t}) \\ &= C_1 s(t) + C_2 s(t)e^{j4\pi f_c t} + C_1 s^*(t)e^{-j4\pi f_c t} + C_2 s^*(t). \end{aligned} \tag{2.26}$$

Then, after passing through the low pass filter (LPF), the high frequency components of $C_2 s(t)e^{j4\pi f_c t}$ and $C_1 s^*(t)e^{-j4\pi f_c t}$ are removed. Then the signal becomes

$$y(t) = \mathrm{LPF}\{r(t)x_{LO}(t)\} = C_1 s(t) + C_2 s^*(t), \tag{2.27}$$

where $y(t) = y_I(t) + y_Q(t)$, $C_1 s(t)$ is desired part, $C_2 s^*(t)$ is undesired part also known as image part, which is caused by I/Q imbalance. In ideal case without I/Q imbalance, the second term $C_2 s^*(t)$ should be zero. From Eq.(2.27), we can see the desired signal is effected by it's image, while I/Q imbalance happens.

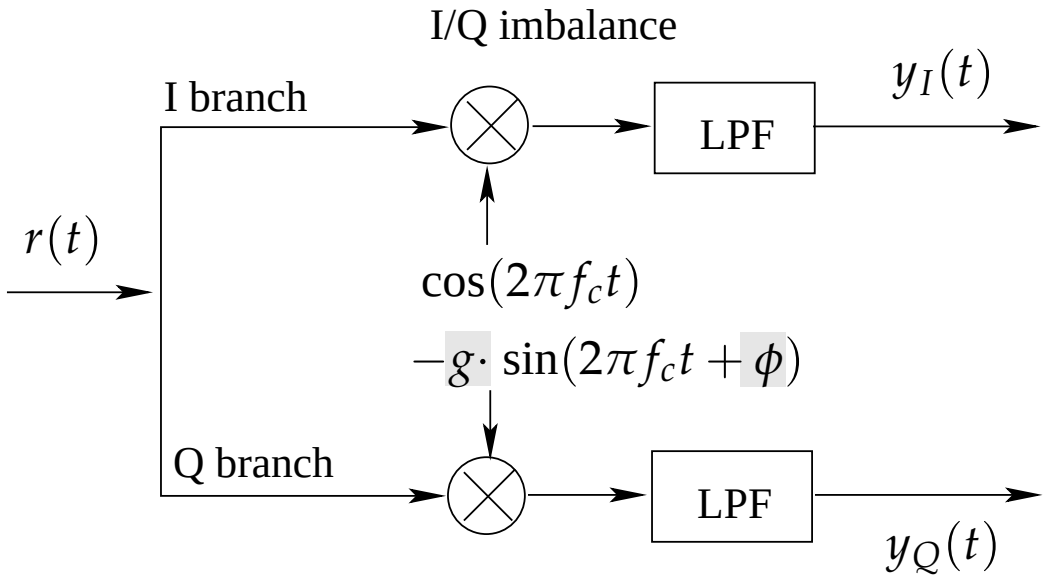

Fig. 2.10. Model of I/Q imbalance.

2.6.3 DC Offset Caused by DCR

DC offset is induced by the self-mixing of leaking LO signal due to the imperfect isolation and is known as the most serious problem [2] of DCR. This offset appears in the middle of the downconverted signal spectrum, and may be larger than the signal itself. While DCO happens, the SNR at the detector input will be very low. The LO signal leaking from the antenna during receive mode may reflect off an external object and self-downconvert to dc in the mixer as shown in Fig. 2.11. Similarly, a large undesired near-channel interferer in the preselect filter passband may leak into the LO port of the mixer and self-downconvert to dc. In order to remove DCO, appropriate circuits is necessary at the receiver. For example, at the I branch in Fig.2.10, let us assume the leaking of LO signal is selfmixed at the mixer, and resuls in DCO. Then it can be expressed as

$$y(t) \quad = cos(2\pi f_c t) \cdot \beta cos(2\pi f_c t) = cos(4\pi f_c t)/2 + \beta/2, \tag{2.28}$$

where β denotes the leaking factor. Then after LPF, the second term $\beta/2$ is left as DCO. In the same way, we can obtain similar result for the Q branch. The spectrum of DCO is shown in Fig.2.12, where we can see that DCO corresponds to zero frequency.

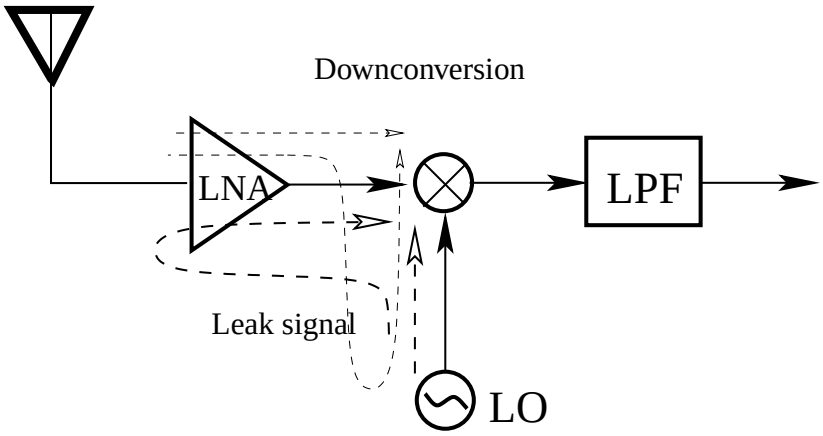

Fig. 2.11. Model of DC offset.

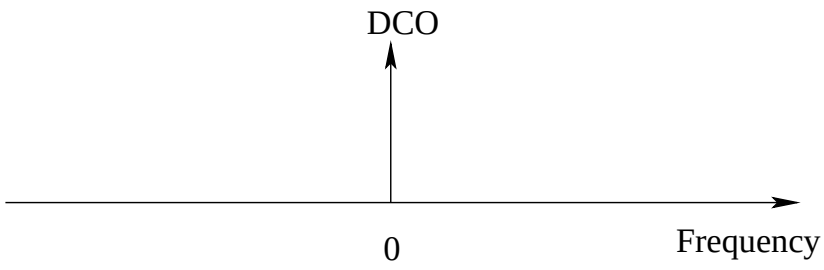

Fig. 2.12. Spectrum of DC offset.

2.7 CONCLUSIONS

In this chapter, we introduced OFDM basis and the analog impairments caused by direct conversion receiver, such as CFO, I/Q imbalance and DCO. Moreover, we analyzed this impairments in detail and expressed by matrix form. In addition, we discussed the ISI problem in OFDM systems without GI, by using matrix form. This will help us to better understand the background knowledge discussed on this thesis.

CHAPTER 3

Robust CFO Estimation in the Presence of TV-DCO

OFDM is known for its sensitivity to CFO, which is mainly caused by frequency mismatch between the transmitter and receiver local oscillators. Since the CFO destroys the orthogonality among subcarriers, the resulting inter-carrier interference (ICI) leads to severe performance degradation [41].

On the other hand, DCR has attracted a lot of attention in recent years, for its smaller size and lower cost over the traditional superheterodyne receivers. However, the price is the additional disturbances, such as DCO, I/Q imbalance, even-order distortion and flicker noise [4]. Among these, DCO, induced by the self-mixing associated with the unperfect isolation, is known as the most serious problem [2]. Obviously, the coexistence of the CFO and DCO is a critical problem in an OFDM DCR.

In the absence of DCO, the CFO can be estimated easily from the autocorrelation of periodic pilot (PP) [14, 26, 30, 40]. Considering DCO, several joint compensation schemes have been proposed in [7, 12, 15, 37], where DCO is assumed time-invariant. In practice, automatic gain control (AGC) is usually used to keep the received signal amplitude proper fixed level. Also, a high pass filter (HPF) is often employed in the DCR to reduce DCO [47]. Therefore, the gain shift in the low noise amplifier (LNA) will cause a TV-DCO [38], whose high frequency components may pass through the HPF. As a result, the ordinary CFO estimation in [7, 12, 15, 37] will be corrupted by the residual TV-DCO. Until now, there is only one CFO estimator taking the residual TV-DCO into account [25]. In this scheme, a differential filter is used to eliminate the residual TV-DCO, and then the CFO is estimated by the conventional autocorrelation-

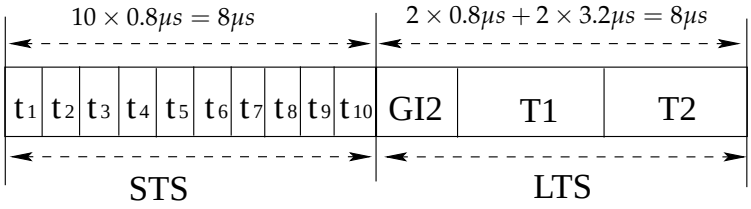

Fig. 3.1. IEEE 802.11a preamble.

based method. Since the differential filter increases the noise variance and the residual TV-DCO cannot be eliminated completely, this method will cause performance loss.

The purpose of this chapter is to develop a novel CFO estimation method in the presence of TV-DCO. As indicated in [25], the residual DCO at the output of the HPF has a linear property. Therefore, it can be approximated by a linear function. On the other hand, it has been shown in [15] that the CFO can be estimated independent of the time-invariant DCO, by exploring the periodicity of the pilot. Motivated by [15] and based on the linear property of the TV-DCO, we propose a PP-aided CFO estimator, which is able to remove the effect of TV-DCO during the CFO estimation process. After the CFO estimation, the residual TV-DCO can be obtained accordingly. Simulations confirm the effectiveness and superiority of the proposed estimator.

3.1 PROBLEM FORMULATION

The pilot used for the joint estimation is the preamble of the IEEE 802.11a [1] shown in Fig.3.1. This preamble has a short training sequence (STS) and a long training sequence (LTS). The STS consists of ten identical K-samples repeated symbols $t_1, \cdots, t_{10}$, and LTS consist of two identical N-samples repeated symbols T_1 and T_2, where $N = 64$ and $K = 16$. Every four repeated symbols of the STS can be treated as an N-subcarriers OFDM symbol, which has only 12 equally-spaced subcarriers loaded, see the generation of the STS in [1]. When the channel is time-invariant during the preamble and the channel length is less than K, the received STS keeps its periodicity after discarding the first symbol. This can be understood that the pattern of the loaded subcarrier in the received STS still is equally-spaced. We can partition IFFT matrix $\mathbf{F}^{\mathcal{H}}$ into two matrices $\mathbf{W}$ and $\mathbf{V}$, corresponding to the loaded and unloaded subcarriers, respectively.

Figure 3.2 shows the mathematical model of the system, where $s(n)$ denotes the nth

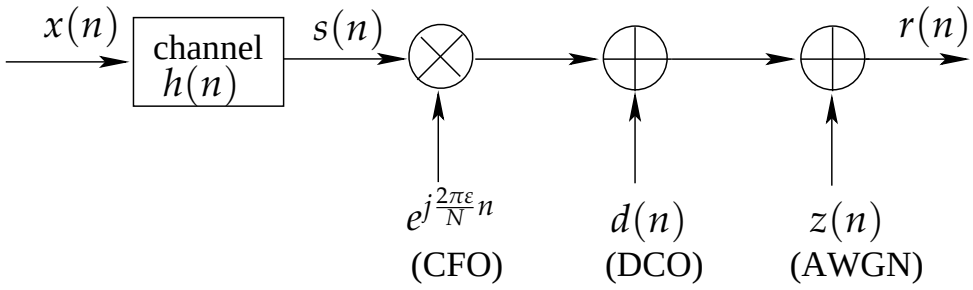

Fig. 3.2. Mathematical model.

sample of the preamble after passing through the channel, ε is the CFO normalized to subcarrier spacing, $d(n)$ and $z(n)$ are the possible DCO and additive white Gaussian noise (AWGN), respectively.

In the absence of DCO, the received sample $r_s(n)$ corresponding to the STS can be written as

$$r_s(n) = s_s(n)e^{j\frac{2\pi\varepsilon}{N}n} + z(n). \tag{3.1}$$

As mentioned above, we have $s_s(n) = s_s(n+K)$ for $K \leq n < 9K$. Then the normalized CFO can be estimated by taking the autocorrelation of the STS as

$$\hat{\varepsilon} = \frac{4}{2\pi}\arg\{\sum_{m=2}^{8}\sum_{k=0}^{K-1} r_s^*(k+mK)r_s(k+(m+1)K)\}, \tag{3.2}$$

where m is the index of the repeated symbols in the STS.

In the presence of a time-invariant DCO d, the received signal becomes

$$r_s(n) = s_s(n)e^{j\frac{2\pi\varepsilon}{N}n} + d + z(n). \tag{3.3}$$

In [7], it is known that the CFO estimation in Eq.(3.2) is biased. Hence, several PP-based joint estimation scheme have been proposed in [7, 12, 15, 37].

3.2 Conventional Method

In practice, in order to keep the proper fixed level of the received signal, AGC circuits are usually employed [38]. In 802.11a WLAN systems, at the middle of STS, the AGC starts to adjust the gain of the received signal, which also changes the gain of DCO.

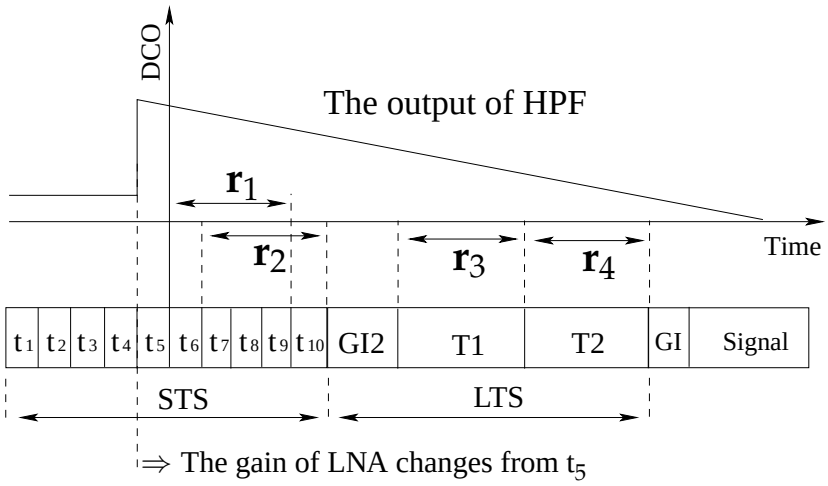

Fig. 3.3. Model of the residual TV-DCO.

On the other hand, a HPF is often used to eliminate DCO [47]. When DCO is time-invariant, a HPF is sufficient to remove the effect of DCO, then enables the CFO estimation in Eq.(3.2). However, the higher frequency components of the AGC-induced TV-DCO may pass through the HPF. In consequence, the CFO estimation will suffer from the residual TV-DCO. In [25], it has been shown that the residual DCO varies in a linear fashion, see the example given in Fig.3.3, where the LNA switches at the beginning of t_5. Then, the authors propose to use a differential filter to counteract the impact of the residual TV-DCO.

At the coarse CFO estimation stage, the STS is used, whose nth sample can be written as

$$r_s(n) = s_s(n)e^{j\frac{2\pi n\varepsilon}{N}} + d(n) + z(n), \tag{3.4}$$

where $d(n)$ denotes the residual TV-DCO. The received STS is passed through a differential filter, and the nth sample of the differential filter's output is given by:

$$\begin{aligned} r_{sd}(n) &= r_s(n) - r_s(n-1) \\ &= s_{sd}(n)e^{j\frac{2\pi n\varepsilon}{N}} + d_{sd}(n) + z_{sd}(n), \end{aligned} \tag{3.5}$$

where

$$\begin{aligned} s_{sd}(n) &= s_s(n) - e^{-j\frac{2\pi\varepsilon}{N}}s_s(n-1), \\ d_{sd}(n) &= d(n) - d(n-1), \\ z_{sd}(n) &= z(n) - z(n-1). \end{aligned}$$

As $s_s(n)$ is a PP with a period of K, so does $s_{sd}(n)$. Then the normalized CFO value $\hat{\varepsilon}_1$ is estimated by replacing $r_s(n)$ with $r_{sd}(n)$ in Eq.(3.2).

At the fine CFO estimation stage, the obtained $\hat{\varepsilon}_1$ is used to compensate the CFO in the LTS, which is also passed through the differential filter. Let $r_{ld}(n)$ denote the nth sample of the LTS after the differential filter and coarse CFO compensation. Since the LTS is a PP with a period of N, the residual normalized CFO is calculated by

$$\hat{\varepsilon}_2 = \frac{1}{2\pi}\arg\{\sum_{n=0}^{N-1} r_{ld}^*(n) r_{ld}(n+N)\}. \tag{3.6}$$

Finally, the CFO estimate is given by $\hat{\varepsilon} = \hat{\varepsilon}_1 + \hat{\varepsilon}_2$.

3.3 Proposed Method

Compared Eq.(3.4) with Eq.(3.5), it is clear that the above mentioned CFO estimation still is biased by $d_{sd}(n)$. Moreover, the noise variance is doubled, which also leads to performance loss. Here, by extending the method in [15], we will derive a novel CFO estimator, which can remove the effect of the TV-DCO completely. Similar to [25], we assume the LNA is switched at the beginning of t_5.

At the coarse estimation stage, without loss of generality, we can form two $N \times 1$ vectors $\mathbf{r}_1$ and $\mathbf{r}_2$ from the received STS symbols $t_6, t_7, \cdots, t_{10}$, which are at a distance of K shown in Fig.3.3. Note that $\mathbf{r}_1$ and $\mathbf{r}_2$ are the symbols corresponding to the sampling range of $t_6 - t_9$ and $t_7 - t_{10}$, respectively. Since the TV-DCO is approximated by a linear function $ax + b$, a denotes the ratio of variation, while b stands for the constant component. Then, $\mathbf{r}_1$ and $\mathbf{r}_2$ can be expressed as

$$\begin{aligned}
\mathbf{r}_1 &= \mathbf{\Gamma}(\varepsilon)\mathbf{S}_s + a\mathbf{x}_1 + b\mathbf{1}_N + \mathbf{z}_1, && (3.7)\\
\mathbf{r}_2 &= e^{j\frac{2\pi K\varepsilon}{N}}\mathbf{\Gamma}(\varepsilon)\mathbf{S}_s + a\mathbf{x}_2 + b\mathbf{1}_N + \mathbf{z}_2, && (3.8)\\
\mathbf{x}_1 &= [0,\ 1,\ \cdots,\ N-1]^T, && (3.9)\\
\mathbf{x}_2 &= [K, K+1, \cdots, K+N-1]^T, && (3.10)
\end{aligned}$$

where

$$\begin{aligned}
\mathbf{\Gamma}(\varepsilon) &= \mathrm{diag}(1, e^{j\frac{2\pi\varepsilon}{N}}, \ldots, e^{j\frac{2\pi\varepsilon(N-1)}{N}}), && (3.11)\\
\mathbf{S}_s &= [\mathbf{s}^T, \mathbf{s}^T, \mathbf{s}^T, \mathbf{s}^T]^T, && (3.12)
\end{aligned}$$

and $\mathbf{s} = [s_s(0), s_s(1), \cdots, s_s(K-1)]^T$ is a distortion free STS symbol, $\mathbf{z}_n$ is an AWGN vector. Meanwhile, the initial phase offset of the CFO is incorporated into the channel.

Then, in the absence of AWGN, we should have

$$e^{j\frac{2\pi K\varepsilon}{N}}(\mathbf{r}_1 - a\mathbf{x}_1 - b\mathbf{1}_N) = \mathbf{r}_2 - a\mathbf{x}_2 - b\mathbf{1}_N. \tag{3.13}$$

Thus, the CFO and DCO can be estimated as

$$(\hat{\varepsilon}, \hat{a}, \hat{b}) = \underset{\tilde{\varepsilon},\tilde{a},\tilde{b}}{\operatorname{argmin}} \parallel \mathbf{r}_2 - e^{j\frac{2\pi K\tilde{\varepsilon}}{N}}\mathbf{r}_1 - \tilde{a}(\mathbf{x}_2 - e^{j\frac{2\pi K\tilde{\varepsilon}}{N}}\mathbf{x}_1) - \tilde{b}(1 - e^{j\frac{2\pi K\tilde{\varepsilon}}{N}})\mathbf{1}_N \parallel^2 . \tag{3.14}$$

This equation indicates a least squares problem for three unknown scalar. The optimal solution is given by

$$\begin{bmatrix} e^{j\frac{2\pi K\hat{\varepsilon}}{N}} \\ \hat{a}(1 - e^{j\frac{2\pi K\hat{\varepsilon}}{N}}) \\ \hat{b}(1 - e^{j\frac{2\pi K\hat{\varepsilon}}{N}}) + \hat{a}K \end{bmatrix} = [\mathbf{r}_1\ \mathbf{x}_1\ \mathbf{1}_N]^{\dagger}\mathbf{r}_2 = \mathbf{R}. \tag{3.15}$$

The first element of $\mathbf{R}$ is given as

$$R(1) = \frac{1}{G}\mathbf{r}_1^{\mathcal{H}}\mathbf{D}\mathbf{r}_2, \tag{3.16}$$

$$\begin{aligned} \mathbf{D} = \{&\mathbf{x}_1^T\mathbf{x}_1\mathbf{1}_N^T\mathbf{1}_N - \mathbf{x}_1^T\mathbf{1}_N\mathbf{1}_N^T\mathbf{x}_1\}\mathbf{I}_N \\ &+\mathbf{1}_N\mathbf{1}_N^T\mathbf{x}_1\mathbf{x}_1^T - \mathbf{x}_1\mathbf{1}_N^T\mathbf{1}_N\mathbf{x}_1^T \\ &+\mathbf{x}_1\mathbf{x}_1^T\mathbf{1}_N\mathbf{1}_N^T - \mathbf{1}_N\mathbf{x}_1^T\mathbf{x}_1\mathbf{1}_N^T, \end{aligned} \tag{3.17}$$

where $\mathbf{I}_N$ is the $N \times N$ identity matrix, and

$$\begin{aligned} G &= \mathbf{r}_1^{\mathcal{H}}\mathbf{r}_1\mathbf{x}_1^T\mathbf{x}_1\mathbf{1}_N^T\mathbf{1}_N + \mathbf{r}_1^{\mathcal{H}}\mathbf{x}_1\mathbf{x}_1^T\mathbf{1}_N\mathbf{1}_N^T\mathbf{r}_1 \\ &+ \mathbf{x}_1^T\mathbf{r}_1\mathbf{r}_1^{\mathcal{H}}\mathbf{1}_N\mathbf{1}_N^T\mathbf{x}_1 - \mathbf{r}_1^{\mathcal{H}}\mathbf{1}_N\mathbf{1}_N^T\mathbf{r}_1\mathbf{x}_1^T\mathbf{x}_1 \\ &- \mathbf{r}_1^{\mathcal{H}}\mathbf{r}_1\mathbf{x}_1^T\mathbf{1}_N\mathbf{1}_N^T\mathbf{x}_1 - \mathbf{r}_1^{\mathcal{H}}\mathbf{x}_1\mathbf{x}_1^T\mathbf{r}_1\mathbf{1}_N^T\mathbf{1}_N \\ &= \mathbf{r}_1^{\mathcal{H}}\mathbf{D}\mathbf{r}_1. \end{aligned} \tag{3.18}$$

Then we have

$$\begin{aligned} \mathbf{r}_1^{\mathcal{H}}\mathbf{D}\mathbf{r}_2 = &e^{j\phi}\dot{\mathbf{S}}_s^{\mathcal{H}}\mathbf{D}\dot{\mathbf{S}}_s + a\dot{\mathbf{S}}_s^{\mathcal{H}}\mathbf{D}\mathbf{x}_2 + b\dot{\mathbf{S}}_s^{\mathcal{H}}\mathbf{D}\mathbf{1}_N \\ &+ae^{j\phi}\mathbf{x}_1^T\mathbf{D}\dot{\mathbf{S}}_s + a^2\mathbf{x}_1^T\mathbf{D}\mathbf{x}_2 + ab\mathbf{x}_1^T\mathbf{D}\mathbf{1}_N \\ &+be^{j\phi}\mathbf{1}_N^T\mathbf{D}\dot{\mathbf{S}}_s + ab\mathbf{1}_N^T\mathbf{D}\mathbf{x}_2 + b^2\mathbf{1}_N^T\mathbf{D}\mathbf{1}_N + R_z, \end{aligned} \tag{3.19}$$

where

$$\begin{aligned} R_z = &e^{j\phi}\mathbf{z}_1^{\mathcal{H}}\mathbf{D}\dot{\mathbf{S}}_s + a\mathbf{z}_1^{\mathcal{H}}\mathbf{D}\mathbf{x}_2 + b\mathbf{z}_1^{\mathcal{H}}\mathbf{D}\mathbf{1}_N \\ &+\mathbf{z}_1^{\mathcal{H}}\mathbf{D}\mathbf{z}_2 + \dot{\mathbf{S}}_s^{\mathcal{H}}\mathbf{D}\mathbf{z}_2 + a\mathbf{x}_1^T\mathbf{D}\mathbf{z}_2 + b\mathbf{1}_N^T\mathbf{D}\mathbf{z}_2, \end{aligned} \tag{3.20}$$

and $\dot{\mathbf{S}}_s = \mathbf{\Gamma}(\varepsilon)\mathbf{S}_s$, $\phi = \frac{2\pi K\varepsilon}{N}$.

It can be proved that the matrix $\mathbf{D}$ is symmetric, $\mathbf{D}\mathbf{1}_N = \mathbf{0}_N$, $\mathbf{D}\mathbf{x}_1 = \mathbf{0}_N$, and $\mathbf{D}\mathbf{x}_2 = \mathbf{0}_N$ (see Appendix B for the proof), where $\mathbf{0}_N$ is an $N \times 1$ all 0 vector. Then we have

$$R(1) = \frac{1}{G}\mathbf{r}_1^{\mathcal{H}}\mathbf{D}\mathbf{r}_2 = \frac{1}{G}(e^{j\phi}\dot{\mathbf{S}}_s^{\mathcal{H}}\mathbf{D}\dot{\mathbf{S}}_s + \dot{R}_z), \tag{3.21}$$

where

$$\dot{R}_z = e^{j\phi}\mathbf{z}_1^{\mathcal{H}}\mathbf{D}\dot{\mathbf{S}}_s + \mathbf{z}_1^{\mathcal{H}}\mathbf{D}\mathbf{z}_2 + \dot{\mathbf{S}}_s^{\mathcal{H}}\mathbf{D}\mathbf{z}_2. \tag{3.22}$$

Obviously, in $R(1)$, all terms containing DCO parameters a and b are removed. Consequently, we obtain a CFO estimate independent of TV-DCO as

$$\hat{\varepsilon}_1 = \frac{4}{2\pi}\arg\{R(1)\}. \tag{3.23}$$

At the fine estimation stage, $\hat{\varepsilon}_1$ is used to compensate the CFO in the received LTS symbols. Let the vectors $\mathbf{r}_3$ and $\mathbf{r}_4$ express the received two LTS symbols, which can be written as

$$\begin{aligned}
\mathbf{r}_3 &= \mathbf{\Gamma}(\varepsilon)\mathbf{S}_l + a\mathbf{x}_3 + b\mathbf{1}_N + \mathbf{z}_3, && (3.24)\\
\mathbf{r}_4 &= e^{j2\pi\varepsilon}\mathbf{\Gamma}(\varepsilon)\mathbf{S}_l + a\mathbf{x}_4 + b\mathbf{1}_N + \mathbf{z}_4, && (3.25)\\
\mathbf{x}_3 &= \mathbf{x}_1 + Q\mathbf{1}_N, && (3.26)\\
\mathbf{x}_4 &= \mathbf{x}_3 + N\mathbf{1}_N, && (3.27)
\end{aligned}$$

where $\mathbf{S}_l$ is a distortion-free LTS symbol, and Q is the distance between $\mathbf{r}_1$ and $\mathbf{r}_3$. Similarly, the initial phase offset of the CFO is absorbed into the channel. After the CFO compensation, we have

$$\begin{aligned}
\tilde{\mathbf{r}}_3 &= \mathbf{\Gamma}(\hat{\varepsilon}_1)^{\mathcal{H}}\{\mathbf{\Gamma}(\varepsilon)\mathbf{S}_l + a\mathbf{x}_3 + b\mathbf{1}_N + \mathbf{z}_3\}, && (3.28)\\
\tilde{\mathbf{r}}_4 &= e^{-j2\pi\hat{\varepsilon}_1}\mathbf{\Gamma}(\hat{\varepsilon}_1)^{\mathcal{H}}\{e^{j2\pi\varepsilon}\mathbf{\Gamma}(\varepsilon)\mathbf{S}_l + a\mathbf{x}_4 + b\mathbf{1}_N + \mathbf{z}_4\}. && (3.29)
\end{aligned}$$

Using the same approach at coarse estimation stage, we have

$$\begin{bmatrix} e^{j2\pi(\hat{\varepsilon}-\hat{\varepsilon}_1)} \\ ae^{-j2\pi\hat{\varepsilon}_1}(1-e^{j2\pi\hat{\varepsilon}}) \\ e^{-j2\pi\hat{\varepsilon}_1}\{b(1-e^{j2\pi\hat{\varepsilon}})+aN\} \end{bmatrix} = [\tilde{\mathbf{r}}_3\ \tilde{\mathbf{x}}_3\ \tilde{\mathbf{1}}_N]^{\dagger}\tilde{\mathbf{r}}_4,$$

where $\tilde{\mathbf{x}}_3 = \mathbf{\Gamma}(\hat{\varepsilon}_1)^{\mathcal{H}}\mathbf{x}_3$ and $\tilde{\mathbf{1}}_N = \mathbf{\Gamma}(\hat{\varepsilon}_1)^{\mathcal{H}}\mathbf{1}_N$. Hence $\hat{\varepsilon}_2 = \hat{\varepsilon} - \hat{\varepsilon}_1$ can be obtained by

$$\hat{\varepsilon}_2 = \frac{1}{2\pi}\arg\{\tilde{R}(1)\}, \tag{3.30}$$

Table 3.1. Computational complexity

	Proposed	Differential
Subtraction	-	$N+K-1$
Addition	$N \times (N+1)$	N
Multiplication	$N \times (N+1)$	N

where $\tilde{R}(1)$ indicates the first element of the 3×1 vector $[\tilde{\mathbf{r}}_3\ \tilde{\mathbf{x}}_3\ \tilde{\mathbf{1}}_N]^{\dagger}\tilde{\mathbf{r}}_4$. Finally, the fine CFO estimation is given by

$$\hat{\varepsilon} = \hat{\varepsilon}_1 + \hat{\varepsilon}_2. \tag{3.31}$$

On the other hand, the residual TV-DCO can be estimated by using $\hat{\varepsilon}$. For $\hat{\varepsilon} \neq 0$, the parameter a of the residual TV-DCO can be calculated from Eq.(3.15) as

$$\hat{a} = \frac{R(2)}{(1 - e^{j\frac{2\pi K\hat{\varepsilon}}{N}})}. \tag{3.32}$$

Then, using $\hat{\varepsilon}$ and $\hat{a}$, we have

$$\hat{b} = \frac{R(3) - \hat{a}K}{(1 - e^{j\frac{2\pi K\hat{\varepsilon}}{N}})}. \tag{3.33}$$

However, this method cannot work when the $\hat{\varepsilon}$ is close to zero. As mentioned in Section 3.1, since the matrix $\mathbf{V}$ consists of the columns of the IFFT matrix that correspond to the unloaded subcarriers, we know $\mathbf{V}^{\mathcal{H}}\mathbf{S}_s = \mathbf{0}$. In the absence of noise, we have

$$\mathbf{V}^{\mathcal{H}}\mathbf{\Gamma}(\hat{\varepsilon})^{\mathcal{H}}\mathbf{r}_1 = a\mathbf{V}^{\mathcal{H}}\mathbf{\Gamma}(\hat{\varepsilon})^{\mathcal{H}}\mathbf{x}_1 + b\mathbf{V}^{\mathcal{H}}\mathbf{\Gamma}(\hat{\varepsilon})^{\mathcal{H}}\mathbf{1}_N. \tag{3.34}$$

Therefore, using least square method, we can obtain $\hat{a}$ and $\hat{b}$ as

$$\begin{bmatrix} \hat{a} \\ \hat{b} \end{bmatrix} = [\mathbf{A}\ \ \mathbf{B}]^{\dagger}\ \mathbf{V}^{\mathcal{H}}\mathbf{\Gamma}(\hat{\varepsilon})^{\mathcal{H}}\mathbf{r}_1, \tag{3.35}$$

where $\mathbf{A} = \mathbf{V}^{\mathcal{H}}\mathbf{\Gamma}(\hat{\varepsilon})^{\mathcal{H}}\mathbf{x}_1$ and $\mathbf{B} = \mathbf{V}^{\mathcal{H}}\mathbf{\Gamma}(\hat{\varepsilon})^{\mathcal{H}}\mathbf{1}_N$.

The computational complexity of the coarse estimation is shown in Table.3.1. The similar result can be found for the fine estimation. From the comparison result, we can see that the proposed method needs more calculation than the differential filter method.

Table 3.2. Simulation setup

Trial number	10000 times
Modulation scheme	QPSK+OFDM
Number of subcarrier	64
Number of loaded subcarrier	12(STS), 52(LTS)
Channel	Rayleigh fading
HPF	1st order Butterworth
LNA gain	35/15[dB]
Normalized frequency offset	-0.5 $\sim$ 0.5

3.4 SIMULATION RESULTS

We performed simulations to demonstrate the validity of the proposed method. The simulation setup is shown in Table.3.2. The channel is 6-path Rayleigh fading channels. Since the cyclic prefix (CP) exceeds the maximum channel delay spread, there is no inter symbol interference (ISI). To investigate the effect of Doppler shift f_d, f_d = 200Hz which corresponds to about 42km/h mobile speed is also considered. The HPF is the first order Butterworth filter, and the cutoff frequencies f_c =1, 10, 50, and 100kHz are selected. The normalized CFO value ε is set to be a random value in the range of $-0.5 \sim 0.5$. The TV-DCO is generated using the same model of the LNA and the mixer as [25], where the gain of LNA changes between 15 and 35dB, the isolation between LO and LNA input is assumed to be -60dB, and the received signal power is set to be -53dBm.

The CFO and DCO estimation results are evaluated in terms of mean square error (MSE). The acronyms DMC, DMF, LMC and LMF denote the differential method coarse and fine estimation, and least square method coarse and fine estimation, respectively. Figures 3.4(a) and (b) show the CFO estimation results, where the cutoff frequency of HPF is f_c =10kHz. From these results, it can be observed that whatever the Doppler shift exists or not, not only the coarse estimation but also the fine estimation of proposed method are better than the existing differential filter method. By comparing (a) and (b) in Fig.3.4, we observed the CFO estimation results have no obvious difference. Figure 3.5 shows TV-DCO MSE versus SNR result for f_c =10kHz and f_d = 200Hz, which

is obtained using the observed TV-DCO and the approximated TV-DCO based on the estimate of a and b. From Fig. 3.5, it can be seen the estimation is performed accurately. Figures 3.6(a), (b) and (c) show the simulation results for different cutoff frequencies f_c =1, 50, and 100kHz respectively. From these figures, we can find that the proposed estimator performs quite accurately in all of these cases. Then, the similar result can be observed for various cutoff frequencies. Figure 3.7 shows CFO MSE versus variant ε, we can see the proposed method is almost independent of frequency offset. Finally, the BER curve is plotted in Fig.3.8 to show the validity of the proposed method.

3.5 CONCLUSIONS

Orthogonality among subcarriers is the fundamental of OFDM systems. While CFO occurs, the spectrum of the received signal will be shifted. This will destroy the required orthogonality and result in severe performance degradation. On the other hand, although DCR is very attractive by its small-size, low-cost, and low-power consumption, it introduces additional analog impairment DCO. More seriously, in practice, automatic gain control (AGC) results in TV-DCO. Therefore, in OFDM-DCR, the estimation/compensation of CFO in the presence of TV-DCO is very crucial.

In this chapter, a novel CFO estimation scheme in the presence of TV-DCO have been proposed. It is shown the residual DCO after high-pass filtering varies in a linear fashion. Based on this observation, we have modeled the residual DCO using a linear function. Then, from the periodicity of the training sequence, we derived a CFO estimator independent of TV-DCO. Also, the residual TV-DCO was estimated using the obtained CFO. Simulations has been performed to show the effectiveness of the proposed method. In the simulation, we have confirmed whatever the Doppler shift exists or not, not only the coarse estimation but also the fine estimation of proposed method are better than the existing differential filter method. Meantime, it has been shown that the proposed CFO estimator is almost independent of frequency offset. Then, TV-DCO estimation result have shown the estimation performed quite accurately. Finally, after compensating CFO and TV-DCO, BER curve has been plotted, where it has been shown the proposed method performs better than conventional method.

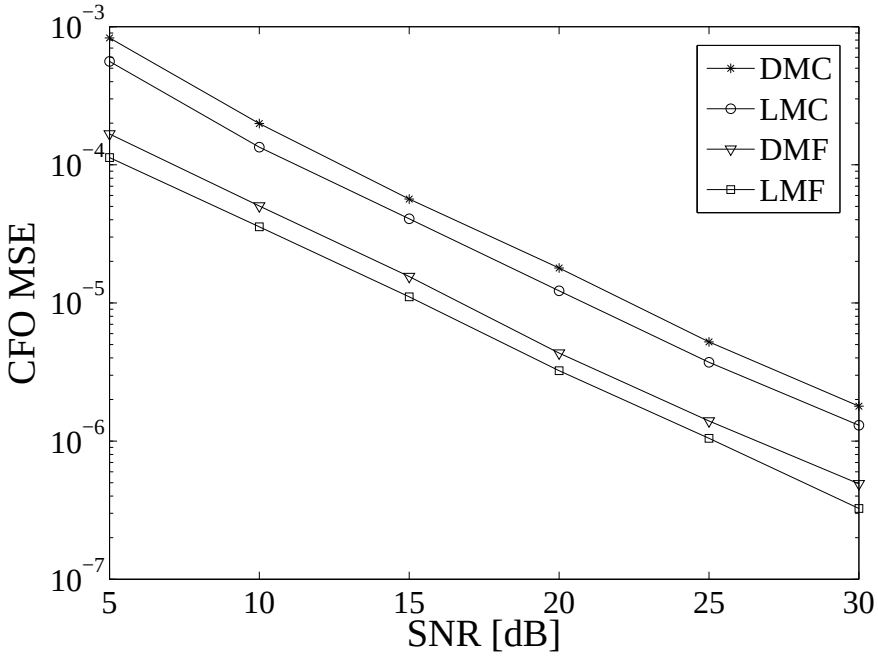

(a) f_d =0Hz

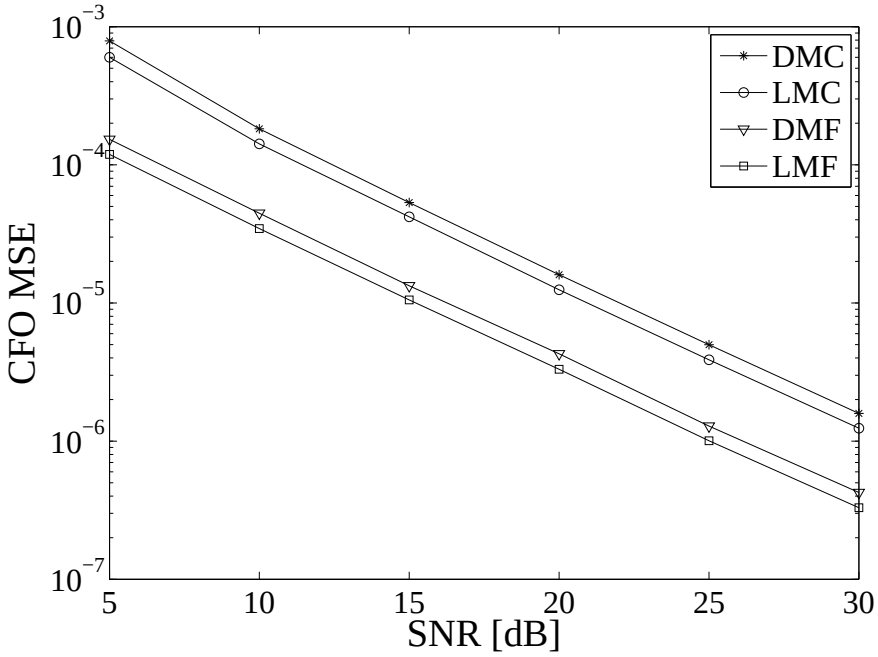

(b) f_d =200Hz

Fig. 3.4. CFO MSE to various f_d, f_c =10kHz

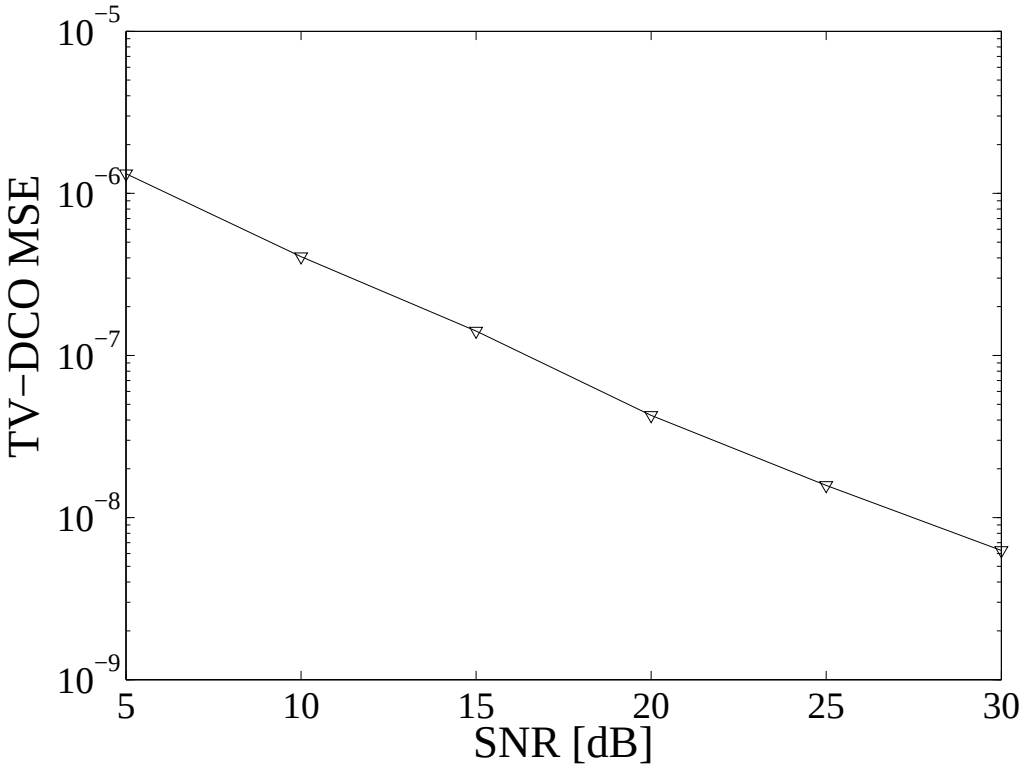

Fig. 3.5. TV-DCO MSE versus SNR, f_c =10kHz, f_d =200Hz

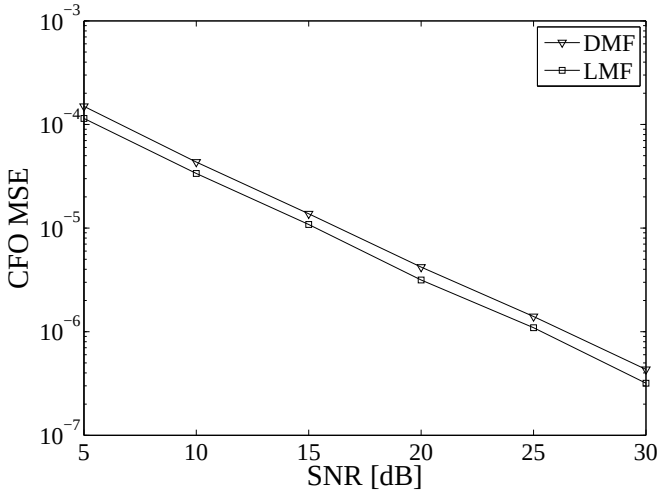

(a) $f_c = 1$kHz

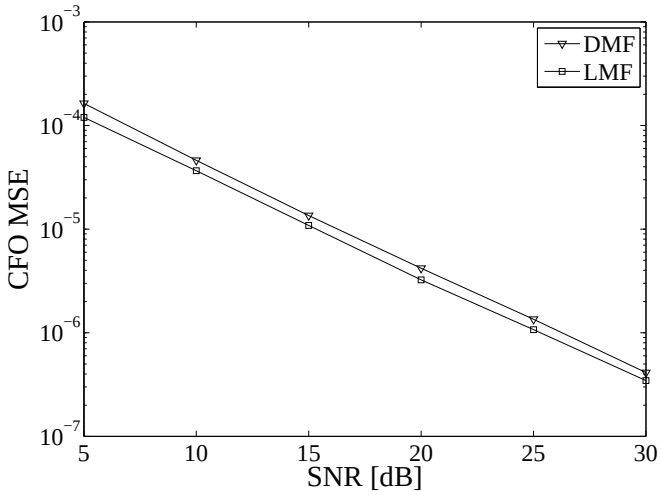

(b) $f_c = 50$kHz

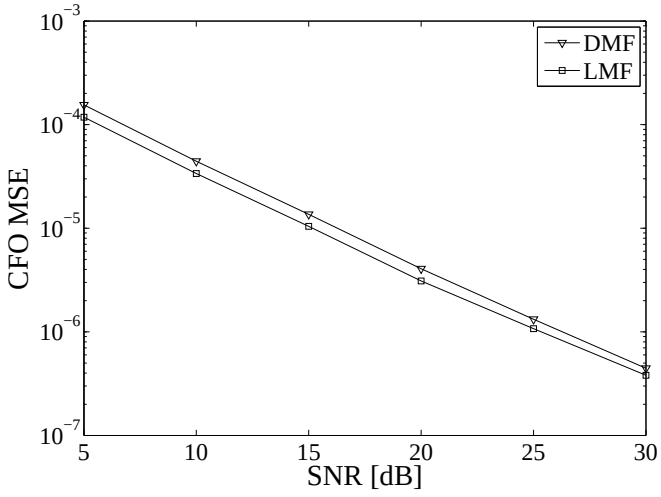

(c) $f_c = 100$kHz

Fig. 3.6. CFO MSE to various f_c, f_d =200Hz

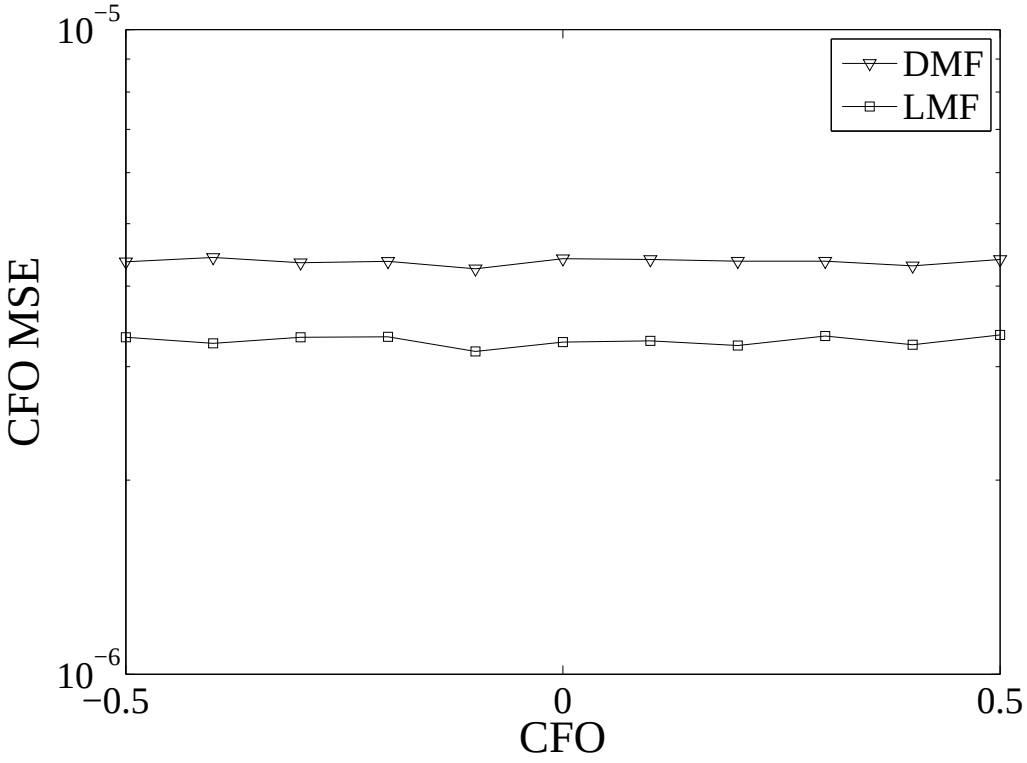

Fig. 3.7. CFO MSE versus ε,f_c =100kHz,f_d =200Hz,SNR=20dB

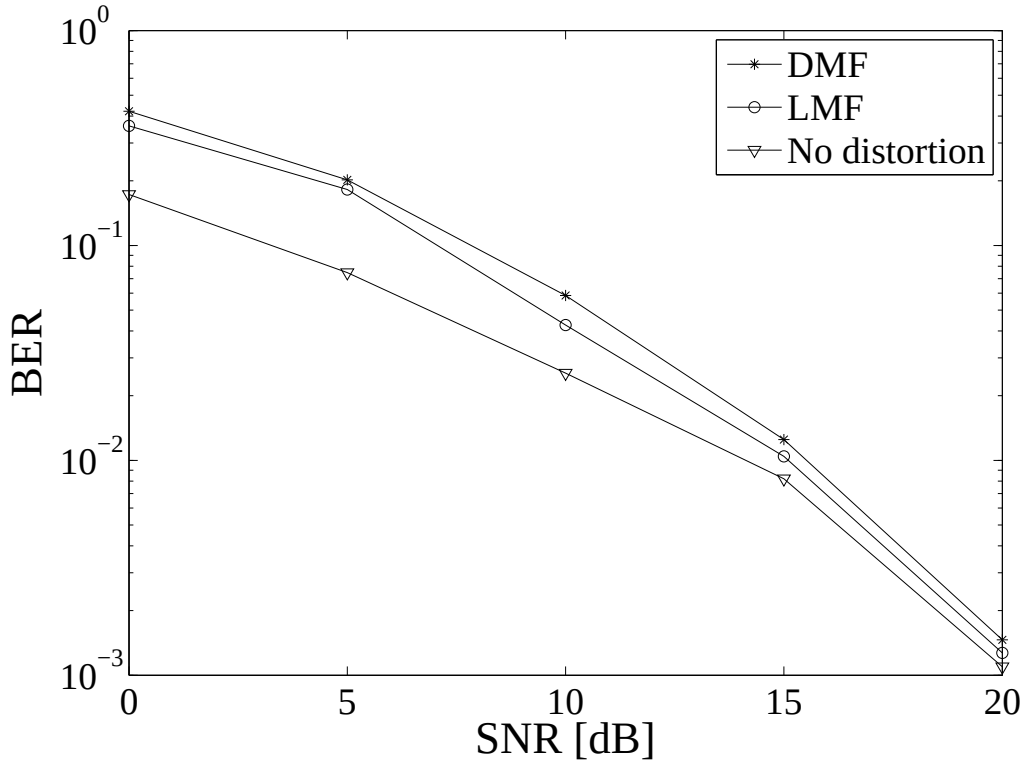

Fig. 3.8. BER versus SNR, f_c =100kHz, f_d =200Hz

CHAPTER 4

Joint Estimation of CFO and I/Q Imbalance in the Presence of TV-DCO

ORTHOGONALITY among subcarriers is the fundamental of OFDM systems. As mentioned before, CFO destroys the required orthogonality and results in severe performance degradation. On the other hand, although DCR is very attractive, it leads to additional impairments, such as I/Q imbalance and DC offset [4]. In a DCR, the I/Q imbalance is basically caused by the mismatched components between the in-phase (I) and quadrature-phase (Q) branches, while the DCO is induced by the self-mixing of leaking LO signal due to the imperfect isolation. Obviously, how to estimate and compensate the CFO, I/Q imbalance and DCO is an inevitable problem in the design of an OFDM DCR.

Traditionally, autocorrelation of periodic pilot is used to estimate the CFO in OFDM systems [14, 26, 30, 40]. The CFO estimators in the presence of DCO and of I/Q imbalance in OFDM DCRs have been proposed in [7, 12, 15, 37] and [9, 11, 19, 35, 36], respectively. Also, the joint estimation of CFO, I/Q imbalance and DCO can be found in [12]. However, all of these works treated the DCO as time-invariant. As mentioned in Chapter 3, in practice, AGC will cause a time-varying DCO (TV-DCO) [38], In the literature, only a few papers [24, 25] studied the effect of TV-DCO. To the best of our knowledge, until now, only [24] considered the scenario of the coexistence of CFO, I/Q imbalance, and TV-DCO. The idea in [24] is to employ a differential filter to ease the effect of the TV-DCO, and then estimate the CFO by the conventional autocorrelation-based method. However, the differential filter not only fails to completely eliminate the TV-DCO, but also enhances the noise. Also, the CFO estimation is severely biased by the remaining

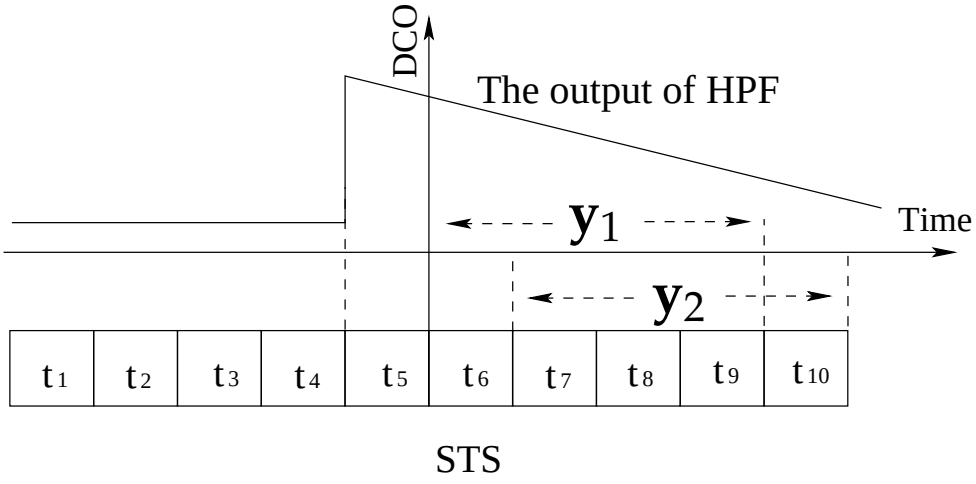

Fig. 4.1. STS preamble and TV-DCO model.

uncompensated I/Q imbalance. Moreover, [24] only proposed a CFO estimator and did not mention how to estimate/compensate the I/Q imbalance in this situation.

The purpose of this chapter is to develop a novel joint estimation method for CFO and I/Q imbalance in the presence of TV-DCO. As indicated in [24,25], the residual TV-DCO at the output of the HPF has a linear property, which means it can be approximated by a linear function. On the other hand, a PP-based joint estimation/compensation of CFO and I/Q imbalance was recently proposed in [16], however in the absence of TV-DCO. Noticing the linear property of the TV-DCO, we extend the approach in [16] to take the existence of the TV-DCO into account. From the periodicity of the pilot, we derive a low-complexity estimator which can obtain the necessary estimates in closed-form. Simulations confirms the effectiveness and superiority of the proposed estimator.

4.1 PROBLEM FORMULATION

Let us consider the IEEE 802.11a short training sequence (STS) [1] shown in Fig. 4.1. As indicated before, the STS consists of ten identical K-samples repeated symbols $t_1, \cdots, t_{10}$, and every four repeated symbols of the STS can be treated as an N-subcarriers OFDM symbol, where $N = 64$ and $K = 16$. When the channel is time-invariant during the preamble and its length is less than K, the received STS keeps its periodicity after discarding the first symbol as a guard interval.

4.1.1 Model of I/Q Imbalance, CFO and DCO

Figure 4.2 shows the architecture of a direct-conversion receiver. Usually, we can assume the LO-induced I/Q imbalance, i.e., imperfect phase difference and unequal amplitudes, is constant over the signal bandwidth. Based on this assumption, the mathematical model of the system is shown in Fig.4.3. $r(t)$ denotes the STS after passing through the channel, f_c is carrier frequency, Δf is the CFO, g and ϕ are the amplitude mismatch and the phase error of I/Q imbalance, and d_I and d_Q are the I and Q components of the DCO d, respectively.

In the presence of I/Q imbalance, the nth sample of the downconverted STS, can be written as

$$y(n) = c_1 s(n) + c_2 s^*(n) + z(n), \tag{4.1}$$

where

$$c_1 = \frac{(1 + g e^{-j\phi})}{2}, \tag{4.2}$$

$$c_2 = \frac{(1 - g e^{j\phi})}{2}, \tag{4.3}$$

$s(n)$ is the baseband equivalent signal of $r(n)$, and $z(n)$ is AWGN. Then, considering the CFO and time-invariant DCO, we have

$$y(n) = c_1 s(n) e^{-j\varphi n} + c_2 s^*(n) e^{j\varphi n} + d + z(n), \tag{4.4}$$

where $\varphi = \frac{2\pi\varepsilon}{N}$, ε is the CFO normalized to subcarrier spacing. The I and Q components of $y(n)$ can be given as

$$\begin{bmatrix} y_I(n) \\ y_Q(n) \end{bmatrix} = \mathbf{AB} \begin{bmatrix} s_I(n) \\ s_Q(n) \end{bmatrix} + \begin{bmatrix} d_I \\ d_Q \end{bmatrix} + \begin{bmatrix} z_I(n) \\ z_Q(n) \end{bmatrix}, \tag{4.5}$$

where

$$\mathbf{A} = \begin{bmatrix} 1 & 0 \\ -g \cdot \sin\phi & g \cdot \cos\phi \end{bmatrix}, \tag{4.6}$$

$$\mathbf{B} = \begin{bmatrix} \cos(\varphi n) & \sin(\varphi n) \\ -\sin(\varphi n) & \cos(\varphi n) \end{bmatrix}. \tag{4.7}$$

Obvously, **A** and **B** correspond to the effect of I/Q imbalance and CFO, respectively.

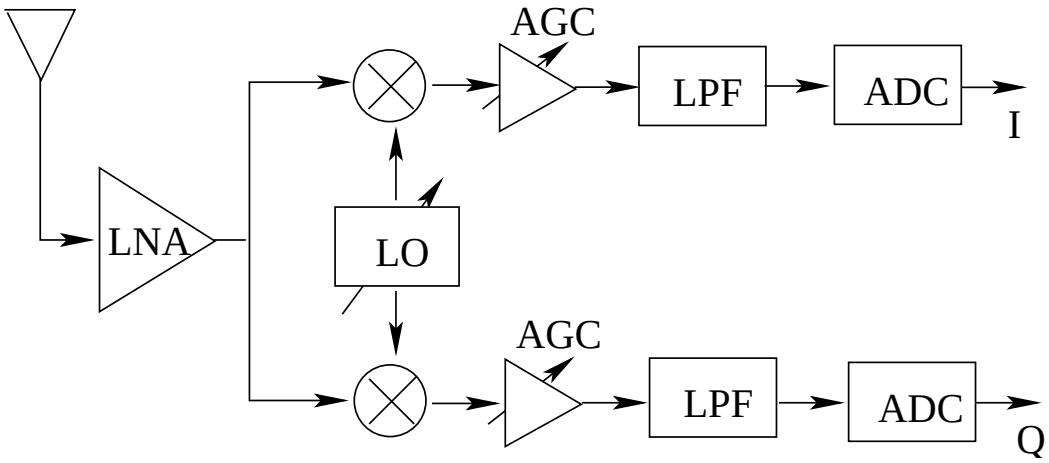

Fig. 4.2. Architecture of a DCR.

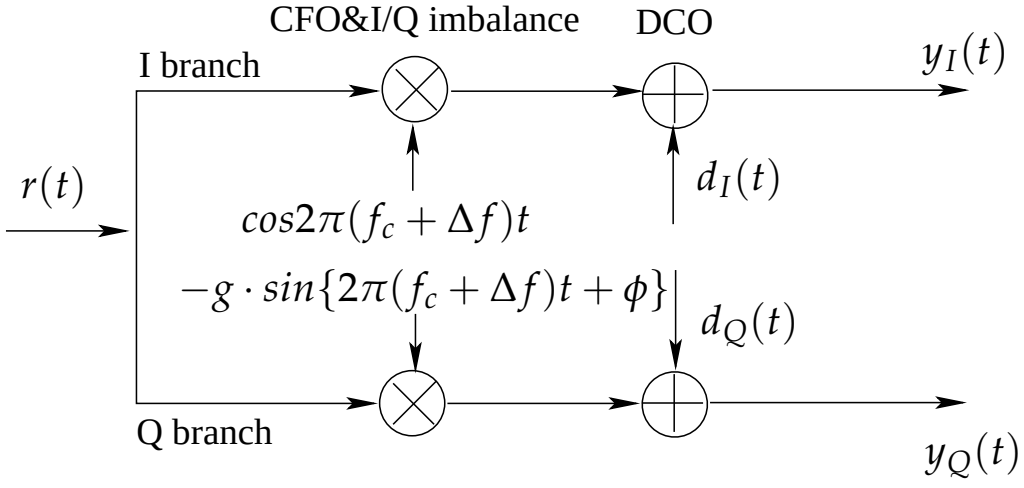

Fig. 4.3. Mathematical model of the system.

4.1.2 Compensation Scheme

From Eq.(4.5), after removing the DCO, we have

$$\begin{bmatrix} \dot{y}_I(n) \\ \dot{y}_Q(n) \end{bmatrix} = \mathbf{AB} \begin{bmatrix} s_I(n) \\ s_Q(n) \end{bmatrix} + \begin{bmatrix} z_I(n) \\ z_Q(n) \end{bmatrix}, \tag{4.8}$$

where

$$\dot{y}_I(n) = y_I(n) - d_I, \tag{4.9}$$

$$\dot{y}_Q(n) = y_Q(n) - d_Q. \tag{4.10}$$

Then, the baseband signal can be recovered by the compensation of I/Q imbalance and CFO as follows

$$\begin{bmatrix} \hat{s}_I(n) \\ \hat{s}_Q(n) \end{bmatrix} = \mathbf{B}^{-1}\mathbf{A}^{-1} \begin{bmatrix} \dot{y}_I(n) \\ \dot{y}_Q(n) \end{bmatrix}, \tag{4.11}$$

where

$$\mathbf{A}^{-1} = \begin{bmatrix} 1 & 0 \\ \tan\phi & 1/(g \cdot \cos\phi) \end{bmatrix}, \tag{4.12}$$

$$\mathbf{B}^{-1} = \begin{bmatrix} \cos(\varphi n) & -\sin(\varphi n) \\ \sin(\varphi n) & \cos(\varphi n) \end{bmatrix}. \tag{4.13}$$

Similarly, $\mathbf{A}^{-1}$ and $\mathbf{B}^{-1}$ correspond to the compensation of the I/Q imbalance and the CFO, respectively.

4.2 Conventional CFO Estimator

In practice, AGC circuits are usually employed to keep the proper fixed level of the received signal [38]. In 802.11a WLAN systems, at the middle of STS, the AGC starts to control the gain of the received signal, which leads to the gain shift of DCO.

On the other hand, an HPF is often used to eliminate DCO [47]. Usually, an HPF is sufficient to remove the effect of the time-invariant DCO. However, in the case of AGC-induced TV-DCO, its higher frequency components may pass through the HPF. In consequence, the CFO estimation will be deteriorated by the residual TV-DCO.

In the presence of TV-DCO $d(n)$, we have following relationship by replacing d with $d(n)$ in Eq.(4.4)

$$y(n) = c_1 s(n) e^{-j\varphi n} + c_2 s^*(n) e^{j\varphi n} + d(n) + z(n). \tag{4.14}$$

In the conventional estimator [24], the received STS is passed through the differential filter to reduce the TV-DCO. The nth sample of the differential filter's output is given by

$$y_d(n) = s_d(n) + d_d(n) + z_d(n), \tag{4.15}$$

where

$$\begin{aligned} y_d(n) &= y(n) - y(n-1), && (4.16)\\ s_d(n) &= c_1 e^{-j\varphi n}\{s(n) - s(n-1)e^{j\varphi}\} \\ &+ c_2 e^{j\varphi n}\{s^*(n) - s^*(n-1)e^{-j\varphi}\}, && (4.17)\\ d_d(n) &= d(n) - d(n-1), && (4.18)\\ z_d(n) &= z(n) - z(n-1). && (4.19) \end{aligned}$$

Then the CFO is estimated by using the autocorrelation of the STS as

$$\begin{aligned} \hat{\varepsilon} &= \frac{4}{2\pi}\arg\{\lambda \sum_{k=0}^{K-1} y_d^*(k+2K) y_d(k+3K) \\ &+ \sum_{m=4}^{8}\sum_{k=0}^{K-1} y_d^*(k+mK) y_d(k+(m+1)K)\}, \end{aligned} \tag{4.20}$$

where λ is the weighting factor.

As indicated in [24], due to the uncompensated I/Q imbalance, the CFO estimation in Eq.(4.20) is severely biased. From Eq.(4.15), we can see that the estimation is also biased by the residual TV-DCO $d_d(n)$ and the noise variance is doubled. Furthermore, [24] only proposed a CFO estimator, how to estimate/compensate I/Q imbalance in such situation was not given.

4.3 PROPOSED JOINT ESTIMATOR

In this section, we derive a joint estimator of CFO and I/Q imbalance, which can remove the effect of TV-DCO completely, when the residual TV-DCO can be approximated by a linear function.

We employ the pilot in [16], where $\pi/2$ phase difference is added between adjacent two repeated STS symbols. Similar to [24], we assume that the LNA is switched at the beginning of t_5. In the absence of I/Q imbalance, CFO, TV-DCO and noise terms, after passing through the channel, whose length is less than K, the received STS symbols satisfy $y(n+K) = e^{j\frac{\pi}{2}} y(n)$, $n > K$. Then, in the presence of CFO, we have $y(n+K) = e^{-j\theta} y(n)$, where $\theta = \tilde{\theta} - \frac{\pi}{2}$, $\tilde{\theta} = \varphi K$.

Without loss of generality, we can form two $N \times 1$ vectors $\mathbf{y}_1$ and $\mathbf{y}_2$ from the received STS symbols $t_6, t_7, \cdots, t_{10}$, which are at a distance of K shown in Fig.4.1. Note that $\mathbf{y}_1$ and $\mathbf{y}_2$ are the symbols corresponding to the sampling range of $t_6, t_7, \cdots, t_9$ and $t_7, t_8, \cdots, t_{10}$, respectively. Therefore, considering the CFO only, the relation between $\mathbf{y}_1$ and $\mathbf{y}_2$ becomes

$$\mathbf{y}_2 = e^{-j\theta}\mathbf{y}_1. \tag{4.21}$$

Since the TV-DCO has a linear property, it is approximated by a linear function $ax + b$, where a denotes the ratio of variation, while b stands for the constant component. Thus, in the presence of CFO, I/Q imbalance and TV-DCO, we have the following relationship for one symbol by replacing DCO with TV-DCO in Eq.(4.5)

$$\begin{bmatrix} \mathbf{y}_I^T \\ \mathbf{y}_Q^T \end{bmatrix} = \mathbf{A} \begin{bmatrix} \tilde{\mathbf{s}}_I^T \\ \tilde{\mathbf{s}}_Q^T \end{bmatrix} + \begin{bmatrix} a_I\mathbf{x}^T + b_I\mathbf{1}_N^T \\ a_Q\mathbf{x}^T + b_Q\mathbf{1}_N^T \end{bmatrix} + \begin{bmatrix} \mathbf{z}_I^T \\ \mathbf{z}_Q^T \end{bmatrix}, \tag{4.22}$$

where $\mathbf{1}_N$ is an $N \times 1$ all 1 vector, $\mathbf{y}_I$,$\mathbf{z}_I$ and $\mathbf{y}_Q$,$\mathbf{z}_Q$ are the real (I) and imaginary (Q) parts of

$$\mathbf{y} = [y(0),\ y(1),\ ...,\ y(N-1)]^T, \tag{4.23}$$
$$\mathbf{z} = [z(0),\ z(1),\ ...,\ z(N-1)]^T, \tag{4.24}$$
$$\mathbf{x} = [0,\ 1,\ \cdots,\ N-1]^T, \tag{4.25}$$

respectively. Clearly, $\tilde{\mathbf{s}} = \tilde{\mathbf{s}}_I + j\tilde{\mathbf{s}}_Q$ is an $N \times 1$ STS vector corrupted by the CFO. To estimate the CFO, we should remove the TV-DCO and compensate I/Q imbalance firstly. From Eq.(4.22), we have

$$\begin{bmatrix} \check{\mathbf{y}}_I^T \\ \check{\mathbf{y}}_Q^T \end{bmatrix} = \mathbf{A}^{-1} \begin{bmatrix} \dot{\mathbf{y}}_I^T \\ \dot{\mathbf{y}}_Q^T \end{bmatrix}, \tag{4.26}$$

where

$$\dot{\mathbf{y}}_I^T = \mathbf{y}_I^T - (a_I\mathbf{x}^T + b_I\mathbf{1}_N^T), \tag{4.27}$$
$$\dot{\mathbf{y}}_Q^T = \mathbf{y}_Q^T - (a_Q\mathbf{x}^T + b_Q\mathbf{1}_N^T). \tag{4.28}$$

Then, using Eqs.(4.12) and (4.26), $\check{\mathbf{y}}_\mathbf{1}$ and $\check{\mathbf{y}}_\mathbf{2}$ corresponding to $\mathbf{y}_1$ and $\mathbf{y}_2$ which are at a

distance of K can be written as

$$\begin{aligned}
\check{\mathbf{y}}_{\mathbf{1}} &= \check{\mathbf{y}}_{1I} + j\check{\mathbf{y}}_{1Q} \\
&= \mathbf{y}_{1I} - (a_I\mathbf{x}_1 + b_I\mathbf{1}_N) \\
&+ j\{\alpha[\mathbf{y}_{1I} - (a_I\mathbf{x}_1 + b_I\mathbf{1}_N)] \\
&+ \beta[\mathbf{y}_{1Q} - (a_Q\mathbf{x}_1 + b_Q\mathbf{1}_N)]\}, \qquad (4.29) \\
\check{\mathbf{y}}_{\mathbf{2}} &= \check{\mathbf{y}}_{2I} + j\check{\mathbf{y}}_{2Q} \\
&= \mathbf{y}_{2I} - (a_I\mathbf{x}_2 + b_I\mathbf{1}_N) \\
&+ j\{\alpha[\mathbf{y}_{2I} - (a_I\mathbf{x}_2 + b_I\mathbf{1}_N)] \\
&+ \beta[\mathbf{y}_{2Q} - (a_Q\mathbf{x}_2 + b_Q\mathbf{1}_N)]\}, \qquad (4.30)
\end{aligned}$$

where $\alpha = \tan\phi$, $\beta = 1/(g\cos\phi)$ and

$$\mathbf{x}_1 = [0,\ 1,\ \cdots,\ N-1]^T, \qquad (4.31)$$

$$\mathbf{x}_2 = [K, K+1, \cdots, K+N-1]^T. \qquad (4.32)$$

Since $\check{\mathbf{y}}_{\mathbf{1}}$ and $\check{\mathbf{y}}_{\mathbf{2}}$ are only corrupted by CFO, they should satisfy Eq.(4.21). As a result, we can define the cost function as

$$(\hat{\varepsilon}, \hat{\alpha}, \hat{\beta}, \hat{a}_I, \hat{a}_Q, \hat{b}_I, \hat{b}_Q) = \underset{\varepsilon,\alpha,\beta,a_I,a_Q,b_I,b_Q}{\operatorname{argmin}} \parallel \check{\mathbf{y}}_2 - e^{-j\theta}\check{\mathbf{y}}_1 \parallel^2 . \qquad (4.33)$$

Substituting Eqs.(4.29) and (4.30) into Eq.(4.33), it can be found that the cost function is minimized when

$$\begin{aligned}
\mathbf{y}_{2I} &= (\cos\theta + \alpha\sin\theta)\mathbf{y}_{1I} + \mathbf{y}_{1Q}\beta\sin\theta \\
&+ \mathbf{x}_1\{a_I(1 - \cos\theta - \alpha\sin\theta) - a_Q\beta\sin\theta\} + \mathbf{1}_N \\
&\times \{b_I(1 - \cos\theta - \alpha\sin\theta) - b_Q\beta\sin\theta + a_I K\}, \qquad (4.34) \\
\mathbf{y}_{1I} &= (\cos\theta - \alpha\sin\theta)\mathbf{y}_{2I} - \mathbf{y}_{2Q}\beta\sin\theta \\
&+ \mathbf{x}_2\{a_I(1 - \cos\theta + \alpha\sin\theta) + a_Q\beta\sin\theta\} + \mathbf{1}_N \\
&\times \{b_I(1 - \cos\theta + \alpha\sin\theta) + b_Q\beta\sin\theta - a_I K\}. \qquad (4.35)
\end{aligned}$$

From Eqs.(4.34) and (4.35), we can obtain

$$\begin{bmatrix} \mathbf{y}_{2I} \\ \mathbf{y}_{1I} \end{bmatrix} = \mathbf{GR}, \qquad (4.36)$$

where

$$\begin{aligned}\mathbf{R} &= [R(1),R(2),R(3),R(4),R(5),R(6),R(7)]^T \\ &= \begin{bmatrix} \cos\theta+\alpha\sin\theta \\ \cos\theta-\alpha\sin\theta \\ a_I(1-\cos\theta-\alpha\sin\theta)-a_Q\beta\sin\theta \\ a_I(1-\cos\theta+\alpha\sin\theta)+a_Q\beta\sin\theta \\ \beta\sin\theta \\ b_I(1-\cos\theta-\alpha\sin\theta)-b_Q\beta\sin\theta+a_IK \\ b_I(1-\cos\theta+\alpha\sin\theta)+b_Q\beta\sin\theta-a_IK \end{bmatrix} \end{aligned} \tag{4.37}$$

$$\mathbf{G} = \begin{bmatrix} \mathbf{y}_{1I} & \mathbf{0}_N & \mathbf{x}_1 & \mathbf{0}_N & \mathbf{y}_{1Q} & \mathbf{1}_N & \mathbf{0}_N \\ \mathbf{0}_N & \mathbf{y}_{2I} & \mathbf{0}_N & \mathbf{x}_2 & -\mathbf{y}_{2Q} & \mathbf{0}_N & \mathbf{1}_N \end{bmatrix} \tag{4.38}$$

and $\mathbf{0}_N$ is an $N\times 1$ all 0 vector. Then, we have

$$\mathbf{R} = \mathbf{G}^{\dagger}\begin{bmatrix} \mathbf{y}_{2I} \\ \mathbf{y}_{1I} \end{bmatrix}. \tag{4.39}$$

Since $\theta = \tilde{\theta}-\frac{\pi}{2} = \frac{2\pi\varepsilon K}{N}-\frac{\pi}{2}$ and $\frac{N}{K}=4$, finally we have a closed-form solution for CFO as follows

$$\hat{\varepsilon} = \frac{4}{2\pi}\arcsin\left\{\frac{R(1)+R(2)}{2}\right\}. \tag{4.40}$$

After the CFO estimation, the terms of I/Q imbalance can be calculated as

$$\hat{\phi} = -\arctan\{\frac{R(1)-R(2)}{2\cos\tilde{\theta}}\}, \tag{4.41}$$

$$\hat{g} = -\frac{\cos\tilde{\theta}}{R(5)\cos\hat{\phi}}, \tag{4.42}$$

where $\tilde{\theta} = \arcsin\{\frac{R(1)+R(2)}{2}\}$. Then using $\hat{\alpha}=\tan\hat{\phi}$ and $\hat{\beta}=1/(\hat{g}\cos\hat{\phi})$, we can obtain the residual TV-DCO parameters as follows

$$\hat{a}_I = \frac{R(3)+R(4)}{2(1-\sin\tilde{\theta})}, \tag{4.43}$$

$$\hat{b}_I = \frac{R(7)+R(6)}{2(1-\sin\tilde{\theta})}, \tag{4.44}$$

$$\hat{a}_Q = \frac{R(4)-R(3)+2\hat{a}_I\hat{\alpha}\cos\tilde{\theta}}{-2\hat{\beta}\cos\tilde{\theta}}, \tag{4.45}$$

$$\hat{b}_Q = \frac{R(7)-R(6)+2\hat{b}_I\hat{\alpha}\cos\tilde{\theta}+2\hat{a}_IK}{-2\hat{\beta}\cos\tilde{\theta}}. \tag{4.46}$$

Table 4.1. Simulation setup

Modulation scheme	QPSK
Number of subcarrier	64
Channel	Rayleigh fading
HPF	1st order Butterworth
LNA gain	35/15[dB]
Normalized frequency offset	-0.5 $\sim$ 0.5

4.4 SIMULATION RESULTS

We performed simulations to demonstrate the validity of proposed joint estimation of CFO and I/Q imbalance. Table 4.1 shows the simulation setup. The channel is 6-path Rayleigh fading channel. There is no inter symbol interference, since the length of cyclic prefix N_{CP}=16 exceeds the maximum channel delay spread. The first order Butterworth filter is used as the HPF, and the cutoff frequency is f_x =100kHz. The normalized CFO value ε is set to be a random value in the range of $-0.5 \sim 0.5$. The TV-DCO is generated using the same model for the LNA and the mixer as [24], where the gain of LNA changes between 15 and 35dB, the isolation between LO and LNA input is assumed to be -60dB, and the received signal power is set to be -53dBm.

The CFO estimation is evaluated in terms of mean square error (MSE), and the compensation of I/Q imbalance is evaluated by image rejection ratio (IRR). Since the conventional estimator [24] did not show a way to obtain λ, and the simulations are only conducted for λ=0, we simply follow this setting. Figure 4.4 shows the results of CFO MSE versus SNR, where $g = 1.25$, $\phi = 6^\circ$, $\varepsilon = 0.2$ and f_x =100kHz. From Fig.4.4, we can find that the proposed estimator performs quite accurately than the conventional differential filter based estimator. Also, it can be observed that the estimation results of the conventional method are not improved along with the SNR. The main reason of this can be considered as the impact of the I/Q imbalance, i.e., the CFO estimator is biased by the uncompensated I/Q imbalance [24]. Figure 4.5 shows CFO MSE versus variant ε, where $g = 1.25$, $\phi = 6^\circ$, f_x =100kHz, SNR=25dB, and ε is in the range of $-0.5 \sim 0.5$. From Fig.4.5, we can see the proposed method is almost independent of frequency off-

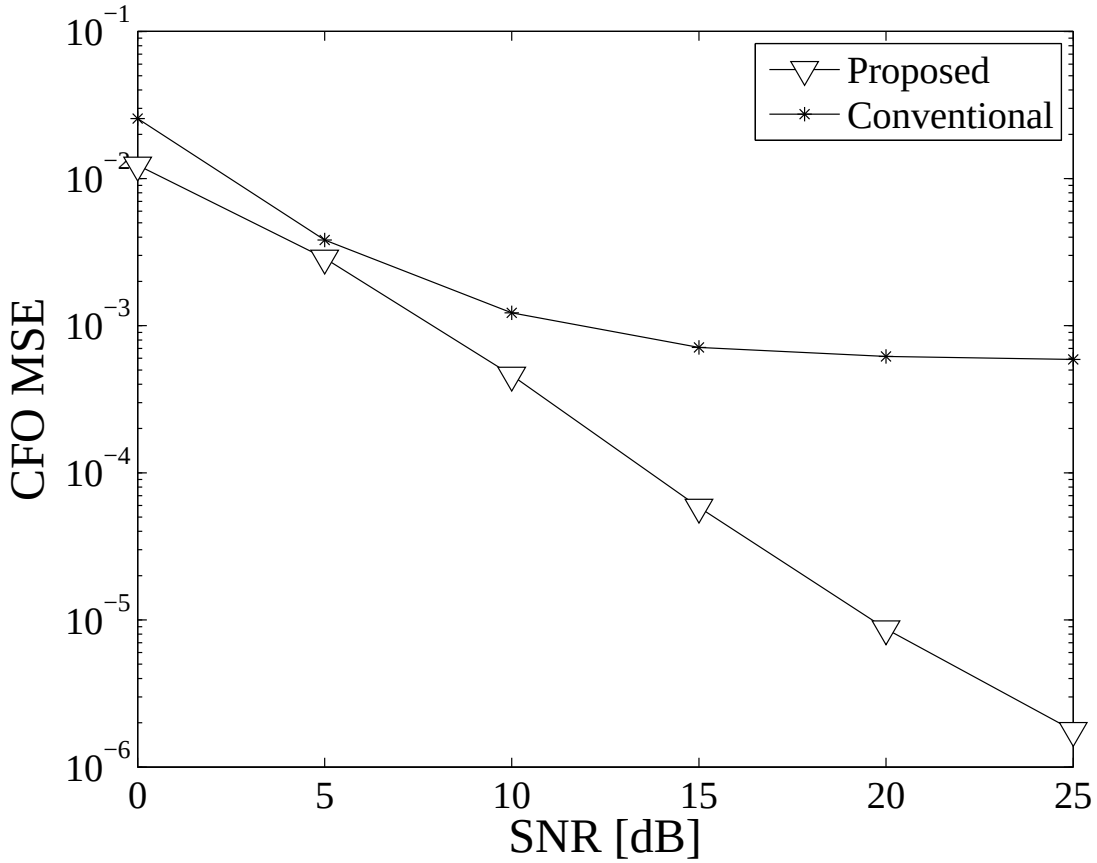

Fig. 4.4. CFO MSE versus SNR, f_x =100kHz, $g = 1.25$, $\phi = 6^\circ$, $\varepsilon = 0.2$

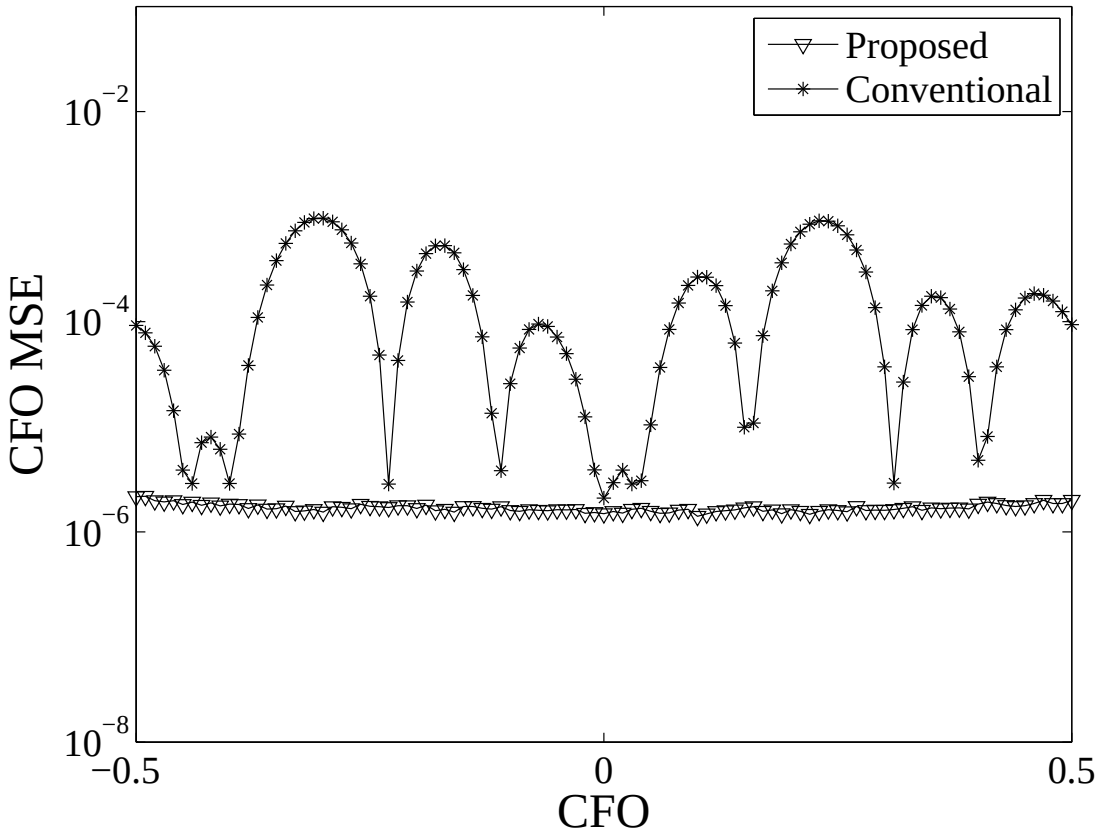

Fig. 4.5. CFO MSE versus ε, f_x =100kHz, $g = 1.25$, $\phi = 6^\circ$, SNR=25dB

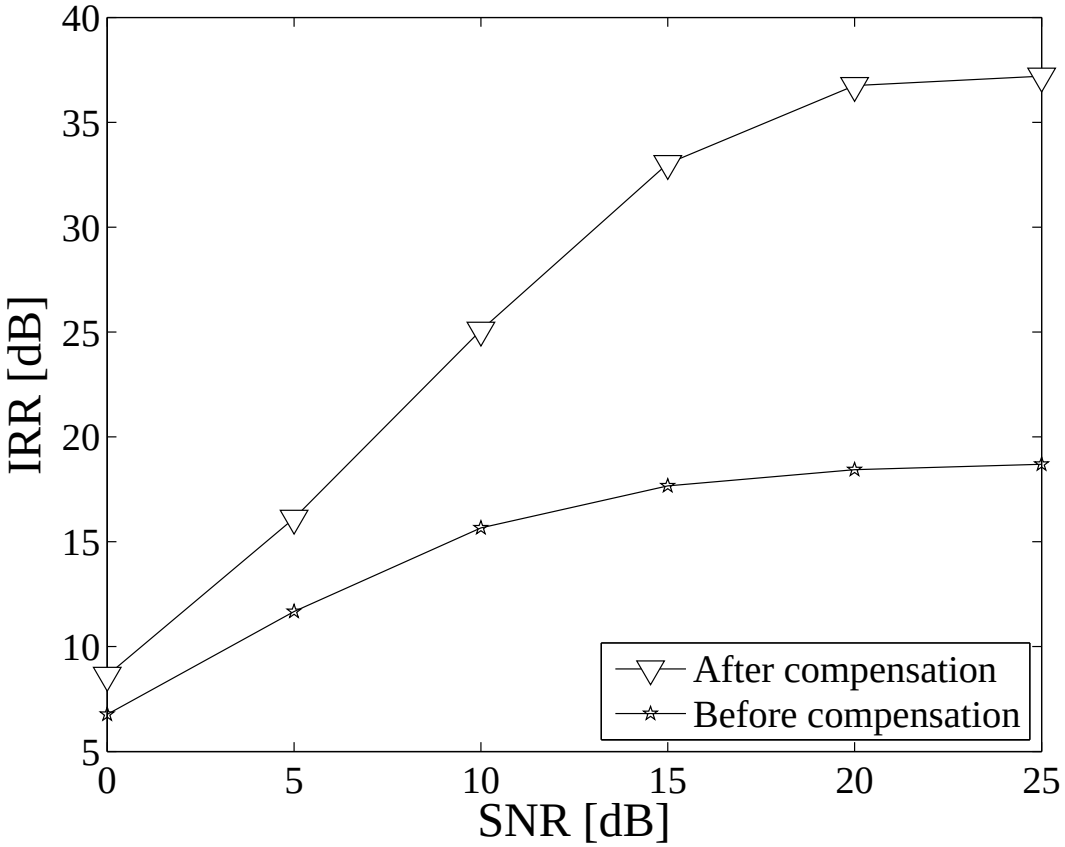

Fig. 4.6. IRR versus SNR, f_x =100kHz, $g = 1.25$, $\phi = 6^\circ$, $\varepsilon = 0.2$

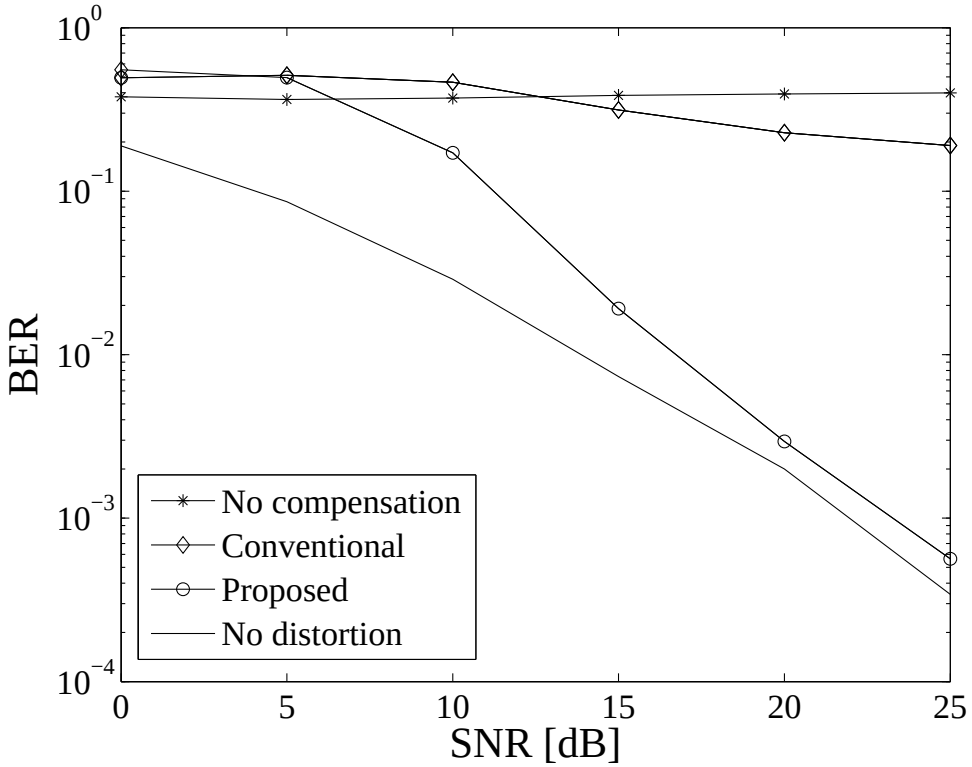

(a) 6-path Rayleigh fading channel

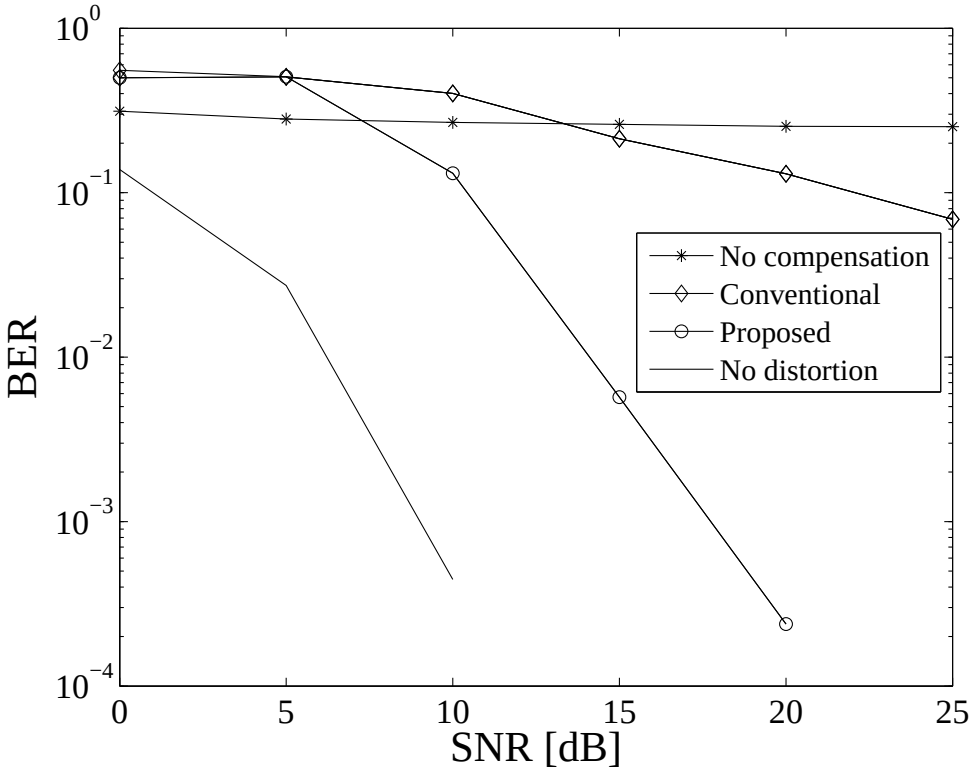

(b) 1-path Static channel

Fig. 4.7. BER versus SNR, f_x =100kHz, $g = 1.25$, $\phi = 6^\circ$, $\varepsilon = 0.2$

set. Figure 4.6 shows IRR versus SNR, where f_x =100kHz, $g = 1.25$, $\phi = 6^\circ$, $\varepsilon = 0.2$. It can be seen that after the I/Q imbalance compensation, the IRR is improved from 18dB to 37dB while SNR=25dB. Finally, the BER results for 6-path Rayleigh fading channel and 1-path static channel are illustrated in Fig.4.7(a) and Fig.4.7(b), respectively. In conventional method [24], only a CFO estimator was proposed, how to estimate/compensate I/Q imbalance in such situation was not given. As a consequence, for the conventional method, we measure the BER without compensating I/Q imbalance. It can be seen that the conventional method presents very poor performance due to the uncompensated I/Q imbalance. In contrast, the proposed estimator shows acceptable performance at the most range of SNR. On the other hand, the proposed method cannot achieve satisfied BER performance for SNR$<$7dB, since there is a severe CFO estimation error at low-SNR, which further corrupts the subsequent CFO-dependent I/Q imbalance estimation.

4.5 CONCLUSIONS

In a DCR, CFO, DCO and I/Q imbalance are considered to be the most serious impairments. Furthermore, AGC leads to TV-DCO. Since OFDM system is sensitive to CFO, the estimation/compensation of CFO in the presence of I/Q imbalance and the TV-DCO is a critical problem in an OFDM-DCR.

In this chapter, a novel joint estimation method for CFO and I/Q imbalance in the presence of TV-DCO has been proposed. Based on the linear property of TV-DCO, we have approximated the TV-DCO using a linear function. Then, a closed-form CFO and I/Q imbalance estimator was derived from the periodicity of training sequence. Simulations were performed to confirm the validity of the proposed estimator. From CFO MSE to both the proposed and the conventional methods, it has been confirmed that the proposed CFO estimator performs quite accurately than the conventional CFO estimator. In contrast to the poor estimation ability of 10^{-3} CFO MSE in 25dB SNR in conventional method, about 10^{-6} CFO MSE can be obtained for the proposed estimator. Meantime, it has been shown that the proposed CFO estimator is independent of CFO, while conventional CFO estimator is dependent on CFO. In the I/Q imbalance estimation results using IRR, it has been shown that the IRR is improved from 18dB to 37dB while SNR=25dB. Finally, after compensating CFO and I/Q imbalance, BER curve has been shown to evaluate the whole compensation, where we can see that in contrast to the poor performance of the conventional method, the proposed method shows acceptable performance.

CHAPTER 5

A Novel ISI Cancellation Method for OFDM Systems without Guard Interval

IN an asynchronous uplink multi-carrier code division multiple access (MC-CDMA) systems, user's individual timing offset exists in the received signal. Since the synchronization of all user's signals is not always available, the resulting multi-user interference (MUI) leads to severe performance degradation. In [27,29], we proposed a novel symbol structure with zero-padding to synchronize all user's signal, which can eliminate the MUI completely. In OFDM or MC-CDMA systems, in order to fight multipath, the cyclic prefix, which is also referred to as guard interval, is inserted between symbols. While the length of GI is longer than channel delay spread, it can protect received signal from ISI. However, the price is transmission speed. In order to increase the transmission speed, several attempts [8, 13, 18, 21–23, 31, 39, 48] have been made to the cancellation of ISI and ICI in OFDM systems with insufficient GI [8, 13, 18, 21–23, 31] or without GI [39, 48]. In [21, 31], time domain equalizer is used to shorten the channel impulse response to combat ISI and ICI. FIR tail cancellation and FIR cyclic reconstruction techniques are used in [18] to cope with ISI and ICI. Precoding techniques and oversampling techniques are used to mitigate ISI and ICI in [22] and [23], respectively. In [8, 13], a decision feed back loop is proposed, which not only results in feedback delay increment and error propagation, but also increases the computational complexity. All these methods only consider OFDM systems with insufficient GI. Since GI insertion reduces transmission efficiency, beside the common GI insertion, some studies [39,48] discussed OFDM systems without GI. In the absence of GI, eliminating ISI between adjacent symbols is a crucial problem. It is proposed a method [39] for compensation of ISI distor-

tion by using null subcarriers, i.e., inactive subcarriers, which is usually being placed at the edges of the frequency band and DC to avoid aliasing and ease transmit filtering. In [48], an iteration method is proposed to eliminate the ISI and ICI. However, the iteration in [48] increases the complexity of computing and also results in error propagation, specially for high-degree constellation.

To obtain a good performance with the low-complexity, a novel ISI cancellation method is derived in this chapter. In order to investigate the effect of channel to OFDM symbols, we studied various channels. Based on the simulations to the both minimum and non-minimum phase channels, our attention is attracted occasionally by following interesting phenomenons. While the channel is minimum phase, after frequency domain equalization (FDE) and then converting the resulting signal into time domain, OFDM symbols are effected by ISI primarily at the beginning part of the symbols. Based on this observation, we consider a novel ISI cancellation method, by using the channel information and signal achieved at the tail part of OFDM symbols, which is almost not effected by ISI. For the channel which is not minimum-phase, the proposed method is also applicable after converting the channel into minimum-phase by using a proper filter.

5.1 SYSTEM FORMULATION

As explained in Chapter 2, for OFDM systems without GI, the received signal, after passing through the channel, can be expressed as follows

$$\mathbf{r}_i = \mathbf{h} \cdot \begin{bmatrix} s_{i-1}^{N-L+1} \\ \vdots \\ s_{i-1}^{N-1} \\ s_i^0 \\ \vdots \\ s_i^{N-1} \end{bmatrix} + \mathbf{z}_i, \tag{5.1}$$

where, s_i^{N-1} is the $(N-1)$th sample of the ith transmitted symbol, $\mathbf{r}_i = [r_i^0, r_i^1, \ldots, r_i^{N-1}]^T$ is an $N \times 1$ vector corresponding to the ith received symbol, $\mathbf{z}_i$ is an $N \times 1$ vector corresponding to additive white Gaussian noise (AWGN), L is the length of the channel, the

channel matrix $\mathbf{h}$ is an $N \times (N + L - 1)$ Toeplitz-like matrix as follows

$$\mathbf{h} = \begin{bmatrix} h_{L-1} & \dots & h_0 & 0 & \dots & \dots & 0 \\ 0 & \ddots & & \ddots & \ddots & & \vdots \\ \vdots & \ddots & h_{L-1} & \dots & h_0 & \ddots & \vdots \\ \vdots & & \ddots & \ddots & & \ddots & 0 \\ 0 & \dots & & 0 & h_{L-1} & \dots & h_0 \end{bmatrix}. \tag{5.2}$$

Then it can be rewritten as

$$\mathbf{r}_i \;=\; \dot{\mathbf{h}} \cdot \mathbf{s}_{i-1,i} + \mathbf{z}_i, \tag{5.3}$$

where, $\mathbf{s}_{i-1,i} = \begin{bmatrix} \mathbf{s}_{i-1} \\ \mathbf{s}_i \end{bmatrix}$ is a $2N \times 1$ vector consist of two consecutive transmitted symbols and $\mathbf{s}_i = [s_i^0,\ s_i^1,\ \dots,\ s_i^{N-1}]^T$ is an $N \times 1$ vector corresponding to ith symbol, and $\dot{\mathbf{h}} = [\mathbf{h_t}\ \ \mathbf{h_x}]$, where $N \times N$ matrices $\mathbf{h_x}$ and $\mathbf{h_t}$ can be expressed as follows

$$\mathbf{h_x} = \begin{bmatrix} h_0 & 0 & \dots & \dots & \dots & 0 \\ \vdots & \ddots & \ddots & & & \vdots \\ h_{L-1} & \dots & h_0 & \ddots & & \vdots \\ 0 & h_{L-1} & \dots & h_0 & \ddots & \vdots \\ \vdots & \ddots & \ddots & & \ddots & 0 \\ 0 & \dots & 0 & h_{L-1} & \dots & h_0 \end{bmatrix}, \tag{5.4}$$

$$\mathbf{h_t} = \begin{bmatrix} 0 & \dots & 0 & h_{L-1} & \dots & h_1 \\ \vdots & \ddots & & \ddots & \ddots & \vdots \\ \vdots & & \ddots & & \ddots & h_{L-1} \\ \vdots & & & \ddots & & 0 \\ \vdots & & & & \ddots & \vdots \\ 0 & \dots & \dots & \dots & \dots & 0 \end{bmatrix}. \tag{5.5}$$

Obviously, these two matrices satisfy

$$\mathbf{h_x} + \mathbf{h_t} = \mathbf{h}_{cycl}, \tag{5.6}$$

where $\mathbf{h}_{cycl}$ is the "ideal" channel matrix, i.e., the matrix that results in a cyclic convolution between the transmitted signal and the channel. As shown in Fig.5.1, after decomposition, finally, we have

$$\mathbf{r}_i = \mathbf{h}_{cycl} \cdot \mathbf{s}_i - \mathbf{h_t} \cdot \mathbf{s}_i + \mathbf{h_t} \cdot \mathbf{s}_{i-1} + \mathbf{z}_i, \tag{5.7}$$

where, $\mathbf{h}_{cycl} \cdot \mathbf{s}_i$, $\mathbf{h_t} \cdot \mathbf{s}_i$ and $\mathbf{h_t} \cdot \mathbf{s}_{i-1}$ represent the desired, ICI and ISI components, respectively.

5.2 ITERATION BASED ISI CANCELLATION METHOD

In this section, we introduce the iteration based interference cancellation method proposed in [48]. After removing ICI and ISI in Eq.(5.7), we have

$$\mathbf{y}_i^j = \mathbf{r}_i - \mathbf{h_t} \cdot \mathbf{s}_{i-1} + \mathbf{h_t} \cdot \mathbf{s}_i^j, \tag{5.8}$$

where j is the iteration index, $\mathbf{y}_i^j$ express the desired signal with AWGN. By using Eq.(5.8), interference cancellation using iterative procedure becomes as follows

Step 1: Remove ISI according to $\mathbf{w}_i = \mathbf{r}_i - \mathbf{h_t} \cdot \mathbf{s}_{i-1}$.

Step 2: Perform initial estimation of $\mathbf{s}_i$ by using $\mathbf{w}_i$, and set iteration index to $j = 1$.

Step 3: Remove ICI by using $\mathbf{y}_i^j = \mathbf{w}_i + \mathbf{h_t} \cdot \mathbf{s}_i^j$.

Step 4: Recover ith symbol and update iteration index to $j + 1$.

Step 5: Repeat Step 3 and Step 4 until convergence occurs or the maximum number of iterations is reached.

However, the disadvantages of this method is that iteration increases the complexity of computing and also results in error propagation, specially for high-degree constellation.

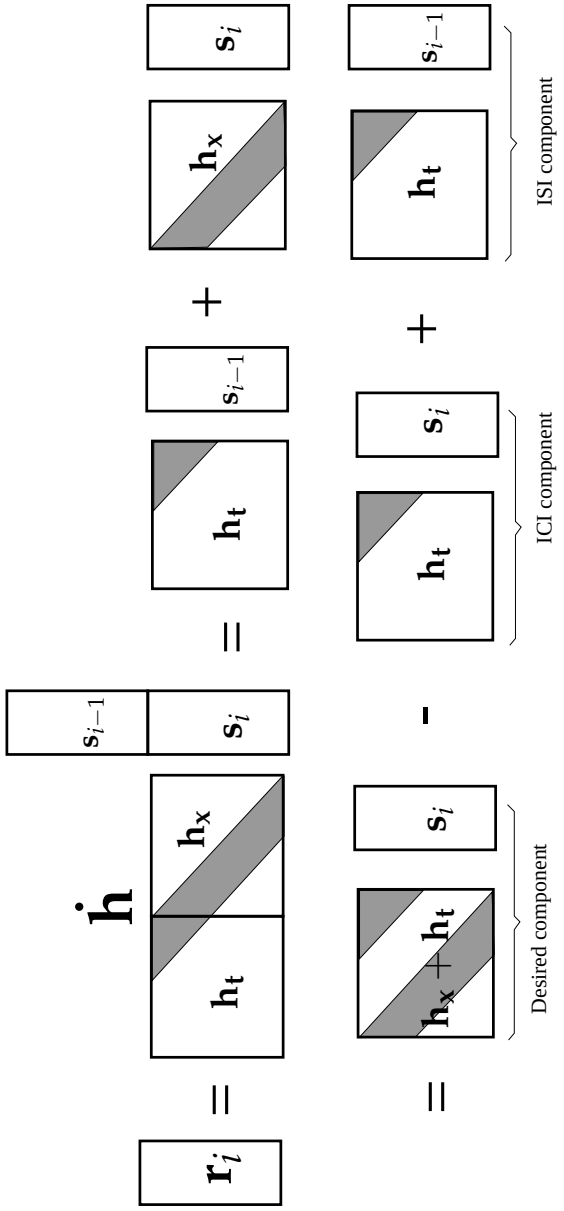

Fig. 5.1. Decomposition model of channel matrix.

5.3 PROPOSED METHOD

The diagram of transmitter and receiver is shown in Fig.5.2. Based on the relationship between frequency domain and time domain, we have

$$\mathbf{s}_i = \mathbf{F}_N^{\mathcal{H}} \mathbf{S}_i, \tag{5.9}$$

where, $\mathbf{S}_i$ denotes the ith symbol in the frequency domain corresponding to the $\mathbf{s}_i$, $\mathbf{F}_N^{\mathcal{H}}$ denotes an $N \times N$ IFFT matrix

$$\mathbf{F}_N^{\mathcal{H}} = \frac{1}{\sqrt{N}} \begin{bmatrix} 1 & 1 & \dots & 1 \\ 1 & e^{j\frac{2\pi}{N}} & \dots & e^{j\frac{2\pi(N-1)}{N}} \\ \vdots & \vdots & \ddots & \vdots \\ 1 & e^{j\frac{2\pi(N-1)}{N}} & \dots & e^{j\frac{2\pi(N-1)(N-1)}{N}} \end{bmatrix}. \tag{5.10}$$

Thus we have

$$\begin{bmatrix} s_{i-1}^{N-L+1} \\ \vdots \\ s_{i-1}^{N-1} \\ s_i^0 \\ \vdots \\ s_i^{N-1} \end{bmatrix} = \begin{bmatrix} \mathbf{F}_{L-1}^{\mathcal{H}} \mathbf{S}_{i-1} \\ \mathbf{F}_N^{\mathcal{H}} \mathbf{S}_i \end{bmatrix}, \tag{5.11}$$

where $\mathbf{F}_{L-1}^{\mathcal{H}}$ is a matrix consist of last $L-1$ rows of the matrix $\mathbf{F}_N^{\mathcal{H}}$ as follows

$$\mathbf{F}_{L-1}^{\mathcal{H}} = \frac{1}{\sqrt{N}} \begin{bmatrix} 1 & e^{j\frac{2\pi(N-L+1)}{N}} & \dots & e^{j\frac{2\pi(N-L+1)(N-1)}{N}} \\ \vdots & \vdots & \ddots & \vdots \\ 1 & e^{j\frac{2\pi(N-1)}{N}} & \dots & e^{j\frac{2\pi(N-1)(N-1)}{N}} \end{bmatrix}. \tag{5.12}$$

The decomposition of channel matrix in the proposed method is shown in Fig.5.3. Based on this, in the absence of noise term, Eq.(5.1) can be rewritten as follows

$$\begin{aligned} \mathbf{r}_i &= \mathbf{h} \cdot \begin{bmatrix} \mathbf{F}_{L-1}^{\mathcal{H}} \mathbf{S}_{i-1} \\ \mathbf{F}_N^{\mathcal{H}} \mathbf{S}_i \end{bmatrix} \\ &= \mathbf{h} \cdot \left\{ \begin{bmatrix} \mathbf{F}_{L-1}^{\mathcal{H}} \mathbf{S}_i \\ \mathbf{F}_N^{\mathcal{H}} \mathbf{S}_i \end{bmatrix} + \begin{bmatrix} \mathbf{F}_{L-1}^{\mathcal{H}} (\mathbf{S}_{i-1} - \mathbf{S}_i) \\ \mathbf{0}_N \end{bmatrix} \right\}, \end{aligned} \tag{5.13}$$

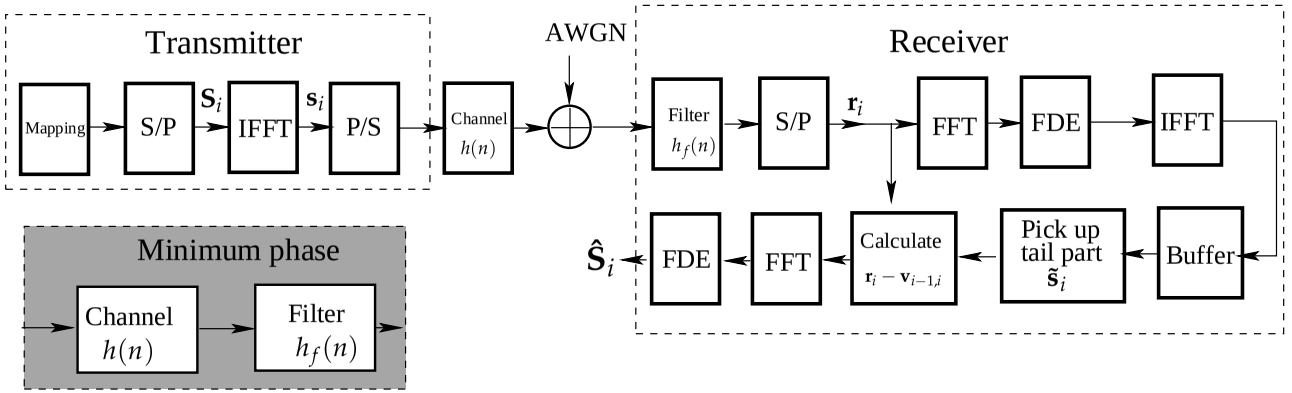

Fig. 5.2. Transmitter and receiver diagram.

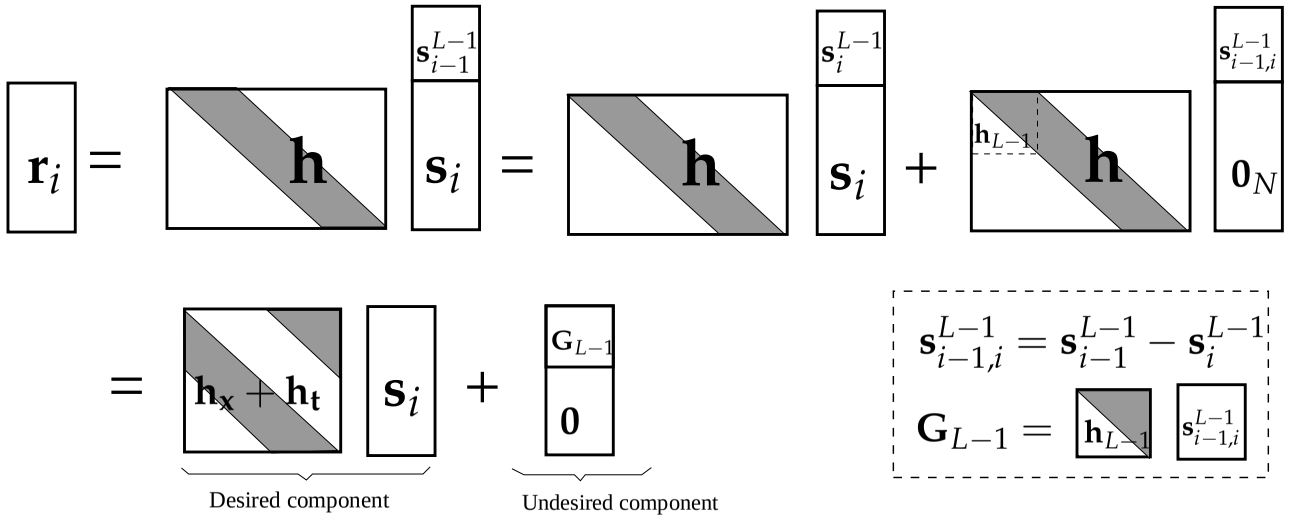

Fig. 5.3. Decomposition model of channel matrix in proposed method.

where $\mathbf{0}_N$ is an $N \times 1$ all zero vector. Then we can acheive

$$\mathbf{r}_i - \mathbf{v}_{i-1,i} = \mathbf{h} \begin{bmatrix} \mathbf{F}_{L-1}^{\mathcal{H}} \mathbf{S}_i \\ \mathbf{F}_N^{\mathcal{H}} \mathbf{S}_i \end{bmatrix}, \tag{5.14}$$

where

$$\begin{aligned} \mathbf{v}_{i-1,i} &= \mathbf{h} \cdot \begin{bmatrix} \mathbf{F}_{L-1}^{\mathcal{H}} (\mathbf{S}_{i-1} - \mathbf{S}_i) \\ \mathbf{0}_N \end{bmatrix} \\ &= \mathbf{h} \cdot \begin{bmatrix} \mathbf{s}_{i-1,i}^{L-1} \\ \mathbf{0}_N \end{bmatrix}, \end{aligned} \tag{5.15}$$

where $\mathbf{s}_{i-1,i}^{L-1} = \mathbf{s}_{i-1}^{L-1} - \mathbf{s}_i^{L-1}$ represents the difference of last $(L-1)$ samples of the $(i-1)$th and the ith symbols, and $\mathbf{s}_i^{L-1} = [s_i^{N-L+1}, s_i^{N-L+2}, \ldots, s_i^{N-1}]^T$. Then, we have

$$\mathbf{v}_{i-1,i} = \begin{bmatrix} \mathbf{G}_{L-1} \\ \mathbf{0}_{N-L+1} \end{bmatrix}, \tag{5.16}$$

where $\mathbf{G}_{L-1} = \mathbf{h}_{L-1} \cdot \mathbf{s}_{i-1,i}^{L-1}$ is an $(L-1) \times 1$ matrix, and $\mathbf{h}_{L-1}$ is a submatrix consist of the non-zero elements of $\mathbf{h_t}$ as follows

$$\mathbf{h}_{L-1} = \begin{bmatrix} h_{L-1} & \ldots & h_1 \\ \vdots & \ddots & \vdots \\ 0 & \ldots & h_{L-1} \end{bmatrix}, \tag{5.17}$$

which is an $(L-1) \times (L-1)$ matrix. Then, after performing FFT to Eq.(5.14), we have

$$\mathbf{F}_N \mathbf{r}_i = \mathbf{F}_N \mathbf{h} \begin{bmatrix} \mathbf{F}_{L-1}^{\mathcal{H}} \mathbf{S}_i \\ \mathbf{F}_N^{\mathcal{H}} \cdot \mathbf{S}_i \end{bmatrix} + \mathbf{F}_N \mathbf{v}_{i-1,i}. \tag{5.18}$$

Note that, $\begin{bmatrix} \mathbf{F}_{L-1}^{\mathcal{H}} \mathbf{S}_i \\ \mathbf{F}_N^{\mathcal{H}} \mathbf{S}_i \end{bmatrix}$ becomes the shape of the symbol by inserting the GI with the length of $(L-1)$. Thus, Eq.(5.18) becomes

$$\begin{aligned} \mathbf{F}_N \mathbf{r}_i &= \mathbf{F}_N \mathbf{h}_{cycl} \mathbf{F}_N^{\mathcal{H}} \mathbf{S}_i + \mathbf{F}_N \mathbf{v}_{i-1,i} \\ &= \mathbf{H}_{diag} \mathbf{S}_i + \mathbf{F}_N \begin{bmatrix} \mathbf{G}_{L-1} \\ \mathbf{0}_{N-L+1} \end{bmatrix}, \end{aligned} \tag{5.19}$$

where $\mathbf{F}_N$ is the FFT matrix given by

$$\mathbf{F}_N = \frac{1}{\sqrt{N}} \begin{bmatrix} 1 & 1 & \dots & 1 \\ 1 & e^{-j\frac{2\pi}{N}} & \dots & e^{-j\frac{2\pi(N-1)}{N}} \\ \vdots & \vdots & \ddots & \vdots \\ 1 & e^{-j\frac{2\pi(N-1)}{N}} & \dots & e^{-j\frac{2\pi(N-1)(N-1)}{N}} \end{bmatrix}, \tag{5.20}$$

and $\mathbf{H}_{diag} = \mathbf{F}_N \cdot \mathbf{h}_{cycl} \cdot \mathbf{F}_N^{\mathcal{H}}$ is a diagonal matrix corresponding to the frequency response. Thus we have

$$\mathbf{F}_N^{\mathcal{H}} \mathbf{H}_{diag}^{-1} \mathbf{F}_N \mathbf{r}_i = \mathbf{s}_i + \mathbf{F}_N^{\mathcal{H}} \mathbf{H}_{diag}^{-1} \mathbf{F}_N \begin{bmatrix} \mathbf{G}_{L-1} \\ \mathbf{0}_{N-L+1} \end{bmatrix}. \tag{5.21}$$

In the right side of the equation, we can see the first term denotes desired signal and second term denotes the ISI. In the second term, the $\mathbf{H}_{diag}^{-1}$ corresponds to the inverse channel. To better understand the effect of ISI, we will consider two various channels (minimum-phase and non-minimum-phase channels) as follows.

5.3.1 Minimum Phase Channel

While the channel is minimum-phase, since all the zeros are inside the unit circle, the channel and its inverse are causal and stable. This means

$$\mathbf{F}_N^{\mathcal{H}} \mathbf{H}_{diag}^{-1} \mathbf{F}_N = \tilde{\mathbf{h}}_{cycl}. \tag{5.22}$$

If the length of inverse channel is m, it can be expressed as

$$\tilde{\mathbf{h}}_{cycl} = \begin{bmatrix} \tilde{h}_0 & 0 & \dots & 0 & \tilde{h}_{m-1} & \dots & \tilde{h}_0 \\ \vdots & \ddots & \ddots & & \ddots & \ddots & \vdots \\ \tilde{h}_{m-2} & \dots & \tilde{h}_0 & \ddots & & \ddots & \tilde{h}_{m-1} \\ \tilde{h}_{m-1} & \dots & & \tilde{h}_0 & \ddots & & 0 \\ 0 & \tilde{h}_{m-1} & \dots & & \tilde{h}_0 & \ddots & \vdots \\ \vdots & \ddots & \ddots & & & \ddots & 0 \\ 0 & \dots & 0 & \tilde{h}_{m-1} & \dots & & \tilde{h}_0 \end{bmatrix}. \tag{5.23}$$

Then, when the length of channel L and that of inverse channel m satisfy $N - m \geq 2(L-1)$, we can obtain

$$\tilde{\mathbf{h}}_{cycl} \begin{bmatrix} \mathbf{G}_{L-1} \\ \mathbf{0}_{N-L+1} \end{bmatrix} = \begin{bmatrix} \mathbf{A}_{N-w} \\ \mathbf{0}_w \end{bmatrix}. \tag{5.24}$$

In this equation, we should note that $w \geq L-1$. Then Eq.(5.21) becomes

$$\tilde{\mathbf{s}}_i = \mathbf{F}_N^{\mathcal{H}} \mathbf{H}_{diag}^{-1} \mathbf{F}_N \mathbf{r}_i = \mathbf{s}_i + \begin{bmatrix} \mathbf{A}_{N-w} \\ \mathbf{0}_w \end{bmatrix}. \tag{5.25}$$

This implies that ISI only occur at the beginning portion of the symbols and without interference, we can obtain $w \geq L-1$ pure samples at the tail part of the symbols. Note that $\mathbf{s}_i^{L-1}$ is the last $L-1$ elements of the ith symbol. As a result, we can obtain the $\mathbf{v}_{i-1,i}$ in Eq.(5.15) by using the tail part of the symbols. By substituting $\mathbf{v}_{i-1,i}$ into Eq.(5.19), we get

$$\mathbf{F}_N \cdot (\mathbf{r}_i - \mathbf{v}_{i-1,i}) = \mathbf{H}_{diag} \cdot \mathbf{S}_i. \tag{5.26}$$

Finally, the symbol can be recovered as follows

$$\hat{\mathbf{S}}_i \;=\; \mathbf{H}_{diag}^{-1} \cdot \mathbf{F}_N \cdot (\mathbf{r}_i - \mathbf{v}_{i-1,i}). \tag{5.27}$$

5.3.2 Non-Minimum Phase Channel

While the channel is non-minimum phase, we can employ proper filter converting it into minimum phase. Then, the above method, which is corresponding to minimum-phase channel, can be used.

To explain the conversion from non-minimum phase to minimum phase, let us see an example, where $\vec{\mathbf{h}} = [h_0,\ h_1,\ h_2,\ h_3]$ is a channel with 4 delay spread. After $z-$transform, it becomes

$$H(z) = h_0 + h_1 z^{-1} + h_2 z^{-2} + h_3 z^{-3}. \tag{5.28}$$

By factorization, we have

$$H(z) = h_0(1 - z_0 z^{-1})(1 - z_1 z^{-1})(1 - z_2 z^{-1}), \tag{5.29}$$

where z_0, z_1 and z_2 are the zeros of the system. In this system, let us assume one of the zeros z_2 is outside the unit circle, and express the corresponding factor with

$H_f(z) = (1 - z_2 z^{-1})$. In order to convert $H(z)$ into minimum phase, it is necessary to remove z_2. This can be achieved by using inverse filter $H'_f(z) = 1/(1 - z_2 z^{-1})$. Unfortunately, since the system $H'_f(z)$ is unstable because of a pole outside the unit circle, it is necessary to approximate it by a realizable filter. Here, we employ the approximation method proposed in [10], where long division is used to find approximate inverse system. The technique finding approximate inverse to the system $H_f(z) = (1 - z_2 z^{-1})$ can be described as follows.

Firstly, write $D(z) = z^n H_f(z)$, where n is chosen to be the peak of the impulse response. Here, impulse response corresponding to $H_f(z)$ can be expressed as $h = [1,\ z_2]$, thus the $n = 1$ due to $\mid z_2 \mid \geq 1$. Then perform long devision to find $1/D(z)$. After the long division, we can write

$$Q(z) = \frac{1 - R(z)}{D(z)} = \frac{1 - R(z)}{z H_f(z)}, \tag{5.30}$$

where $Q(z)$ and $R(z)$ represent the quotient polynomial and remainder polynomial respectively. Since $1/H_f(z)$ is unstable and has a divergent expansion, $R(z)$ will eventually have large coefficients. In Eq.(5.30), neglecting 1 with respect to $R(z)$, we have

$$\frac{z^{-1}}{H_f(z)} \simeq Q(z)\frac{-1}{R(z)}. \tag{5.31}$$

Then, after long division to $D(z) = z(1 - z_2 z^{-1})$, we get

$$\begin{aligned} Q(z) &= z^{-1} + z_2 z^{-2} + z_2^2 z^{-3} ... + z_2^{k-1} z^{-k}, & (5.32)\\ R(z) &= z_2^k z^{-k}, & (5.33) \end{aligned}$$

where k denotes the highest index of truncated serious, i.e, the highest power of z in the series. By substituting $Q(z)$ and $R(z)$ into Eq.(5.31), we can obtain

$$\begin{aligned} H'_f(z) &= z^{-k}\left\{-\frac{Q(z)}{R(z)}\right\} \\ &= \frac{z^{-1} + z_2 z^{-2} + z_2^2 z^{-3} ... + z_2^{k-1} z^{-k}}{-z_2^k}. \end{aligned} \tag{5.34}$$

To varify that $H'_f(z)$ is a very good approximation to the inverse of $H_f(z)$, let us see

$$H_f(z) \cdot H'_f(z) = -\frac{1}{z_2^k} z^{-1} + z^{-l}. \tag{5.35}$$

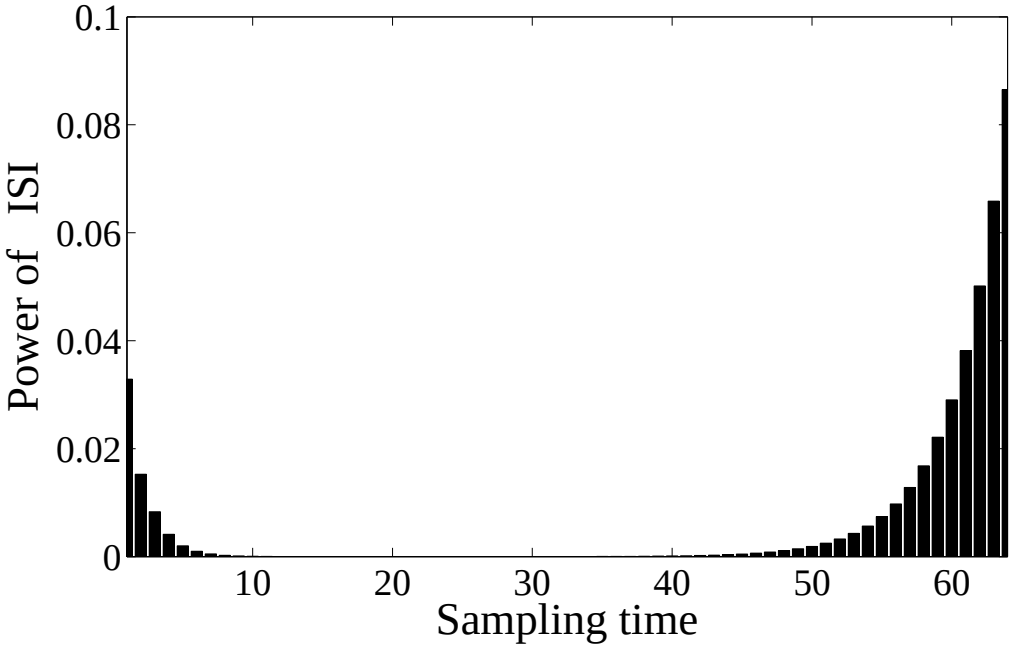

(a) Non-minimum phase channel

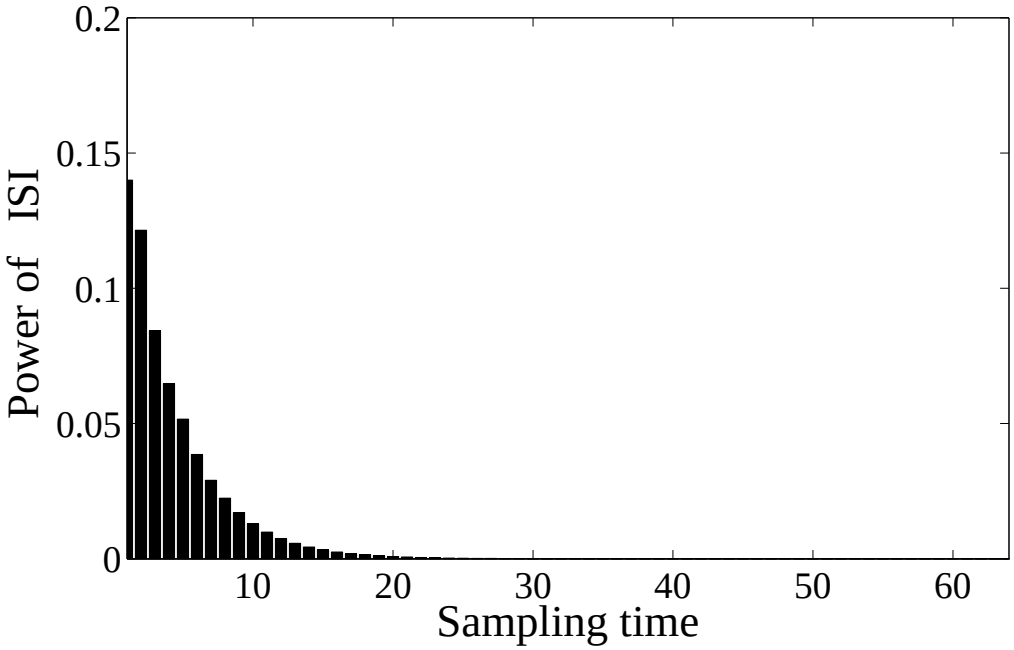

(b) Minimum phase channel

Fig. 5.4. Power of ISI versus sampling time, after FDE.

In Eq.(5.35), if k is big enough, the first term can be neglected and it becomes

$$H_f(z) \cdot H'_f(z) \simeq z^{-l}, \tag{5.36}$$

where $l = n + k$. From this, we can see the approximate inverse filter will cause a delay of l units, and this can be incorporated into the channel.

As a conclusion, by using approximate inverse system like this, we can design a FIR filter to convert the non-minimum phase channel into the minimum phase channel. Figure 5.4 shows an example of the ISI power versus sampling time in the symbol $\tilde{\mathbf{s}}_i$ after FDE. We can observe that ISI only affected in the beginning part of the symbol, after channel becomes minimum phase. Then, the method for the minimum phase can be used.

5.4 Simulation Results

We performed simulations to demonstrate the validity of the proposed method. The symbol length as well as FFT size are $N = 64$. The simulations are performed to the modulation schemes of QPSK, 16QAM and 64QAM respectively. The channel is 6-path static channel. To comparison, we also show the SER results of conventional iteration based ISI cancellation method and that of GI inserted OFDM system. In the iteration based ISI cancellation method, the iteration is conducted for 4 times, since higher iteration almost has no clear improvement. The length of GI is selected as long as 20% of symbol interval. In the figures, the acronyms PICM, GI and IICM denote the proposed ISI cancellation method, conventional method with GI, and iteration based ISI cancellation method, respectively.

Figures 5.5, 5.6, and 5.7 show the SER results versus SNR respectively for QPSK, 16QAM and 64QAM, where the channel is 6 path static channel. From these figures, we can observe that the proposed ISI cancellation method performs as good as the system with GI. We also can see that the conventional iteration based ISI cancellation method although performs good at QPSK modulation, but results in error propagation in high-degree constellation such as 16QAM and 64QAM.

5.5 Conclusions

In OFDM systems, since GI insertion reduces transmission efficiency, some challenges are attempted for OFDM systems without GI. In the absence of GI, eliminating ISI between adjacent symbols is a crucial problem.

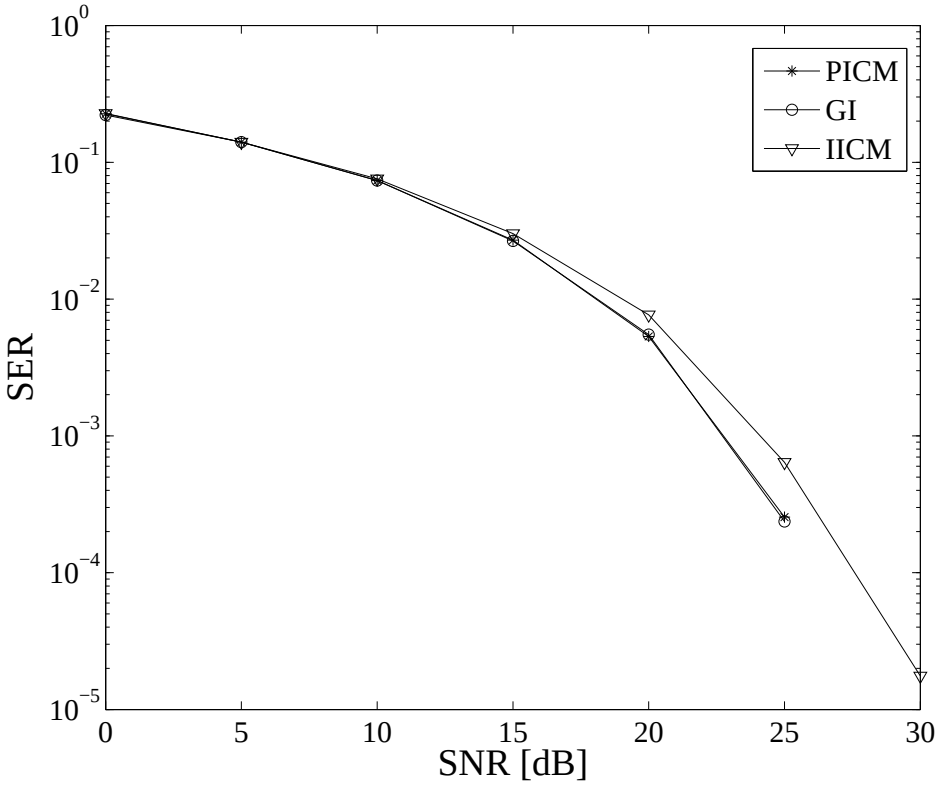

Fig. 5.5. SER versus SNR, QPSK.

In this chapter, in order to upgrade the transmission efficiency, we have discussed OFDM systems without GI. Then, a novel ISI cancellation method has been proposed. We find that, while the channel is minimum phase, after performing FDE to received signal and converting the resulting signal to time domain, every symbol is effected by the ISI only at the beginning part of the symbols. Based on this observation, we derived a interference cancellation method according to the tail part of every symbol, which is not effected by ISI. To a channel which is not minimum-phase, it has been indicated that the proposed method is also applicable after converting the channel into minimum-phase by using proper filter. In order to confirm the validity of proposed method, the simulation is performed. Symbol error rates (SER) results show that even without GI, ISI can be canceled perfectly by using the proposed method.

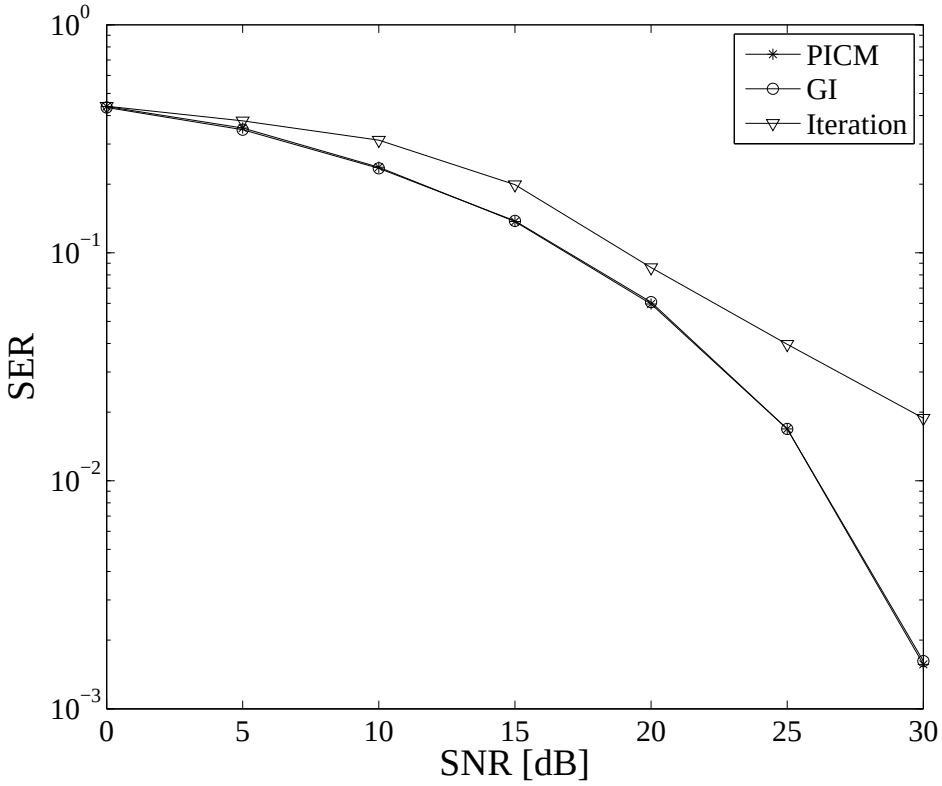

Fig. 5.6. SER versus SNR, 16QAM.

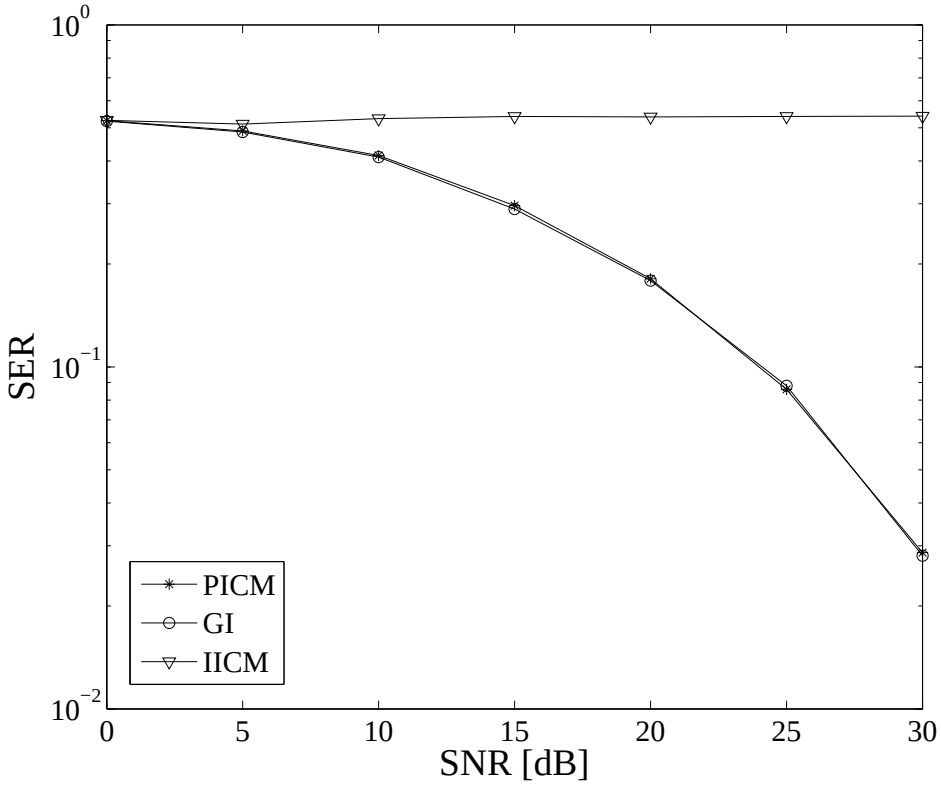

Fig. 5.7. SER versus SNR, 64QAM.

CHAPTER 6

Conclusions and Future Research

THIS thesis addresses the issues of CFO and I/Q imbalance estimation in the presence of TV-DCO. In addition, ISI cancellation problem for OFDM systems without GI is discussed. Our focus has been on designing CFO and I/Q imbalance estimators by using linear approximation to TV-DCO, and developing ISI cancellation method by using proper filter and frequency domain equalization.

Orthogonality among subcarriers is the fundamental of OFDM systems. While CFO occurs, the spectrum of the received signal will be shifted. This will destroy the required orthogonality and result in severe performance degradation. On the other hand, although DCR is very attractive by its small-size, low-cost, and low-power consumption, it introduces additional analog impairment DCO. More seriously, in practice, automatic gain control (AGC) results in TV-DCO. Therefore, in OFDM-DCR, the estimation/compensation of CFO in the presence of TV-DCO is very crucial. In this thesis, a novel CFO estimation scheme in the presence of TV-DCO have been proposed. It is shown the residual DCO after high-pass filtering varies in a linear fashion. Based on this observation, we have modeled the residual DCO using a linear function. Then, from the periodicity of the training sequence, we derived a CFO estimator independent of TV-DCO. Also, the residual TV-DCO was estimated using the obtained CFO. Simulations has been performed to show the effectiveness of the proposed method. In the simulation, we have confirmed whatever the Doppler shift exists or not, not only the coarse estimation but also the fine estimation of proposed method are better than the existing differential filter method. Meantime, it has been shown that the proposed CFO estimator is almost independent of frequency offset. Then, TV-DCO estimation result have

shown the estimation performed quite accurately. Finally, after compensating CFO and TV-DCO, BER curve has been plotted, where it has been shown the proposed method performs better than conventional method.

In a DCR, CFO, DCO and I/Q imbalance are considered to be the most serious impairments. Furthermore, AGC leads to TV-DCO. Since OFDM system is sensitive to CFO, the estimation/compensation of CFO in the presence of I/Q imbalance and the TV-DCO is a critical problem in an OFDM-DCR. In this thesis, a novel joint estimation method for CFO and I/Q imbalance in the presence of TV-DCO has been proposed. Based on the linear property of TV-DCO, we have approximated the TV-DCO using a linear function. Then, a closed-form CFO and I/Q imbalance estimator was derived from the periodicity of training sequence. Simulations were performed to confirm the validity of the proposed estimator. From CFO MSE to both the proposed and the conventional methods, it has been confirmed that the proposed CFO estimator performs quite accurately than the conventional CFO estimator. In contrast to the poor estimation ability of 10^{-3} CFO MSE in 25dB SNR in conventional method, about 10^{-6} CFO MSE can be obtained for the proposed estimator. Meantime, it has been shown that the proposed CFO estimator is independent of CFO, while conventional CFO estimator is dependent on CFO. In the I/Q imbalance estimation results using IRR, it has been shown that the IRR is improved from 18dB to 37dB while SNR=25dB. Finally, after compensating CFO and I/Q imbalance, BER curve has been shown to evaluate the whole compensation, where we can see that in contrast to the poor performance of the conventional method, the proposed method shows acceptable performance.

In OFDM systems, since GI insertion reduces transmission efficiency, some challenges have been attempted for OFDM systems without GI. In the absence of GI, eliminating ISI between adjacent symbols is a crucial problem. In this thesis, in order to upgrade the transmission efficiency, we have discussed OFDM systems without GI. Then, a novel ISI cancellation method has been proposed. We find that, while the channel is minimum phase, after performing FDE to received signal and converting the resulting signal to time domain, every symbol is effected by the ISI only at the beginning part of the symbols. Based on this observation, we derived a interference cancellation method according to the tail part of every symbol, which is not effected by ISI. To a channel which is not minimum-phase, it has been indicated that the proposed method is also applicable after converting the channel into minimum-phase by using proper filter. In order to confirm the validity of proposed method, the simulation has been performed. Symbol error rates (SER) results show that even without GI, ISI can be canceled perfectly by

using the proposed method. However, this method is not applicable for asynchronous uplink MC-CDMA systems. In [27, 29], we proposed a novel symbol structure with zero-padding to synchronize all user's signal, which can eliminate the MUI completely. However, due to long zero padding between symbols, transmission speed would be decreased. In order to increase the transmission speed, I will attempt to derive a multi-user interference cancellation method for MC-CDMA systems without GI or zero-padding in coming future.

Appendix

Appendix A:

We describe brief proofs of signal effected by CFO as $d(k) = y(k)e^{j\frac{2\pi\varepsilon k}{N}}$. The one block of OFDM transmitted signal can be expressed by

$$s(t) = \sum_{n=0}^{N-1} \{a_n cos[2\pi(f_c + n\Delta f)t] - b_n sin[2\pi(f_c + n\Delta f)t]\} \quad \text{(A-1)}$$

Since we just want to observe the effect of CFO, for the simplicity, we assume $H(f) = 1$, $r(t) = s(t)$. Thus, in I branch after downconversion , we have

$$\begin{aligned} & r(t)cos[2\pi(f_c + \Delta f_c)t] \quad \text{(A-2)} \\ = & \sum_{n=0}^{N-1} \{a_n cos[2\pi(f_c + n\Delta f)t] - b_n sin[2\pi(f_c + n\Delta f)t]\} cos[2\pi(f_c + \Delta f_c)t] \\ = & \frac{1}{2}\sum_{n=0}^{N-1} \{a_n cos[2\pi(2f_c + \Delta f_c + n\Delta f)t] + a_n cos[2\pi(n\Delta f - \Delta f_c)t]\} \\ - & \frac{1}{2}\sum_{n=0}^{N-1} \{b_n sin[2\pi(2f_c + \Delta f_c + n\Delta f)t] + b_n sin[2\pi(n\Delta f - \Delta f_c)t]\} \quad \text{(A-3)} \end{aligned}$$

after passing $2 \times LPF$, I branch becomes

$$r_I(t) = \sum_{n=0}^{N-1} \{a_n cos[2\pi(n\Delta f - \Delta f_c)t]\} - \sum_{n=0}^{N-1} \{b_n sin 2\pi(n\Delta f - \Delta f_c)t\}. \quad \text{(A-4)}$$

Similarly, Q branch becomes

$$\begin{aligned} & - r(t)sin[2\pi(f_c + \Delta f_c)t] \\ = & -\sum_{n=0}^{N-1} \{a_n cos[2\pi(f_c + n\Delta f)t] - b_n sin[2\pi(f_c + n\Delta f)t]\} sin[2\pi(f_c + \Delta f_c)t] \\ = & -\frac{1}{2}\sum_{n=0}^{N-1} \{a_n sin[2\pi(2f_c + \Delta f_c + n\Delta f)t] - a_n sin[2\pi(n\Delta f - \Delta f_c)t]\} \\ - & \frac{1}{2}\sum_{n=0}^{N-1} \{b_n cos[2\pi(2f_c + \Delta f_c + n\Delta f)t] - b_n cos[2\pi(n\Delta f - \Delta f_c)t]\} \quad \text{(A-5)} \end{aligned}$$

after passing $2 \times LPF$

$$r_Q(t) = \sum_{n=0}^{N-1} \{a_n sin[2\pi(n\Delta f - \Delta f_c)t]\} + \sum_{n=0}^{N-1} \{b_n cos[2\pi(n\Delta f - \Delta f_c)t]\} \quad \text{(A-6)}$$

Therefore

$$\begin{aligned} r_I(t) + jr_Q(t) &= \sum_{n=0}^{N-1} \{a_n cos[2\pi(n\Delta f - \Delta f_c)t]\} - \sum_{n=0}^{N-1} \{b_n sin[2\pi(n\Delta f - \Delta f_c)t]\} \\ &+ j\{\sum_{n=0}^{N-1} \{a_n sin[2\pi(n\Delta f - \Delta f_c)t]\} + \sum_{n=0}^{N-1} \{b_n cos[2\pi(n\Delta f - \Delta f_c)t]\}\} \\ &= \sum_{n=0}^{N-1} (a_n + jb_n)\{cos[2\pi(n\Delta f - \Delta f_c)t] + jsin[2\pi(n\Delta f - \Delta f_c)t]\} \\ &= \sum_{n=0}^{N-1} (a_n + jb_n)e^{j2\pi(n\Delta f - \Delta f_c)t} \end{aligned} \quad \text{(A-7)}$$

while sampling interval is $\frac{1}{N\Delta f}$, we denote normalized frequency offset to be $\varepsilon = \frac{\Delta f_c}{\Delta f}$. Thus, we get

$$d(k) = \{\sum_{n=0}^{N-1} (a_n + jb_n)e^{j\frac{2\pi nk}{N}}\}e^{j\frac{2\pi\varepsilon k}{N}} = y(k)e^{j\frac{2\pi\varepsilon k}{N}} \quad \text{(A-8)}$$

where $y(k) = \sum_{n=0}^{N-1}(a_n + jb_n)e^{j\frac{2\pi nk}{N}}$ is baseband equivalent signal.

Appendix B:

We describe brief proofs of $\mathbf{D}^T = \mathbf{D}$, $\mathbf{D}\mathbf{1}_N = \mathbf{0}_N$, $\mathbf{D}\mathbf{x}_1 = \mathbf{0}_N$, $\mathbf{D}\mathbf{x}_2 = \mathbf{0}_N$. We should notice $\{\mathbf{x}_1^T\mathbf{1}_N\}$, $\{\mathbf{x}_1^T\mathbf{x}_1\}$, $\{\mathbf{1}_N^T\mathbf{x}_1\}$ and $\{\mathbf{1}_N^T\mathbf{1}_N\}$ are scalar, and $\mathbf{1}_N^T\mathbf{1}_N = N$. Following this, it can be easily proved $\mathbf{D}$ is symmetric , since

$$\begin{aligned}\mathbf{D}^T &= \{\mathbf{x}_1^T\mathbf{x}_1\mathbf{1}_N^T\mathbf{1}_N - \mathbf{x}_1^T\mathbf{1}_N\mathbf{1}_N^T\mathbf{x}_1\}\mathbf{I}_N^T \\ &\quad +\{\mathbf{1}_N\mathbf{1}_N^T\mathbf{x}_1\mathbf{x}_1^T + \mathbf{x}_1\mathbf{x}_1^T\mathbf{1}_N\mathbf{1}_N^T\}^T \\ &\quad -\{\mathbf{x}_1\mathbf{1}_N^T\mathbf{1}_N\mathbf{x}_1^T + \mathbf{1}_N\mathbf{x}_1^T\mathbf{x}_1\mathbf{1}_N^T\}^T = \mathbf{D}. \end{aligned} \tag{B-1}$$

At the same time, we can compute $\mathbf{D}\mathbf{1}_N$ as

$$\begin{aligned}\mathbf{D}\mathbf{1}_N &= \mathbf{x}_1^T\mathbf{x}_1\{\mathbf{1}_N^T\mathbf{1}_N\}\mathbf{1}_N - \mathbf{x}_1^T\mathbf{1}_N\mathbf{1}_N^T\mathbf{x}_1\mathbf{1}_N \\ &\quad +\mathbf{1}_N\{\mathbf{1}_N^T\mathbf{x}_1\}\{\mathbf{x}_1^T\mathbf{1}_N\} - \mathbf{x}_1\{\mathbf{1}_N^T\mathbf{1}_N\}\mathbf{x}_1^T\mathbf{1}_N \\ &\quad +\mathbf{x}_1\mathbf{x}_1^T\mathbf{1}_N\{\mathbf{1}_N^T\mathbf{1}_N\} - \mathbf{1}_N\{\mathbf{x}_1^T\mathbf{x}_1\}\{\mathbf{1}_N^T\mathbf{1}_N\} \\ &\quad = N\mathbf{x}_1^T\mathbf{x}_1\mathbf{1}_N - \mathbf{x}_1^T\mathbf{1}_N\mathbf{1}_N^T\mathbf{x}_1\mathbf{1}_N \\ &\quad +\{\mathbf{x}_1^T\mathbf{1}_N\}\{\mathbf{1}_N^T\mathbf{x}_1\}\mathbf{1}_N - N\mathbf{x}_1\mathbf{x}_1^T\mathbf{1}_N \\ &\quad +N\mathbf{x}_1\mathbf{x}_1^T\mathbf{1}_N - N\{\mathbf{x}_1^T\mathbf{x}_1\}\mathbf{1}_N = \mathbf{0}_N, \end{aligned} \tag{B-2}$$

from which we have $\mathbf{D}\mathbf{1}_N = \mathbf{0}_N$.

Also, we can calculate $\mathbf{D}\mathbf{x}_1$ as

$$\begin{aligned}\mathbf{D}\mathbf{x}_1 &= \{\mathbf{x}_1^T\mathbf{x}_1\}\{\mathbf{1}_N^T\mathbf{1}_N\}\mathbf{x}_1 - \mathbf{x}_1^T\mathbf{1}_N\mathbf{1}_N^T\mathbf{x}_1\mathbf{x}_1 \\ &\quad +\mathbf{1}_N\{\mathbf{1}_N^T\mathbf{x}_1\}\{\mathbf{x}_1^T\mathbf{x}_1\} - \mathbf{x}_1\{\mathbf{1}_N^T\mathbf{1}_N\}\{\mathbf{x}_1^T\mathbf{x}_1\} \\ &\quad +\mathbf{x}_1\{\mathbf{x}_1^T\mathbf{1}_N\}\{\mathbf{1}_N^T\mathbf{x}_1\} - \mathbf{1}_N\mathbf{x}_1^T\mathbf{x}_1\mathbf{1}_N^T\mathbf{x}_1 \\ &\quad = N\mathbf{x}_1\{\mathbf{x}_1^T\mathbf{x}_1\} - \mathbf{x}_1^T\mathbf{1}_N\mathbf{1}_N^T\mathbf{x}_1\mathbf{x}_1 \\ &\quad +\mathbf{1}_N\{\mathbf{x}_1^T\mathbf{x}_1\}\{\mathbf{1}_N^T\mathbf{x}_1\} - N\mathbf{x}_1\{\mathbf{x}_1^T\mathbf{x}_1\} \\ &\quad +\{\mathbf{x}_1^T\mathbf{1}_N\}\{\mathbf{1}_N^T\mathbf{x}_1\}\mathbf{x}_1 - \mathbf{1}_N\mathbf{x}_1^T\mathbf{x}_1\mathbf{1}_N^T\mathbf{x}_1 \\ &\quad = \mathbf{0}_N, \end{aligned} \tag{B-3}$$

which proves $\mathbf{D}\mathbf{x}_1 = \mathbf{0}_N$.

Since $\mathbf{x}_2 = \mathbf{x}_1 + K\mathbf{1}_N$, we have $\mathbf{D}\mathbf{x}_2 = \mathbf{D}\mathbf{x}_1 + K\mathbf{D}\mathbf{1}_N = \mathbf{0}_N$.

Bibliography

[1] "Part 11: Wireless LAN Medium Access Control and Physical Layer (PHY) Specifications: High-Speed Physical Layer in the 5GHz Band," *IEEE Standard 802.11a-1999*.

[2] A.A.Abidi, "Direct-conversion radio transceivers for digital communications," *IEEE Journal of Solid-State Circuits*, vol. 30, pp. 1399–1410, Dec. 1995.

[3] A.Peled and A.Ruiz, "Frequency domain data transmission using reduced computational complexity algorithms," in *Proc. IEEE ICASSP'80*, pp. 964 – 967, Apr. 1980.

[4] B.Razavi, "Design considerations for direct-conversion receivers," *IEEE Trans. Circuits Syst. II*, vol. 44, pp. 428–435, Jun. 1997.

[5] C.E.Shannon, "A mathematical theory of communication," *Bell System Technical Journal*, vol. 27, pp. 379–423, 623–656, Jul., Oct. 1948.

[6] ——, "Communications in the presence of noise," in *Proc. IRE*, vol. 37, pp. 10 – 21, Jan. 1949.

[7] C.K.Ho, S.Sun, and P.He, "Low complexity frequency offset estimation in the presence of DC offset," in *Proc. IEEE ICC'03*, pp. 2051–2055, May 2003.

[8] D.Kim and G.L.Stuber, "Residual ISI cancellation for OFDM with applications to HDTV broadcasting," *IEEE J. Sel. Areas Commun.*, vol. 16, pp. 1590–1599, Oct. 1998.

[9] D.Tandur and M.Moonen, "Joint adaptive compensation of transmitter and receiver IQ imbalance under carrier frequency offset in OFDM-based systems," *IEEE Trans. Signal processing*, vol. 55, pp. 5246 – 5252, Nov. 2007.

[10] E.Newhall, S.Qureshi, and C.Simone, "A technique for finding approximate inverse systems and its applications to equalization," *IEEE Trans. Commun.*, vol. COM-19, pp. 1116–1127, Dec. 1971.

[11] F.Horlin, A.Bourdoux, E. Estraviz, and L. der Perre, "Low complexity EM-based joint CFO and IQ imbalance acquisition," in *Proc. IEEE ICC'07*, pp. 2871 – 2876, Jun. 2007.

[12] G.Gil, I.Sohn, J.Park, and Y.H.Lee, "Joint ML estimation of carrier frequency, channel, I/Q mismatch, and DC offset in communication receivers," *IEEE Trans. Veh. Technol.*, vol. 54, pp. 338–349, Jan. 2005.

[13] H.Jung and M.D.Zoltowski, "Turbo multi-user receiver for asynchronous multi-user OFDM systems," in *Proc. IEEE ICASSP'05*, pp. 693–696, Mar. 2005.

[14] H.K.Song, Y.H.You, J.H.Paik, and Y.S.Cho, "Frequency-offset synchronization and channel estimation for OFDM-based transmission," *IEEE Commun. Lett.*, vol. 4, pp. 95–97, Mar. 2000.

[15] H.Lin, X.Wang, and K.Yamashita, "A low-complexity carrier frequency offset estimator independent of DC offset," *IEEE Commun. Lett.*, vol. 12, pp. 520–522, Jul. 2008.

[16] H.Lin, X.Zhu, and K.Yamashita, "Pilot-aided low-complexity CFO and I/Q imbalance compensation for OFDM systems," in *Proc. IEEE ICC'08*, pp. 713 – 717, May 2008.

[17] H.Shoki and Y.Tanabe, "How fast will be required, how fast can be realized in future wireless communications," *IEICE communication society*, vol. 11, pp. 12–22, 2009.

[18] J.M.Cioffi and A.C.Bingham, "A data-driven multitone echo canceller," *IEEE Trans. Commun.*, vol. 42, pp. 2853–2869, Oct. 1994.

[19] J.Tubbax, A.Ford, L. der Perre, S.Donnay, M.Moonen, and H.D.Man, "Joint compensation of IQ imbalance and frequency offset in OFDM systems," in *Proc. IEEE GLOBECOM'03*, pp. 2365–2369, Dec. 2003.

[20] K.Uehara, "Trends in broadband wireless communication systems and software defined radios," *Interdisciplinary Information Sciences*, vol. 12, pp. 163–172, 2006.

[21] K.V.Acker, G. Lens, M. Moonen, O. V. de Wiel, and T. Pollet, "Per tone equalization for DMT receivers," in *Proc. IEEE Global Telecommun.*, pp. 2311–2315, May 1999.

[22] K.W.Cheong and J.M.Cioffi, "Precoder for DMT with insufficient cyclic prefix," in *Proc. IEEE International Conf. on Commun.*, pp. 339–343, Jun. 1998.

[23] M.D.Courville, P.Duhamel, P.Madec, and J.Palicot, "Blind equalization of OFDM systems based on the minimization of a quadratic criterion," in *Proc. IEEE International Conf. on Commun.*, pp. 1318–1322, Jun. 1996.

[24] M.Inamori, A.M.Bostamam, Y.Sanada, and H.Minami, "Frequency offset estimation scheme in the presence of time-varying DC offset and IQ imbalance for OFDM direct conversion receivers," in *Proc. IEEE PIMRC'07*, pp. 1 – 5, Sept. 2007.

[25] ——, "Frequency offset estimation scheme in the presence of time-varying DC offset for OFDM direct conversion receivers," *IEICE Trans. Commun.*, vol. E90-B, pp. 2884–2890, Oct. 2007.

[26] M.Morelli and U.Mengali, "An improved frequency offset estimator for OFDM applications," *IEEE Commun. Lett.*, vol. 3, pp. 75–77, Mar. 1999.

[27] M.Nishikawa, U.Yunus, H.Lin, and K.Yamashita, "Lattice-reduction based multiuser detection for asynchronous MC-CDMA systems," in *Proc. MITA'09*, pp. 102–103, Aug. 2009.

[28] M.Sawahashi, S.Abeta, H.Atarashi, K.Higuchi, M.Tanno, and T.Ihara, "Broadband packet wireless access," *NTT DoCoMo Technical Journal*, vol. 2, pp. 18–31, Sept. 2004.

[29] N.Shoji, U.Yunus, H.Lin, and K.Yamashita, "Multiuser detection for asynchronous uplink MC-CDMA systems," in *Proc. MITA'09*, pp. 96–97, Aug. 2009.

[30] P.H.Moose, "A technique for orthogonal frequency division multiplexing frequency offset correction noise," *IEEE Trans. Communications*, vol. 42, pp. 2908–2914, Oct. 1994.

[31] P.J.W.Melsa, R.C.Younce, and C.E.Rohrs, "Impulse response shortening for discrete multitone transceivers," *IEEE Trans. Commun.*, vol. 44, pp. 1662–1672, Dec. 1996.

[32] R.W.Chang, "Synthesis of band-limited orthogonal signals for multichannel data tramsmission," *Bell System Technical Journal*, vol. 45, pp. 1775–1796, Dec. 1966.

[33] R.W.Chang and R.Gibby, "A theoretical study of performance of an orthogonal multiplexing data transmission scheme," *IEEE Trans. Commun.*, vol. 16, pp. 529–540, Aug. 1968.

[34] S.B.Weinstein and P.M.Ebert, "Data transmission by frequency-division multiplexing using the discrete Fourier transform," *IEEE Trans. Communications*, vol. 19, pp. 628–634, Oct. 1971.

[35] S.D.Rore, E.L.Estraviz, F.Horlin, and L.V.D.Perre, "Joint estimation of carrier frequency offset and IQ imbalace for 4G mobile wireless systems," in *Proc. IEEE ICC'06*, pp. 2066–2071, Jun. 2006.

[36] S.Fouladifard and H.Shafiee, "Frequency offset estimation in OFDM systems in presence of I/Q imbalance," in *Proc. IEEE ICC'03*, pp. 2071–2075, May 2003.

[37] S.Marsili, "DC offset estimation in OFDM based WLAN application," in *Proc. IEEE GLOBECOM'04*, pp. 3531–3535, Dec. 2004.

[38] S.Otaka, T.Yamaji, R.Fujimoto, and H.Tanimoto, "A low offset 1.9-GHz direct conversion receiver IC with spurious free dynamic range of over 67 dB," *IEICE Trans. Fundamentals*, vol. E84-A, pp. 513–519, Feb. 2001.

[39] S.Trautmann and N.J.Fliege, "Perfect equalization for DMT systems without guard interval," *IEEE J. Select. Areas Commun.*, vol. 20, pp. 987–996, Jun. 2002.

[40] T.M.Schmidl and D.C.Cox, "Robust frequency and timing synchronization for OFDM," *IEEE Trans. Communications*, vol. 45, pp. 1613–1621, Dec. 1997.

[41] T.Pollet, M. Bladel, and M.Moeneclaey, "BER sensitivity of OFDM systems to carrier frequency offset and Wiener phase noise," *IEEE Trans. Communications*, vol. 43, pp. 191–193, Feb./Mar./Apr. 1995.

[42] U.Yunus, H.Lin, and K.Yamashita, "Frequency offset estimation in the presence of I/Q imbalance and time-varying DC offset," in *Proc. APWCS'09*, pp. 1–4, Aug. 2009.

[43] ——, "Pilot-based frequency offset estimation in the presence of time-varying DC offset," in *Proc. IEEE PIMRC'09*, pp. 1–4, Sept. 2009.

[44] ——, "Robust frequency offset estimation in the presence of time-varying DC offset," *IEICE Trans. On Commun.*, vol. E92-B, pp. 2577–2583, Aug. 2009.

[45] ——, "Joint estimation of carrier frequency offset and I/Q imbalance in the presence of time-varying DC offset," *IEICE Trans. On Commun.*, vol. E93-B, pp. 16–21, Jan. 2010.

[46] ——, "A novel ISI cancellation method for OFDM systems without guard interval," in *Proc. IEEE GLOBECOM'10*, pp. 1–7, Dec. 2010 (Submitted).

[47] W.Namgoong and T.H.Meng, "Direct-conversion RF receiver design," *IEEE Trans. Commun.*, vol. 49, pp. 518–529, Mar. 2001.

[48] X.Wang, P.Ho, and Y.Wu, "Robust channel estimation and ISI cancellation for OFDM systems with suppressed features," *IEEE J. Select. Areas Commun.*, vol. 23, pp. 963–972, May 2005.